

**NEXT GENERATION
NETWORKS**

Harmonic Mitigation

**Work Package One –
Model Development**





Report Title	:	Work Package One – Model Development
Report Status	:	Issue 1
Project Ref	:	Harmonic Mitigation
Date	:	24.07.2020

Document Control		
	Name	Date
Prepared by:	Atheer Habash Grazia Todeschini	17.07.2020
Reviewed by:	Zia Emin	22.07.2020
Approved (WPD):	Chris Harrap	24.07.2020

Revision History		
Date	Issue	Status
24/07/2020	1.0	Issued

Table of Contents - Report

1	Introduction.....	7
2	Construction of underlying MATLAB/Simulink model	9
2.1	Model development	9
2.2	Definition of the snapshot power flow cases.....	13
2.3	Comparison of frequency sweep results.....	14
2.4	Comparison of the results for power flow analysis.....	17
2.5	Conclusions on underlying MATLAB/Simulink Model	21
3	MATLAB/Simulink EMT simulations	22
3.1	Model Development – Loads and PV farms	23
3.1.1	Dynamic load model (11 kV busses).....	23
3.1.2	PV farm model	26
3.1.3	PV Inverter model and associated controls	28
3.1.4	PV Farm dynamic model.....	29
3.2	Model Development - harmonic sources.....	31
3.2.1	Dynamic harmonic Load model.....	32
3.2.2	Dynamic PV farm harmonic model.....	33
3.2.3	Upstream network distortion.....	34
3.3	Model performance.....	36
3.4	Fundamental frequency results and validation.....	37
3.4.1	TIVS5 (Load bus) – Dynamic load model and voltage profiles	37
3.4.2	TIV3 (BSP) – Analysis of 132/33 transformer tap changer	41
3.4.3	CMPV3, STFA3 and AYH3 - Validation of inverter model.....	46
3.4.4	AYSH3 (PV farm) – Validation of dynamic PV farm model	49
3.4.5	EXET1 (System boundary) –Active and Reactive Power Exchange	52
3.4.6	Conclusions on fundamental frequency results of EMT simulations..	58
3.5	Harmonic results and validation.....	59
3.5.1	Harmonic current levels at the PV farms	59
3.5.2	Harmonic voltage levels at the PV farms	63
3.5.3	TIVE3 - Overall power quality assessment	66
3.5.4	Conclusions on harmonic aspects of EMT simulations	69
4	WP1 Conclusions	70
5	Lessons learned	71
6	Bibliography.....	72

Table of Contents - Appendices

Appendix A	Literature Review - Executive Summary	74
Appendix B	Description of the Tiverton Network	76
Appendix C	Description of the data files provided by WPD.....	78
C.1	SCADA data	78
C.2	Power Quality (PQ) data	79
C.3	Modelling of the data for EMT simulations.....	79
Appendix D	Validation of frequency sweep results within MATLAB/Simulink	82
D.1	Frequency dependence of upstream system	82
D.2	Harmonic frequency scans	83
Appendix E	Dynamic simulation results for 1 October 2019.....	96
E.1	Results for PV farms	96
E.2	Results for 33 kV buses – voltage rms	102
E.3	Results for 11 kV buses – voltage rms (with tap changing).....	105
E.4	Results for system boundary	107
E.5	Results for 11 kV buses - Load active and reactive power, and current	110
Appendix F	Dynamic simulation results for 1-21 October 2019.....	118
F.1	Results for PV farms	119
F.2	Results for 33 kV buses – voltage rms	120
F.3	Results for 11 kV busses – Load active and reactive power.....	127
F.4	Results for system boundary	135

DISCLAIMER

Neither WPD, nor any person acting on its behalf, makes any warranty, express or implied, with respect to the use of any information, method or process disclosed in this document or that such use may not infringe the rights of any third party or assumes any liabilities with respect to the use of, or for damage resulting in any way from the use of, any information, apparatus, method or process disclosed in the document.

© Western Power Distribution 2020

No part of this publication may be reproduced, stored in a retrieval system or transmitted, in any form or by any means electronic, mechanical, photocopying, recording or otherwise, without the written permission of the Future Networks Manager, Western Power Distribution, Herald Way, Pegasus Business Park, Castle Donington. DE74 2TU. Telephone +44 (0) 1332 827446. E-mail wpdinnovation@westernpower.co.uk

Glossary

Abbreviation	Term
BSP	Bulk Supply Point
CB	Circuit Breaker
DP	DigSILENT PowerFactory
EMT	Electromagnetic transient (simulations)
MS	MATLAB/Simulink
PI	Proportional integral
PQ	Power quality
PLL	Phase locked-loop
PWM	Pulse-width modulation
Rms	Root mean square
SCADA	Supervisory control and data acquisition
THD	Total harmonic distortion
WPD	Western Power Distribution

Executive Summary

The work reported here describes the creation and validation of a modelling environment that is ultimately intended to support the development and testing of harmonic mitigation algorithms to be overlaid on existing (modelled) PV inverters.

The chosen modelling environment for this work is MATLAB/Simulink. This tool provides component libraries and analysis tools for fundamental frequency modelling and time-series simulation of electrical power systems and also facilitates harmonic time-series modelling and analysis. Additionally, MATLAB/Simulink is fully integrated with the real-time simulation software RT-LAB, thus allowing hardware-in-the-loop analysis in Work Package 4.

Establishing a modelling environment has been undertaken in a number of steps that fall into two key stages of development. Stage One was the development of a network model within MATLAB/Simulink, based on a WPD provided model. Stage Two was demonstration that the MATLAB/Simulink model can appropriately perform electromagnetic transient (EMT) simulation and analysis of the modelled network. This EMT simulation covered a period of three weeks, and included fundamental and harmonic components. Validation was carried out within each development stage.

Stage One validation was aimed at demonstrating that the developed network model effectively represented the topology and electrical characteristics (such as impedances) of the actual network. This was achieved through a series of six power flow studies plus a frequency sweep assessment. Results from the developed model were compared to a reference WPD-provided model. Good agreement has been found between the results of these tests from the two models, and where appropriate to SCADA; it is concluded that the MATLAB/Simulink model provides a satisfactory representation of the system under study.

Stage Two validation was aimed at demonstrating EMT simulation and realism of simulation results over time. Initially this focused on fundamental frequency behaviour; where modelled active and reactive power flows across the system boundary were compared to SCADA and found to be realistic. Modelled voltages from the simulation (which excluded tap changer control) were also investigated and found to be satisfactory. Modelled harmonic behaviour was assessed by comparison to measurement data from temporarily installed power quality monitors. Assessment included current and voltage harmonics, considering overall levels and variation between phases for the 5th, 7th, 11th and 13th orders. It is concluded that the developed model EMT simulations provide a realistic representation of the fundamental and harmonic behaviour of the actual network over a three-week time series.

Overall, it is concluded that the established modelling environment provides a realistic representation of the actual network for the purpose of developing and testing harmonic mitigation algorithms to be overlaid on already included PV inverter models.

The following report sets out the details of what is summarised above. In addition, an overview of the validation work is contained in a set of slides included here.


WP1 - Summary of
modelling key point

1 Introduction

The aim of Work Package 1 is to:

- Complete a literature review on approaches to the use of power converters to mitigate harmonics; and
- Establish an appropriate modelling environment in which algorithms added to existing solar inverters can be developed and tested.

The Literature Review was separately reported in January 2020, and provided a detailed summary of previous research and development completed on the subject. This review provided appropriate material for the project on how power converters may provide harmonic compensation as an additional, or “ancillary service”. The Executive Summary from the Literature Review is shown in Appendix A, the complete review is available separately.

The focus of work reported here is therefore the development of an appropriate modelling environment.

The modelling environment chosen for this work is MATLAB/Simulink [1]. This tool provides component libraries and analysis tools for modelling and simulating electrical power systems. Harmonic analysis, calculation of total harmonic distortion (THD), load flow, and other electrical power system analyses are automated. Additionally, MATLAB/Simulink is fully integrated with the real-time simulation software RT-LAB [2], thus allowing hardware-in-the-loop analysis in Work Package 4.

Establishing a modelling environment has been undertaken in a number of steps that broadly fall into two key stages of development:

1. Development of a static network model within MATLAB/Simulink, based on a WPD provided reference network model, with demonstration that the model effectively represents the topology and impedances of the actual network through a series of six power flow and frequency sweep studies
2. Demonstration that the MATLAB/SIMULINK model can appropriately perform EMT analysis of the modelled network over a period of time (approximately one operational month). This simulation is conducted using:
 - a. The already developed static model of the network (topology and impedances etc.);
 - b. Dynamic Load models developed from WPD provided half hourly average SCADA data;
 - c. A combination of PV inverter models and PV dynamic models used to represent the three 33 kV connected PV farms. The PV dynamic model data is obtained from the 10 sec power quality measurements provided by WPD.

Construction and validation of the MATLAB/Simulink model relies on the information and data provided by WPD:

- A DigSILENT PowerFactory model of Tiverton Network and surrounding power system;
- Half hourly SCADA data collected across the system between 01/11/2018 and 01/11/2019.
- Harmonic measurements collected between 01/10/2019 and 21/10/2019. The harmonic measurements took place at Tiverton 33 kV busbar (voltage measurement only), and at the PV farms 33 kV busbars (both voltage and current measurements).

The single-line diagram of the Tiverton Network is shown in Appendix B. A more detailed description of the data provided by WPD is given in Appendix C.

2 Construction of underlying MATLAB/Simulink model

The first step of model development consisted in creating a MATLAB/Simulink representation of the Tiverton Network based on a DlgSILENT PowerFactory model provided by WPD¹.

The MATLAB/Simulink model was validated by conducting a frequency sweep for various network configurations and by undertaking power flow studies using six power flow cases. The results from the frequency sweeps and the load flow analysis were compared to those obtained from DlgSILENT PowerFactory. The results of the power flow analysis were also compared against the SCADA data provided by WPD.

The objective of this analysis was to confirm that the underlying network topology and the network impedance created in MATLAB/Simulink can be relied upon. The success criteria were:

- Agreement of frequency sweep between MATLAB/Simulink and DlgSILENT PowerFactory; and
- Agreement of the load flow results between MATLAB/Simulink, DlgSILENT PowerFactory and SCADA data in terms of voltages at load busses and power flow at the system boundary.

The outline steps undertaken to develop the MATLAB/Simulink model and its validation using power flow studies are described in the next sections.

2.1 Model development

A single-line diagram of the Tiverton Network is shown in Figure 1. The network is supplied by a 132 kV bus (EXET1) and by two parallel-connected 67.5 MVA transformers. Five feeders are connected to the main 33 kV busbar (TIVE3). Three PV farms connected to the 33 kV systems are included in the model: Ayshford (AYSH3), Cullompton (CMPV3) and Stoneshill (STFA3).

Three circuits can be identified in the single line diagram, identified as follows:

- Loop 1, identified by the circuit breakers 1L5 and 4L5
- Loop 2, identified by the circuit breakers 2L5 and 3L5
- Radial feeder, identified by the circuit breaker 6L5.

These three circuits will be referred to in the report.

¹ The DlgSILENT PowerFactory version used in this project is 2019 SP4, build 19.0.6. The MATLAB version is 9.7.0 (R2019b), Update 5; Simulink version is 10.0 (R2019b).

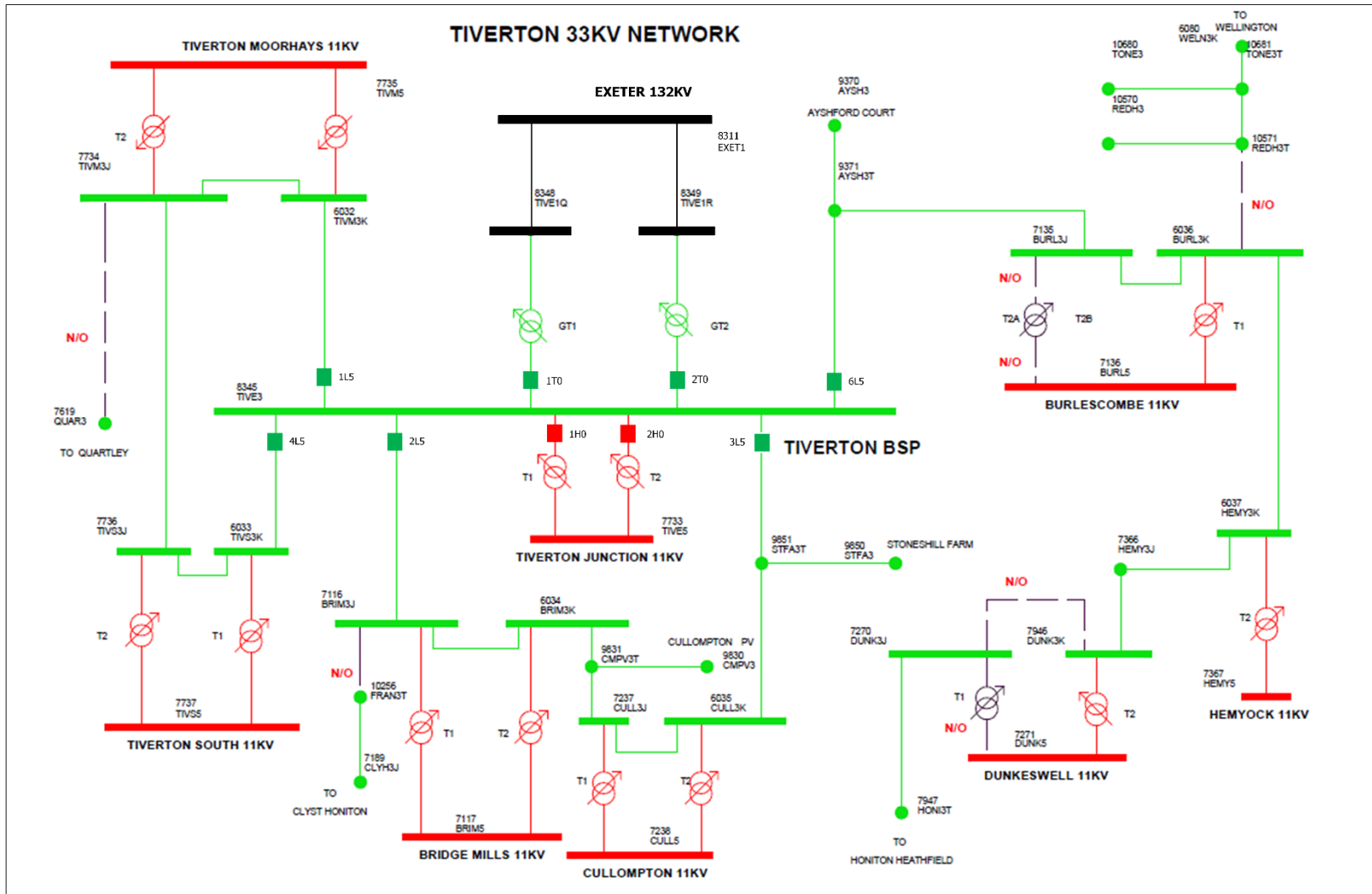


Figure 1: Single-Line Diagram of the Tiverton Network. Only the circuit breakers connected to Tiverton BSP are shown to maintain the figure readability.

A snapshot of the MATLAB/Simulink model is shown in Figure 2. The main features of this model are:

- The transformer and line models employ component models that are very similar to the those used in DigSILENT PowerFactory.
- The 11 kV loads use as input values the active and reactive power readings from the SCADA data.
- The 33 kV PV farm models use as input values the readings from the power quality monitors.
- 132/33 kV and 33/11kV transformers are modelled with fixed winding ratios
- The 132 kV system fundamental impedance is modelled from the short circuit current included in DigSILENT PowerFactory. The harmonic impedance is modelled as a cascade of parallel-connected branches.
- The upstream distortion is modelled by assuming that it contributed to 10% harmonic distortion at TIVE3.

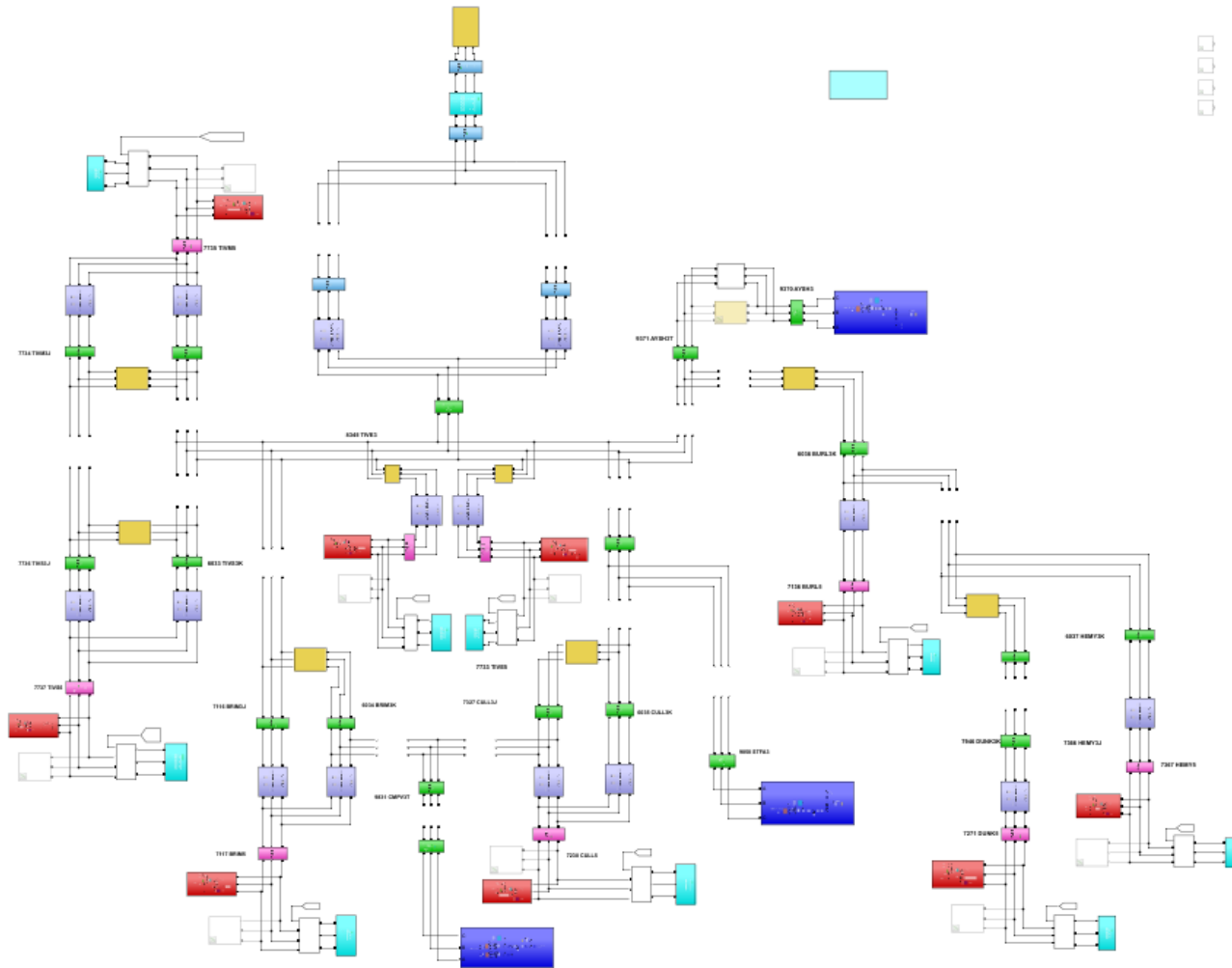


Figure 2: Overview of the MATLAB/Simulink model.

2.2 Definition of the snapshot power flow cases

The power flow solution calculates the magnitude and phase angle of the voltage at all buses in the network and the values of real power, reactive power and losses throughout the system, when the type and status of the generators and loads are given [4]. The solution is accomplished by solving non-linear power flow equations. Various iterative mathematical methods have been developed to calculate power flow solutions. Power flow studies are used by utilities for planning, operation, economic scheduling, and studies such as stability and contingency analysis.

In this project, different power flow cases (snapshots) are defined featuring varying operating conditions. Analysis was undertaken to ensure that both the DigSILENT model and the MATLAB/Simulink models converged to the same solutions, therefore confirming that the same underlying network topology and parameter values were being used.

The SCADA data provided by WPD allowed the identification of six power flow cases. For each case below, a short description is provided, together with an indication of the date and time of the case, and the active power exchange at the system boundary (EXET1, shown in Figure 1):

Case 1: Winter maximum generation and minimum demand
24/02/2019, 13:30: P=3.13 MW at EXET1

Case 2: Winter minimum generation and maximum demand
31/01/2019, 18:00: P= 50.96 MW at EXET1

Case 3: Summer maximum generation and minimum demand
25/08/2019, 13:30: P=-8.2 MW at EXET1 (reverse power flow)

Case 4: Summer minimum generation and maximum demand
12/06/2019, 8:30: P=38.72 MW at EXET1

Case 5: Contingency case 1
26/06/2019, 10:00: P=31.29 MW at EXET1
This contingency case is obtained directly from the SCADA data, as it shows a case where Circuit Breaker (CB) 2L5 is opened. The location of this breaker is shown in Figure 1.

Case 6: Contingency case 2
24/01/2019, 18:30: P= 48.74 MW at EXET1
This contingency case is built in the simulation environment from the data provided. Initially, the loads are set up according to the date and time above in the simulation environment, identified in the result tables as Case 6A. The circuit breaker CB 3L5 is tripped to derive a contingency identified in the result tables as Case 6B. The location of this breaker is shown in Figure 1. This case is investigated to explore the load unbalance that appears to exist between breakers CB 2L5 and CB 3L5.

The six cases described above were built in both simulation environments – i.e. DlgSILENT Power Factory and MATLAB/Simulink. MATLAB scripts were developed to define the loads for each case, using the same underlying network model.

2.3 Comparison of frequency sweep results

The impedance of any electrical systems is a function of the frequency and it depends on the resistance, inductance and capacitance of individual components and on their connection. For the Tiverton Network, the harmonic impedance is the result of the interaction between the network components and with the upstream network.

Appendix D provides a comprehensive description of the extensive work undertaken to arrive at a MATLAB/Simulink model that matched the frequency response of WPD's DlgSILENT PowerFactory model.

The frequency scans for the complete network are shown in Figure 3, - Figure 6:

- Figure 3 shows the total impedance seen at EXET1, i.e. the high-voltage side of the substation transformers connecting the Tiverton Network to the upstream network;
- Figure 4 shows the total impedance seen at TIVE3, i.e. the low-voltage side of the substation transformers.
- Figure 5 shows a zoomed in version of Figure 3 in the region below the 50th harmonic. This graph is shown because TIVE3 is the main busbar of the Tiverton Network and it is critical to assess that the frequency response in the low frequency range matches closely the DlgSILENT PowerFactory model.
- Figure 6 shows the phase angle associated to the impedances of Figure 5.

These results indicate that the two models match in term of resonant frequencies, impedance amplitude and impedance phase angle across a broad frequency range (up to the 200th order).

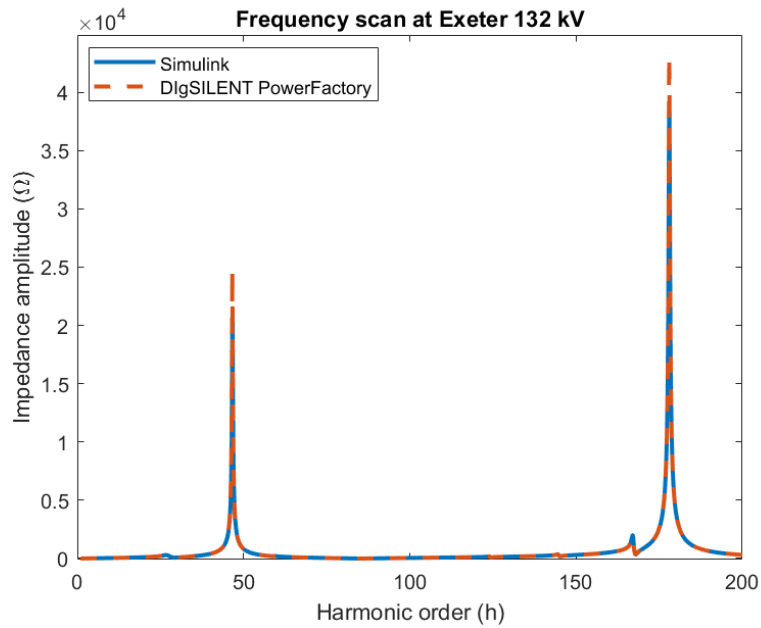


Figure 3: Comparison between Simulink and DlgSILENT PowerFactory – EXET1 bus.

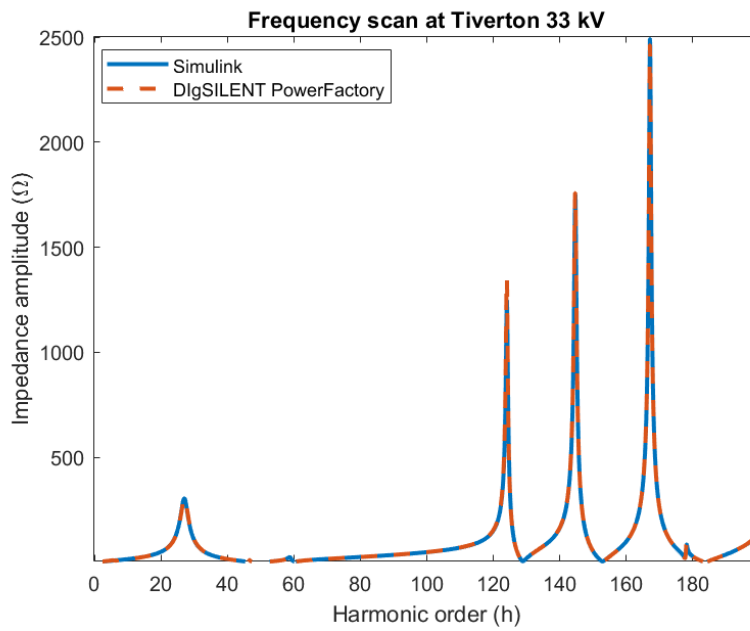


Figure 4: Comparison between Simulink and DlgSILENT PowerFactory for the complete network – TIVE3 bus.

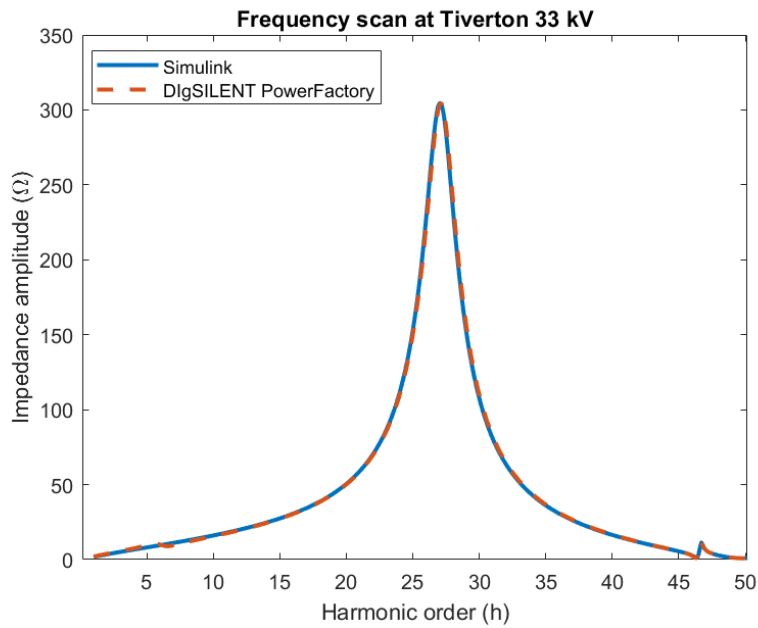


Figure 5: Comparison between Simulink and DlgSILENT PowerFactory for the complete network

2.3.1.1 – TIVE3 bus, zoomed in version.

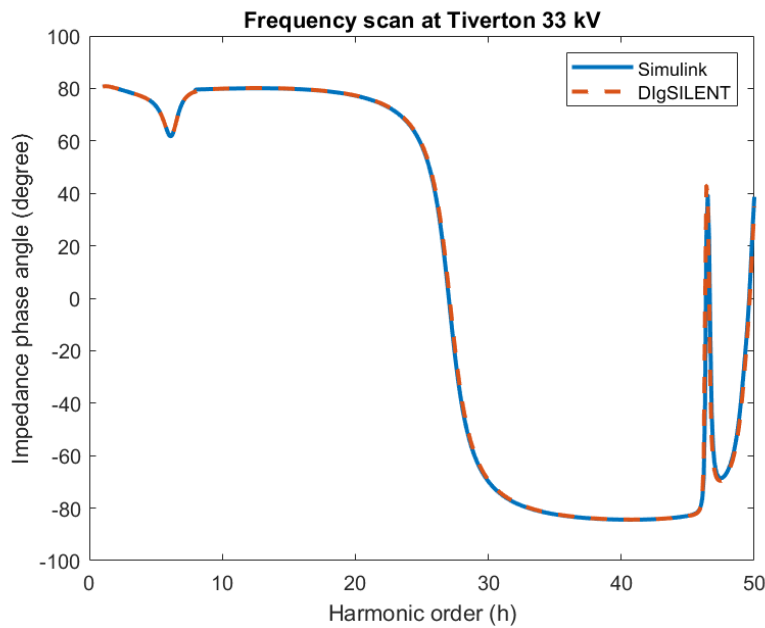


Figure 6: Comparison between Simulink and DlgSILENT PowerFactory for the complete network – TIVE3 bus, phase angle of the impedance for the zoomed in version.

2.4 Comparison of the results for power flow analysis

Two key sets of results will be compared in this section to demonstrate the reliability of the MATLAB model:

1. Active and reactive power (P and Q) at the system boundary (EXET1 in Figure 1). These results are shown in Table 1.
2. Voltage at the 11 kV busses and voltages at the 33 kV busses where the PV farms are connected. These results are shown in Table 2 and Table 3.

The bus numbers indicated in the tables correspond to the ones shown in the Single Line Diagram shown in Figure 1

Table 1: Comparison of the active and reactive power values (P and Q) at the system boundary (EXET1).

Case	DIgSILENT PowerFactory Model		MATLAB/Simulink Model		SCADA data	
	P (MW)	Q (Mvar)	P (MW)	Q (Mvar)	P (MW)	Q (Mvar)
1	3.06	3.45	3.07	3.48	3.13	3.79
2	51.16	7.77	51.19	7.95	50.96	6.96
3	-8.27	4.68	-8.22	4.69	-8.21	4.02
4	39.00	8.95	39.08	9.53	38.72	9.27
5	31.68	7.81	31.79	8.30	31.29	8.43
6A	48.57	6.20	48.92	6.48	48.74	6.92
6B	49.12	5.69	49.15	5.84	NA	NA

Table 1 shows P and Q values at the system boundary for the six power flow cases investigated, as calculated by the two models, and as recorded by SCADA.

From these results it can be seen that:

1. The active power values obtained from DIgSILENT PowerFactory and MATLAB/Simulink are very similar, indicating a good agreement between the two modelling environments. Modelled active power values also compared well to recorded SCADA values.
2. The reactive power values obtained from DIgSILENT PowerFactory and MATLAB/Simulink are also similar, indicating a good agreement between the two modelling environments. Modelled Q values are also comparable to recorded SCADA values.

Moving on to consider the voltage comparison between the two models, Table 2 shows voltages throughout the system for Case 1 – Case 3, while Table 3 shows the results for Cases 4 – 6. Both tables show results as calculated by the two models, and as recorded by SCADA.

From these results it can be seen that:

1. The voltage levels throughout the system show a high level of agreement between the two models.
2. Differences do exist between the two models, and SCADA values. This is to be expected as the SCADA values reflect the action of tap changer controllers, where the models are operated with fixed transformer winding ratios.

Table 2: Comparison of the voltages at the 11 kV busses and at the 33 kV buses.

Bus	Text Ref	Rated Voltage	Case 1			Case 2			Case 3		
			SCD ² data	DP ³ Model	ML ⁴ Model	SCD data	DP Model	ML Model	SCD data	DP Model	ML Model
9830	CMPV3T (PV)	33 kV	1.003	1.014	1.014	0.964	0.985	0.984	0.992	1.020	1.022
9850	STFA3 (PV)	33 kV	1.006	1.016	1.016	0.976	0.992	0.991	0.992	1.021	1.021
9370	AYSH3 (PV)	33 kV	1.013	1.020	1.019	0.975	0.993	0.993	0.999	1.025	1.025
7136	BURL5	11 kV	1.005	1.020	1.019	1.007	0.983	0.983	1.001	1.026	1.027
7367	HEMY5	11 kV	0.995	1.028	1.029	0.995	1.008	1.008	1.012	1.040	1.041
7271	DUNK5	11 kV	1.007	1.023	1.024	0.991	0.975	0.975	0.998	1.030	1.031
7733	TIVE5-T1	11 kV	0.999	1.016	1.016	0.995	0.985	0.985	0.998	1.021	1.022
7733	TIVE5-T2	11 kV	0.999	1.017	1.017	0.995	0.988	0.988	0.998	1.021	1.022
7735	TIVM5	11 kV	0.992	1.009	1.009	1.006	0.979	0.979	0.988	1.014	1.014
7737	TIVS5	11 kV	1.004	1.008	1.008	1.001	0.980	0.979	0.996	1.011	1.011
7117	BRIM5	11 kV	1.001	1.004	1.004	0.986	0.974	0.974	0.999	1.018	1.018
7238	CULL5	11 kV	1.002	1.009	1.009	0.990	0.984	0.983	0.999	1.014	1.014

² SCADA Data

³ DigSILENT PowerFactory

⁴ MATLAB

Harmonic Mitigation Work Package One – Model Development

Table 3: Comparison of the voltages at the 11 kV busses and at the 33 kV busses.

Bus	Text Ref	Voltage	Case 4			Case 5			Case 6A ⁵			Case 6B	
			SCD data	DP Model	ML Model	SCD data	DP Model	ML Model	SCD data	DP Model	ML Model	DP Model	ML Model
9830	CMPV3T(PV)	33 kV	0.984	0.996	0.996	0.979	0.989	0.989	0.968	0.995	0.995	0.984	0.986
9850	STFA3(PV)	33 kV	0.993	1.001	1.001	0.990	1.000	1.000	0.979	1.001	1.001	0.993	0.996
9370	AYSH3(PV)	33 kV	0.988	1.000	1.000	0.992	1.002	1.002	0.978	0.995	0.994	0.988	0.990
7136	BURL5	11 kV	1.001	0.998	0.988	0.993	0.995	0.995	0.998	0.983	0.983	1.001	1.003
7367	HEMY5	11 kV	0.999	1.014	1.014	0.992	1.006	1.006	0.994	0.955	0.955	0.999	1.001
7271	DUNK5	11 kV	0.987	0.988	0.988	0.996	0.992	0.992	0.990	0.974	0.974	0.987	0.988
7733	TIVE5-T1	11 kV	0.995	0.993	0.993	0.995	0.999	0.999	0.990	0.991	0.991	0.995	0.993
7733	TIVE5-T2	11 kV	0.995	0.993	0.993	0.932	0.999	0.999	0.990	0.991	0.991	0.995	0.993
7735	TIVM5	11 kV	0.990	0.990	0.990	0.989	0.994	0.994	0.998	0.997	0.997	0.990	0.990
7737	TIVS5	11 kV	0.990	0.980	0.980	0.987	0.984	0.984	0.985	0.999	0.999	0.990	0.988
7117	BRIM5	11 kV	0.999	0.988	0.980	0.988	0.975	0.975	0.991	1.000	1.000	0.999	0.998
7238	CULL5	11 kV	0.988	0.990	0.981	0.990	0.985	0.983	1.000	0.992	0.992	0.988	0.990

⁵ Case 6A is the original case obtained from the SCADA data, Case 6B is built in simulation environment only and therefore SCADA data are not available.

2.5 Conclusions on underlying MATLAB/Simulink Model

The topology and component parameters contained in the developed MATLAB/Simulink model have been validated by undertaking a series of power flow studies and frequency response checks and comparing the results with those from a WPD DigSILENT PowerFactory model, and where appropriate to SCADA data.

Good agreement has been found between the results for these tests from the two models and where appropriate to SCADA, and it is concluded that the MATLAB/Simulink model provides a satisfactory representation of the system under study.

3 MATLAB/Simulink EMT simulations

Having established a satisfactory underlying network model within MATLAB/Simulink, it was necessary to demonstrate that the environment could perform EMT simulations that reasonably model fundamental frequency behaviour the actual system.

EMT models are developed using continuous-time differential equations that describe the instantaneous behaviour of the system. Digital computers cannot solve continuous-time equations; therefore, they are approximated by a series of solutions at discrete time-steps [5]. The underlying differential equations become more complex in systems with power electronic converters, since the state of the switches change with each time-step forcing a recalculation of the admittance matrix. Such systems also require very short time-steps comparable with the converter switching frequency.

For this project, the solver makes use of the trapezoidal rule of integration and the backward differentiation formula [6]. The simulation time step is 8 μ s and is determined by the length of the shortest distributed line in the model. This time step is comparable to the one required for running the inverter model (including the future harmonic mitigation algorithm), and therefore the use of distributed parameters lines do not pose an additional overly onerous requirement on the time step.

While the same underlying network topology developed for the power flow analysis was retained, dynamic models for both the 11 kV loads and the 33 kV connected PV farms are introduced for the EMT analysis. The dynamic models differ from the ones used for the power flow studies – therefore, it is necessary to select the correct load model (i.e. static or dynamic) depending on the analysis being carried out. This can be easily achieved in Simulink: with the ‘comment out’ option, the user can exclude from the simulation the load models that are not required.

Load values and PV generation values were derived from the data supplied by WPD, as described in the following subsections. The period considered for the EMT analysis is October 2019, this being the period for which temporarily installed power quality monitoring equipment was operating for, specifically for the project.

The simulation time is an acceleration of real time: in other words, 0.1 s of simulation time represents 30 min of real time and 4.8 s simulation time represents 1 day in real time. This is done because of the computational effort required to solve the network in time domain: as it will be seen later on, the time-domain simulation generates large amount of data and therefore only a few seconds simulation can be run with a standard PC.

The next sections will describe the dynamic load model and the dynamic PV farm model, and then validate them against the data provided by WPD.

The success criteria will consist in the MATLAB/Simulink model being able to closely represent time-varying operating conditions described by the SCADA data. These conditions include: voltage levels across the system and power exchange at the system boundary (EXET1), at the load busses and at the PV farms.

3.1 Model Development – fundamental sources

This section describes key details of how the dynamic load and generation models have been built, plus the requirement for the model to run with a short initialisation period.

3.1.1 Dynamic load model (11 kV busses)

The Tiverton Network includes eight 11 kV busbars and the load on each one of them is represented by means of a load time series. The time series for each load is derived from the half-hourly SCADA data from the period 1-21/10/2019.

Because the source 11 kV load data only changes every 30 minutes, values for each simulation step (8 μ s) are linearly interpolated from the half-hourly SCADA data, providing 12,500 load steps to cover 0.1 s of simulation time.

For six of the eight busbars, the SCADA data includes active and reactive power values. For the TIVE5 and BURL5 busbars, the SCADA data is only available as apparent power. Therefore at these nodes, further processing is required to calculate active and reactive power.

Figure 7 shows the dynamic simulation model used to represent the load connected at the TIVS5 busbar, used as an example of any of the eight 11kV busses. The 'dynamic load' block is a built-in component in MATLAB, and it is highlighted in blue. The block is connected to terminals 'A', 'B' and 'C' of the TIVS5 busbar (to the right of the figure). Each terminal represents one phase of the three-phase systems.

The inputs to the block are active and reactive power values (lower part of the figure). These values are imported from an Excel workbook, containing the SCADA readings organised in a way to make them readable from Simulink. More specifically, a column containing the simulation time was created in an excel spreadsheet, containing time readings with an increment of 0.1 s. Corresponding P and Q values were associated to the time stamp for each bus. The excel data is imported in Simulink using the 'From Spreadsheet' block, highlighted in yellow in Figure 7. The readings are then interpolated by the solver. A scaling factor equal to 10^6 is applied because the SCADA readings are provided in MW and Mvar, while the 'Dynamic Load' block requires input in W and var.

The dynamic block adjusts the load parameters to match active and reactive power demand at each simulation point.

A shunt resistance is added in parallel to the dynamic load to allow the numerical solution to converge. This resistance is required because the dynamic load model includes various algorithms to convert the power values to corresponding electrical components, and upon initialisation of the model these electrical components are modelled as open circuits. Therefore, the shunt resistors provide a reference to the ground for the numerical solution to converge. The value of the shunt resistor varies between loads, but it is in the order of 10^4 - $10^6 \Omega$ to avoid draining large currents from the network.

The model includes one monitoring block (highlighted in green) used to visualise both instantaneous and rms voltage, current, active and reactive power profile at each load, and to compare the results with the SCADA data.

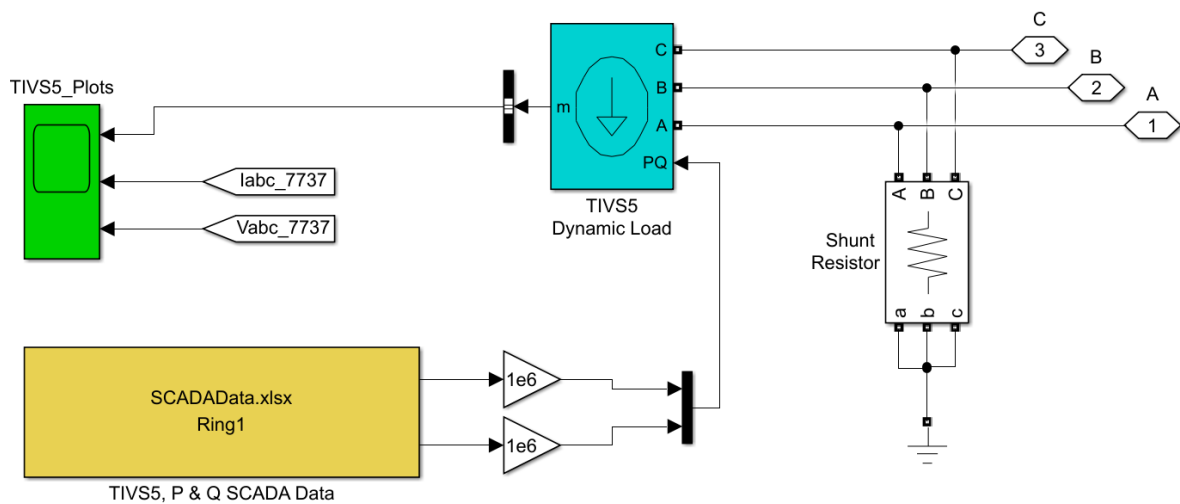


Figure 7: Dynamic load model For TIV5S.

As previously noted, for TIVE5 and BURL5 busbars only the apparent power SCADA data was available. Therefore, for these two busses, active and reactive power were calculated using additional information within the SCADA data. The process adopted for BURL5 load is explained in detail by referring to Figure 8. In this figure, P and Q are available at all points, except for BURL5, where only apparent power (MVA) is provided.

Therefore, active and reactive power at BURL5 are calculated as follows:

$$P_{BURL5} = P_{6L5} - P_{HEMY5} - P_{DUNK5} - P_{AYSH3} \quad (1)$$

$$Q_{BURL5} = Q_{6L5} - Q_{HEMY5} - Q_{DUNK5} - Q_{AYSH3} \quad (2)$$

A similar process is applied for TIVE5 loads, where the formulae are:

$$P_{TIVE5} = P_{GT1} + P_{GT2} - P_{1L5} - P_{2L5} - P_{3L5} - P_{4L5} - P_{6L5} \quad (3)$$

$$Q_{TIVE5} = Q_{GT1} + Q_{GT2} - Q_{1L5} - Q_{2L5} - Q_{3L5} - Q_{4L5} - Q_{6L5} \quad (4)$$

The approach above resulted in generating a new dataset including P and Q values for the two busses. These values were added to the Excel workbook used as input to the MATLAB/Simulink model.

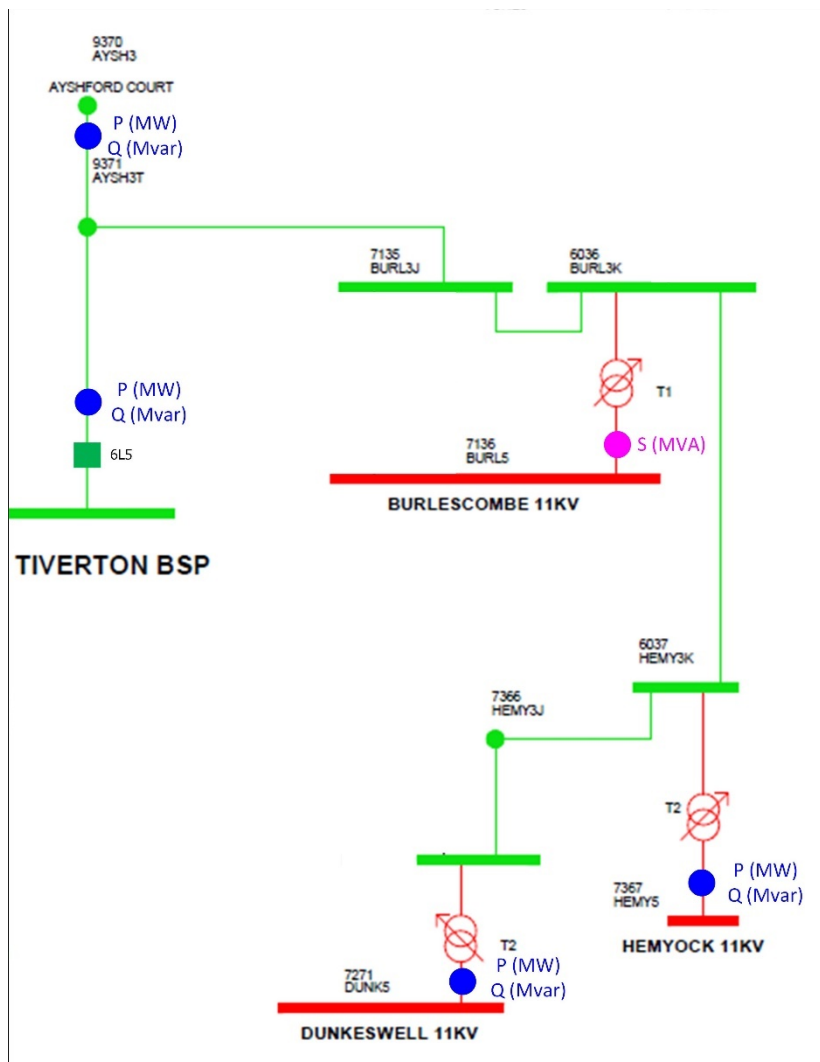


Figure 8: Power measurements available at the feeder including BURL5 busbar.

3.1.2 PV farm model introduction

Similarly to the 11 kV busbars, the three PV farm nodes require a set of time-varying power generation values (a generation time series), that are fed into the simulation.

Keeping in mind that Work Package 2 will require the development of an active filter algorithm for the PV inverters, it is important to develop an underlying inverter model that includes the control algorithms in details. As described in Appendix B, the PV farms connected to the Tiverton Network include a large number of inverters. When such a large system is considered, it is beyond the agreed scope of this work to model each unit in detail.

Therefore, each PV farm representation in MATLAB/Simulink consists of a composite model, shown in Figure 9. This model includes:

1. One detailed inverter model, sized to be representative of the inverters installed at the site (upper element of Figure 9).
2. A dynamic generation model to model the balance of generation capacity at the site. This element consists of two parts:
 - a. A fundamental frequency power generation model (middle element of Figure 9); and
 - b. A harmonic generation model (lower element of Figure 9).

The detailed inverter model and the fundamental frequency generation model are described in Section 3.1.3 and Section 3.1.4, respectively. The harmonic generation model will be described in Section 3.2.2.

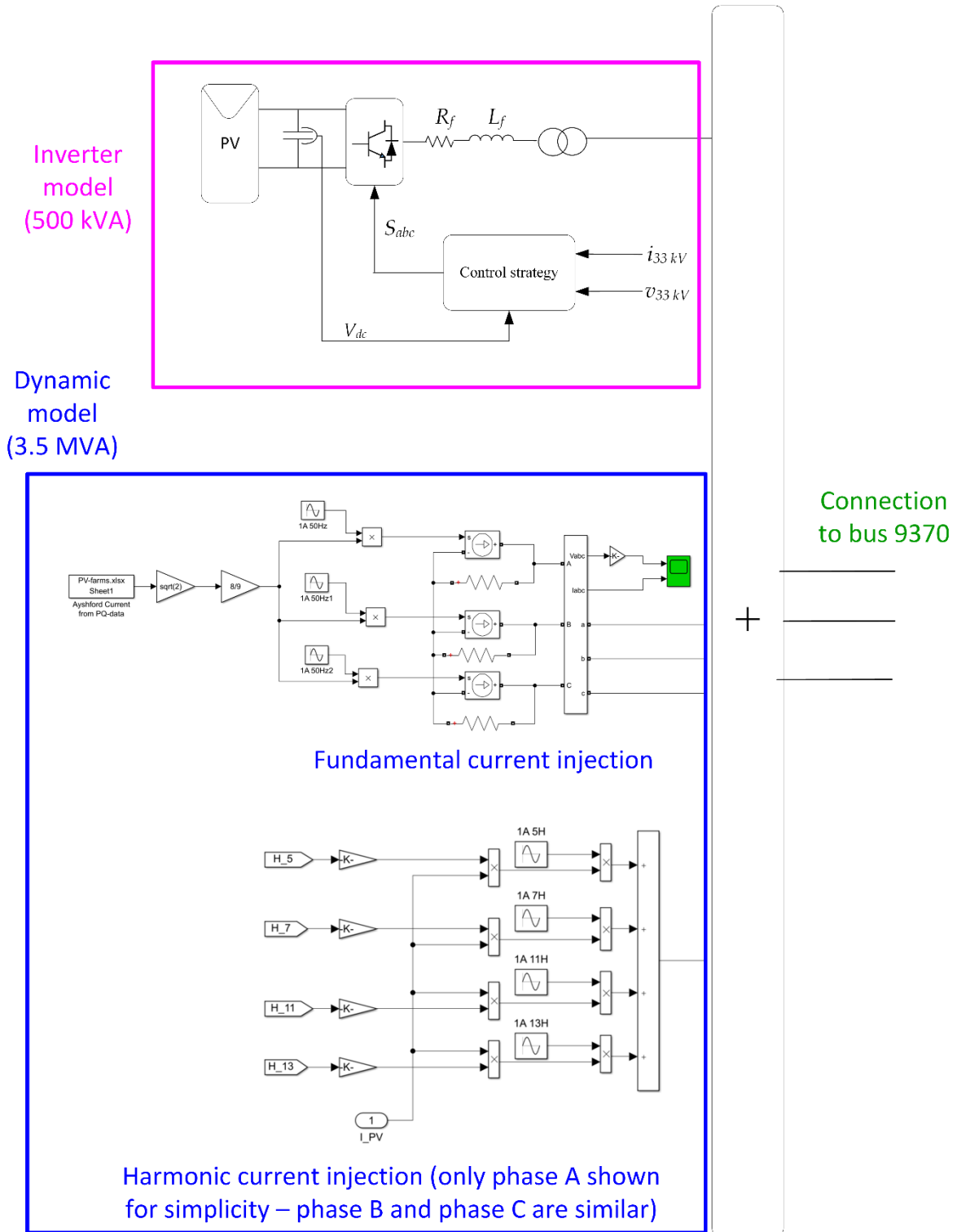


Figure 9: Overall representation of the Ayshford PV farm model in MATLAB/Simulink: the first part of the drawing shows the inverter model, and the second part the dynamic model (including both fundamental current and harmonic injection).

This composite PV node model provides both fundamental and harmonic content.

Load time-series for the three PV farm nodes are derived from the 10 second power quality data provided by WPD for October 2019. Due to the different sampling time of the PQ data and of the SCADA data, appropriate time scaling needs to be applied, as explained in Appendix C.

In the next two sections the underlying element components of the PV farm model are described.

3.1.3 PV Inverter model and associated controls

An overview of the inverter model and associated controls deployed for the Ayshford PV farm is shown in Figure 10. A conventional three-phase two-level converter is used, with a control algorithm developed in the equivalent dq domain⁶ [8]. The PV panel model, the inverter output filter and the step-up transformer are also shown.

The control algorithm includes the following elements:

- A Phase-Lock Loop (PLL) calculates the system angular frequency ωt from the voltage measurements. The angular frequency is used to convert the voltage and currents measurements from the abc domain into the dq reference frame by using the Park transformation [9].
- A dc voltage regulator is used to calculate the d -axis fundamental reference current i_{Sd}^* . The q -axis fundamental reference current i_{Sq}^* is obtained from the power factor setting. For this model, it is assumed that the power factor is unity and therefore the reference current is zero.
- The actual currents are subtracted from the reference currents to obtain the error terms that are fed to PI (proportional integral) controllers.
- The output of the PI controller is the reference output voltage that is used to generate the inverter switching signal. The inverter switching signal is generated by using a Pulse-Width-Modulation (PWM) algorithm.

The general inverter model shown in Figure 10 is configured for each PV farm with the aim to match as closely as possible the equipment installed on the field. Therefore, the following inverters have been included in the model for each PV farm:

- Ayshford: 1 x 500 kVA converter, 400 Vac (broadly representing inverters behind one step-up transformer)
- Stoneshill: 1 x 800 kVA converter, 380 Vac (broadly representing inverters behind one step-up transformer)
- Cullompton: 2 x 900 kVA converter, 400 Vac (broadly representing inverters behind one step-up transformer)

⁶ More details on the terminology related to the control systems can be found in the literature review report.

Two inverters have been included for Cullompton as the required output power from a single unit (1800 kVA) would result in high currents making the proposed converter control less stable in the modelled environment. Introducing higher numbers of inverters would slow the simulation significantly and make the model not manageable. The model built for Cullompton PV inverters is shown in Figure 10.

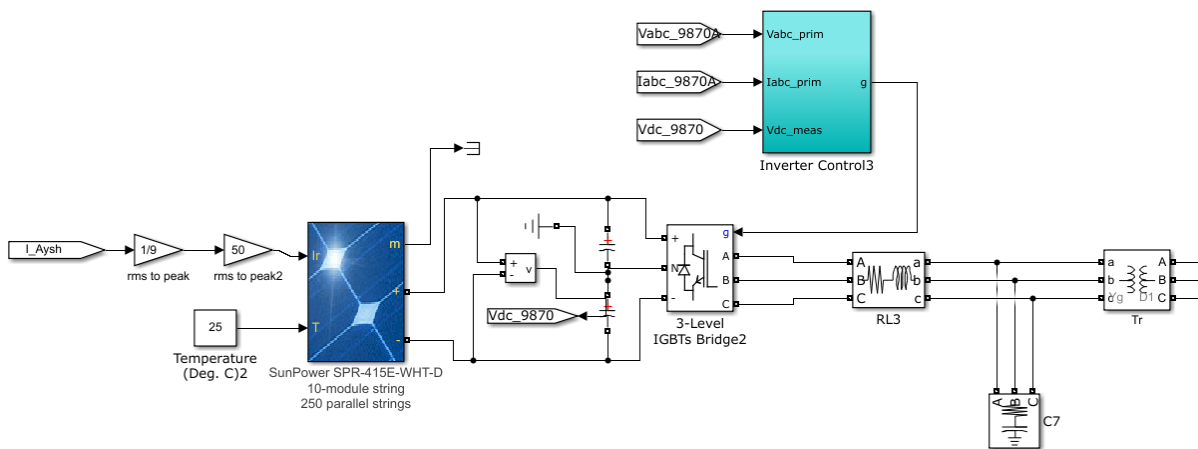


Figure 10: PV inverter configuration implemented in MATLAB/Simulink for Cullompton PV farm.

3.1.4 PV Farm dynamic model

The capacity at PV farms not described by the detailed inverter element of the model is modelled as controlled current sources as illustrated in Figure 11. The block to the left represents the source data – this block performs as described for the dynamic load model, with the difference that for the PV farm model, the source data consists of the high-resolution PQ data, rather than SCADA readings. The source data provides the current amplitude used to modulate the current generation from the PV farm. Because the data provided consist of rms current amplitudes, it is first multiplied by $\sqrt{2}$ to calculate the peak value. A second factor is introduced to adjust the power output of the dynamic model taking into account the contribution of the inverter. In the case of Ayshford PV farm, this factor is 8/9, because the total rating of the PV farm is 4.5 MW, and the inverter is contributing 500 kW. For the case of Stoneshill, the factor is 0.8, and for Cullompton PV farm it is 0.6. This signal is used to modulate the current sources in each phase to provide 50 Hz signals.

Each current source requires a large resistance connected in parallel to allow the model to be compiled. In any computer simulation, independent of the software tools used, it is not possible to connect multiple current sources to the same node because this results in a

simulation error. Therefore, a large resistance is connected in parallel to the current sources, similarly to what was done for the dynamic loads. The value of the resistance is $10^9 \Omega$.

The other blocks shown in Figure 4 consist of a monitoring block, and of the ports used to connect the model to the rest of the network (numbered as 1, 2 and 3 for phase A, phase B and phase C, respectively).

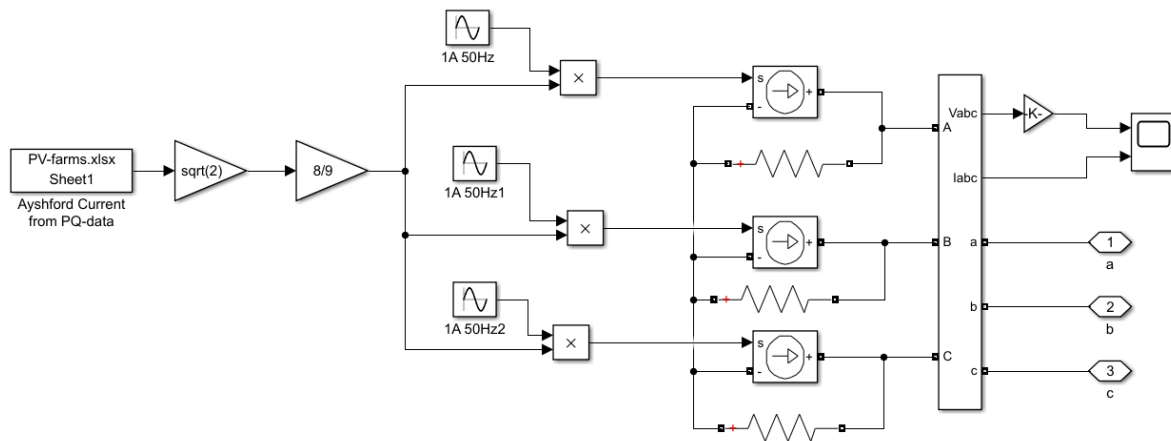


Figure 11: Dynamic model for Ayshford PV farm.

3.2 Model Development - harmonic sources

The sources of harmonic distortion in the system are: the loads connected at the 11 kV busses, the PV farms and distortion from the upstream 132 kV (and above) system.

Since harmonic measurements are provided only for a few points in the Tiverton Network, (voltage harmonics at the Tiverton 33 kV bus, plus voltage and current harmonics at the three PV sites), the remaining harmonic sources are unknown: upstream network distortion and harmonic distortion at the 11 kV busbars (where the loads are located).

From the power quality monitor data, it can be seen that the odd harmonics are the ones that contribute the most to harmonic distortion. The most relevant harmonics are the 5th, 7th, 11th, and 13th, characteristic harmonics associated with 6-pulse and 1-pulse converters. Therefore, the MATLAB/ Simulink harmonics injection model is developed to duplicate these harmonics.

The approach described below is adopted for modelling of each harmonic source⁷. More details for each source will be provided in the next subsections.

- **Dynamic load harmonic injection**
The simulated harmonic current amplitudes at a particular site are made proportional to the fundamental current measured at that same site. The current amplitude for each harmonic is scaled using a coefficient which is used for that harmonic across all sites. These coefficients are manually tuned such that the modelled voltage distortion at Tiverton 33 kV matches the measured voltage distortion, taking into account the contribution of the other harmonic sources (described in the next sections).
- **PV farms harmonic injection**
The harmonic current amplitudes at each site are modelled to match the harmonic measurements provided for each site. This is achieved by combining the harmonics generated by the inverter model and the harmonic generated by the dynamic model.
- **Upstream network distortion**
Upstream network distortion is modelled as a harmonic voltage source. Since no information on this quantity is available, upstream network distortion is modelled to provide an amplitude that contributes 10% of the measured voltage distortion at Tiverton 33 kV.
- **Loads – harmonic current phase angle**
The phase angle is kept to zero for all load harmonic current components injected by the dynamic load model.
- **PV farms – harmonic current phase angle**

⁷ Given the number of variables (harmonic currents amplitude and phase angles) and unknowns, various different approaches are possible to model harmonic distortion. The approach described below is one of the possibilities.

The phase angle of the PV farms is adjusted to match voltage distortion at Tiverton 33 kV. Adjusting the phase angle to be approximately 180 degrees for all PV farms provides results that match the measurements.

- Upstream network distortion – harmonic voltage phase angle
Voltage distortion is modelled with zero phase angle.

3.2.1 Dynamic harmonic Load model

The dynamic harmonic injection model is based on controlled current sources as shown in Figure 12. This figure shows the approach adopted for generation of Phase A harmonic current. The same approach is adopted for Phase B and Phase C. The fundamental current amplitude is calculated from voltage, active and reactive power data provided by the SCADA system (as discussed in Section 3.1.1). This current is indicated as 'Iabc_TM_rms' on the diagram. The current readings are multiplied by $\sqrt{2}$ to calculate the peak value, and the next step consists in scaling the magnitude of the individual harmonic current components. The harmonic scaling factors for the 5th, 7th, 11th, and 13th harmonic currents, are listed in Table 4. These factors are multiplied with the fundamental rms current value to generate the amplitude of each individual harmonic components. The output is then multiplied by a sinusoidal waveform with the appropriate harmonic frequency, i.e., 250 Hz for 5th harmonic.

The sum of the four harmonic component is used as a drive signal for a controllable current source, one for each phase. This method allows the magnitude of each individual harmonic to be easily tuned.

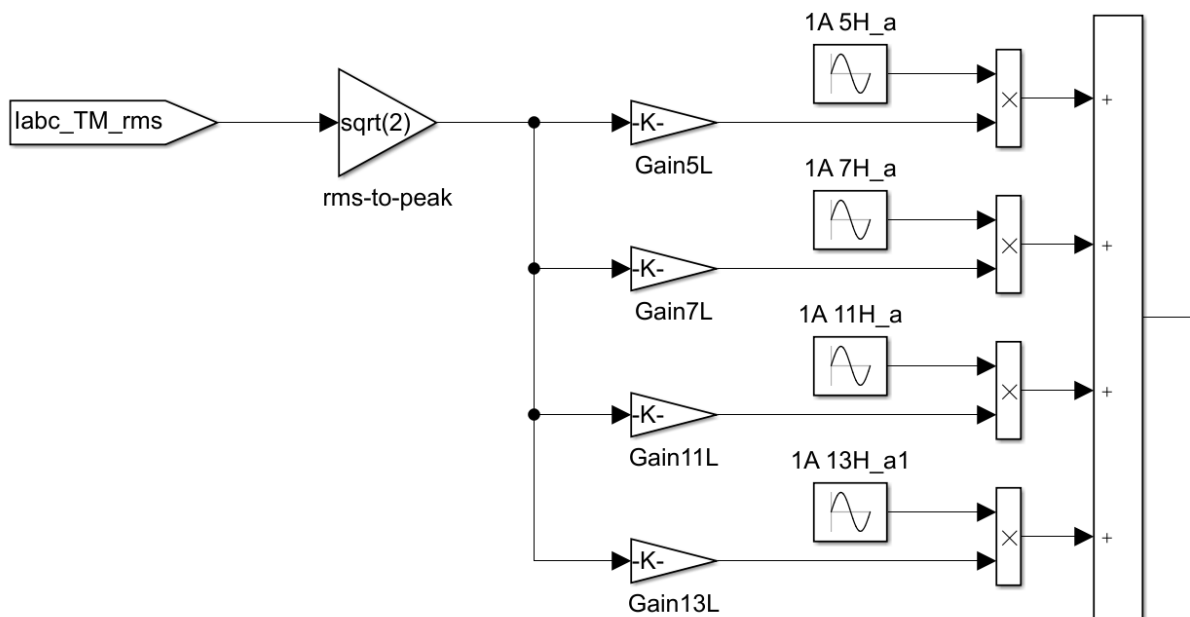


Figure 12: Harmonics injection load model for phase A currents. Phase B and Phase C employs the same approach, and they are not shown here.

Table 4: List of coefficients adopted for the dynamic harmonic load model, PV farm model and upstream network.

Harmonic scaling factor	Loads	Ayshford PV farm	Cullompton PV farm	Stoneshill PV farm	Upstream network
5 th	0.0253	0.0145	0.0203	0.01160	0.002755
7 th	0.0139	0.0055	0.00825	0.00275	0.000935
11 th	0.00178	0.00105	0.00105	0.00084	0.000105
13 th	0.00138	0.00150	0.0009	0.00090	0.000105

3.2.2 Dynamic PV farm harmonic model

Figure 13 shows the dynamic harmonic injection model for the PV farm. This model is identical to the one illustrated in the lower element of Figure 9.

The fundamental current amplitude read from the PQ monitors is multiplied by $\sqrt{2}$; the resulting signal, labelled 'I_PV' is then scaled by using appropriate coefficients. The coefficients used for each PV farm harmonic models are listed in Table 4. These coefficients are then multiplied by a sinusoidal waveform with the appropriate harmonic frequency, i.e., 250 Hz for 5th harmonic. The harmonic currents are then subtracted from the fundamental current. This effectively means that the phase angle for the harmonics is 180 degrees out of phase compared to the loads.

Both the tuning factors for the harmonics and the phase shift are based on manual trial and error method, and the approach described has been adopted because it results in the best match with the measured data.

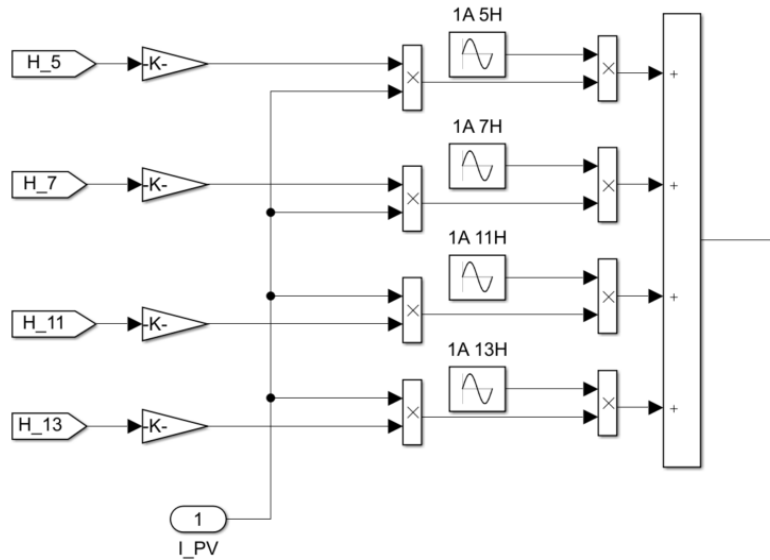


Figure 13: Harmonic current generation model for PV farm. Only Phase A harmonic current generation is shown Harmonic generation for Phase B and Phase C is carried out implementing the same model.

3.2.3 Upstream network distortion

The upstream network distortion is implemented as a harmonic voltage source connected in series with the equivalent system impedance as shown in Figure 14 (a), while Figure 14 (b) shows the connection of the blocks inside the 'harmonic voltage source' subsystem. In this model four harmonics, 5th, 7th, 11th, and 13th are generated for each phase.

The amplitude is determined by using a scaling factor for each harmonic frequency, similarly to the approach described for the load and PV farm harmonic dynamic models. The coefficients applied to the upstream network are shown in Table 4. The output of this model is used to drive a controlled voltage source.

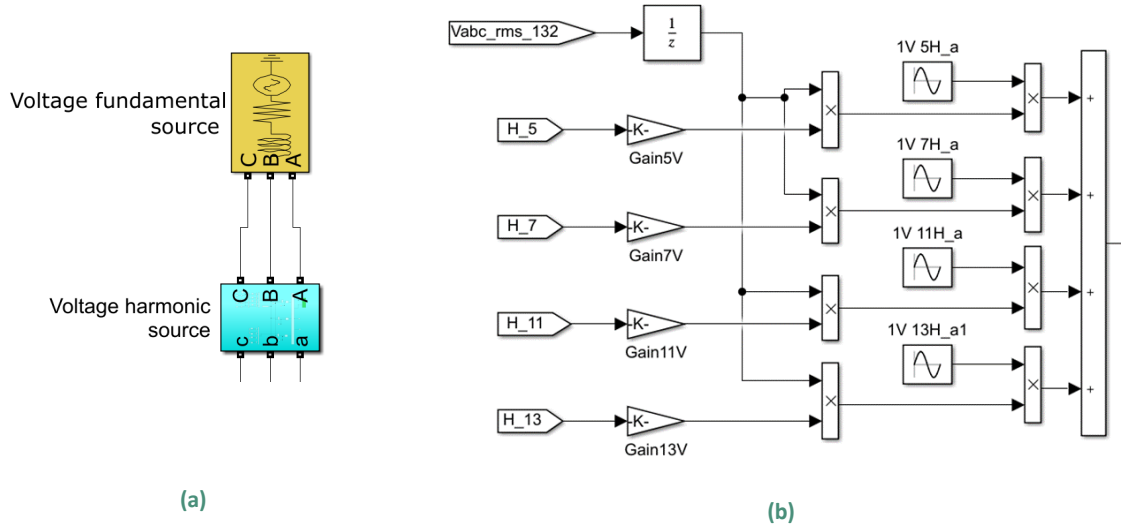


Figure 14: Controllable voltage source for background voltage harmonic injection:(a) connection of the fundamental and harmonic voltage sources, (b) harmonic voltage source model included in the 'harmonic voltage source' subsystem.

3.3 Model performance

The model needs to be correctly initialised before the dynamic load and PV generation data are applied. More specifically:

- In the first 0.39 seconds of the simulation, no load and no PV generation is applied; therefore, the system current is equal to zero. This is done to allow the model to initialise correctly.
- At the simulation start, due to the presence of the capacitances and inductances in the system, the voltage waveforms across the network show high-frequency oscillations corresponding to the system natural resonant frequencies. This is a normal behaviour and these initial transients extinguish after a few milliseconds.

Based on the above, the simulation is set up in a way that loads are applied starting at $t = 0.4$ s. The total simulation time is therefore 5.2 seconds for one day (48 data points, leading to 4.8 s in addition to an initialisation time of 0.4 s).

Table 5: Dynamic model performance overview.

Day/Time	Simulation time	Data generated	Note
Oct 1 st	20 minutes	~1 G	
Oct 1 st – Oct 8 th	~2 hours	~8 GB	
Oct 1 st – Oct 31 st	12 hours	NA	Model failed to save data

The main limitation on running the simulation for more than a week is caused by the size of the data generated. However, this limitation can be overcome by using the same network model and using as input varying files containing data readings, corresponding to the different weeks in October 2019.

3.4 Fundamental frequency results and validation.

In the following sections, example simulation results from the EMT simulations are presented, to show convergence and stability of the model. The complete set of results for 1 October 2019 are shown in Appendix E. The set of results for 1-21 October 2019 are shown in Appendix F.

The simulation results are compared with the SCADA voltage measurements throughout the system and SCADA power flows at the system boundary to show that the model represents real system behaviour.

3.4.1 TIVS5 (Load bus) – Dynamic load model and voltage profiles

Figure 15 shows the SCADA readings for 1st October 2019: between 0 and 0.39 seconds, active and reactive power are equal to zero (the orange markers overlay the blue markers). The SCADA readings are applied at $t = 0.4$ second as explained in Section 3.3. While the active power value shows an expected visible jump, the reactive power remains close to zero throughout the considered time window. The simulation window ends at $t = 5.2$ s, corresponding to the beginning of data reading for 2nd October 2019.

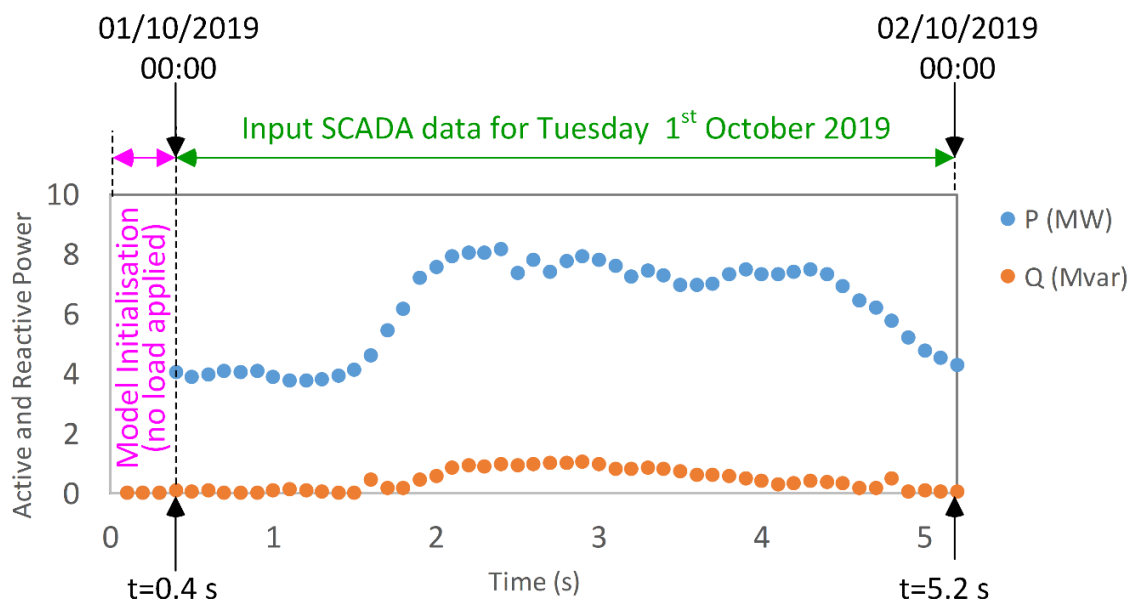


Figure 15: Active and reactive power SCADA readings for TIVS5

Figure 16 shows the simulation results: the first graph illustrates the active and reactive power values used as inputs to the dynamic model. The input values are a linear interpolation of the SCADA readings shown in Figure 15: in other words, the solver fits a line between two

adjacent points, and for each simulation time step, the active and reactive power readings are extrapolated from the fitted line. The second graph in Figure 16 shows the instantaneous load current corresponding to these signals. The third graph shows a zoomed-in version of the current waveform, between 3 s and 3.2 s, to illustrate that the three-phase currents are sinusoidal and symmetrical.

By comparing Figure 15 and Figure 16a, it can be seen that the active and reactive power modelled and input at the TIV5 busbar matches the SCADA measurements. The active and reactive power values between the readings are linearly interpolated in the simulation.

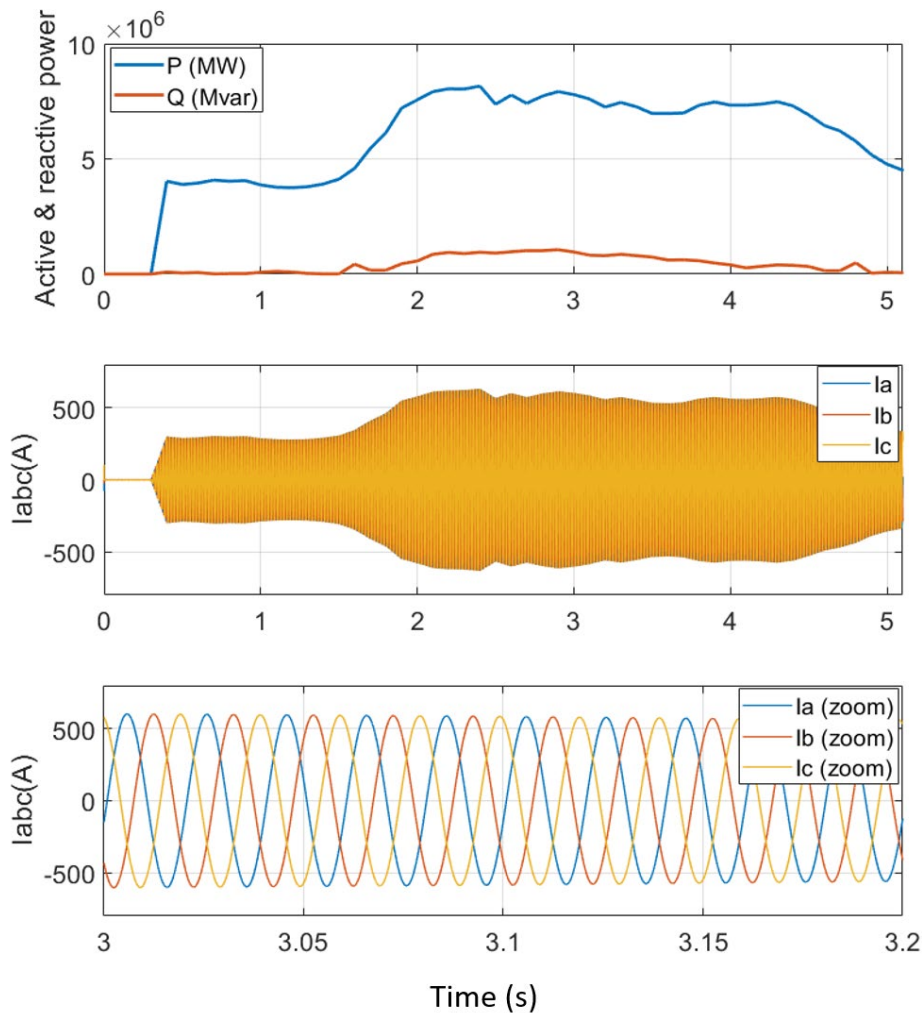


Figure 16: TIV5 waveforms (top) active and reactive power. (middle) Three-phase current. (bottom) Zoomed-in three-phase current

The three-phase current rms at the 11 kV busbar upstream and downstream of the load shunt resistance are given in Figure 17. The value of the shunt resistance for this bus is $10^4 \Omega$ and its connection is shown in Figure 7.

The first graph shows the behaviour for one simulation day, while the second graph shows a zoomed-in version between 0.8 and 0.9 s. In the first graph, the six curves appear to overlap because the system is balanced and the shunt resistance is drawing a very small current. In the second graph, a small difference between the current rms values can be observed (less than 1 A, or 0.5% of the current amplitude).

Based on the results shown in Figure 18, it can be concluded that the shunt resistance has no impact on the power flow in the system

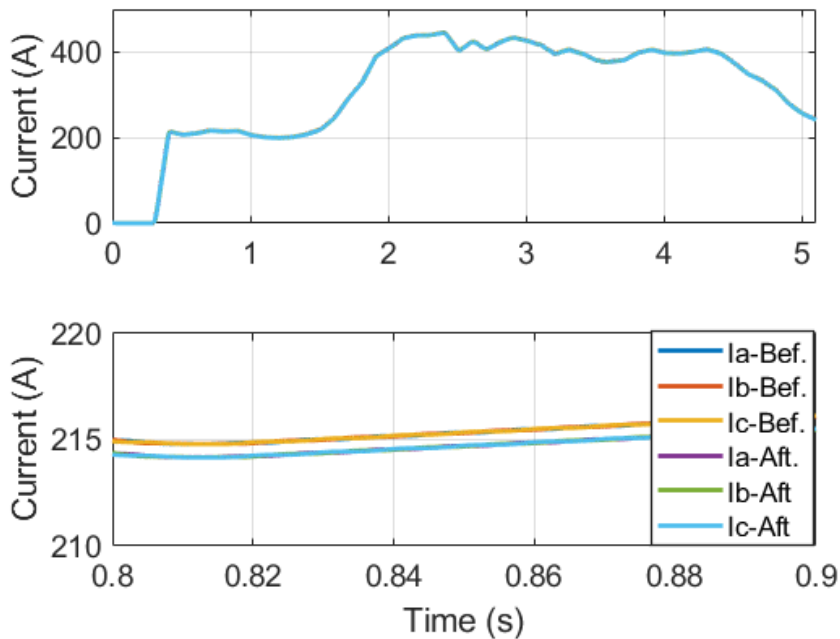


Figure 17: TIVS5 rms current waveforms: (top): overall simulation result; (bottom): zoomed-in three-phase rms current.

Figure 18 shows the instantaneous three-phase voltage at TIVE5 and a zoomed-in version between 3 s and 3.2 s. As discussed in Section 3.3 (model initialisation), the first instants of the simulation show some high-frequency oscillations due to the charging currents in the line-capacitances. During steady-state operation, the voltage profile is symmetrical and shows no distortion.

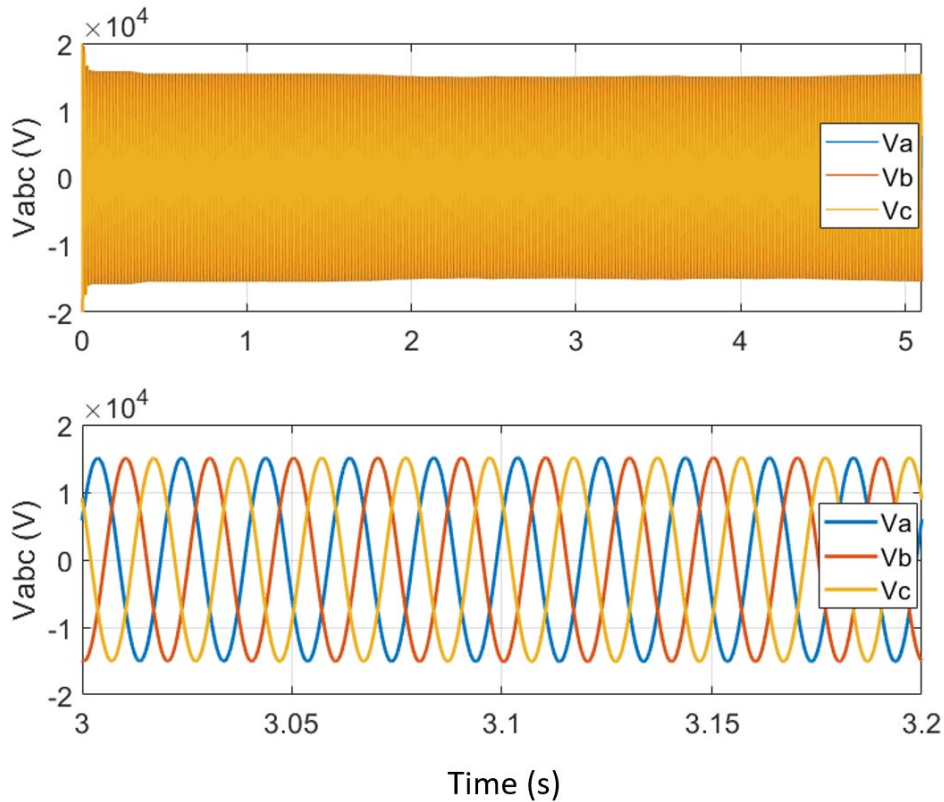


Figure 18: TIVS5 waveforms: (top) Three-phase voltage and (bottom) Zoomed-in three-phase voltage.

In Figure 19, the rms voltage obtained from the simulations is compared with the rms voltage recorded at TIVS5 busbar (SCADA data). The figure shows the rms values of the three-phase voltages obtained from the simulation as a red, yellow and purple curve: however, these three curves are not distinguishable because the system is symmetrical and balanced and therefore the lines are overlaid. The simulation results show some oscillations around the average value for a time between 2.5 seconds and 3.5 seconds (corresponding to the time 10:30 till 15:30 on 1st October 2019), due to the rapid fluctuations of PV farm generation. The SCADA data are sampled every 30 minutes and therefore do not show this behaviour.

With the increase of the load connected to the system, a voltage drop occurs in the Simulink model. While the SCADA readings show a voltage variation, a similar drop does not occur. This discrepancy is due to the SCADA data including the action of automatic tap-changer transformers to maintain a target voltage during load variation. The transformer blocks used in the Simulink model do not provide the capability for implementing tap changing.

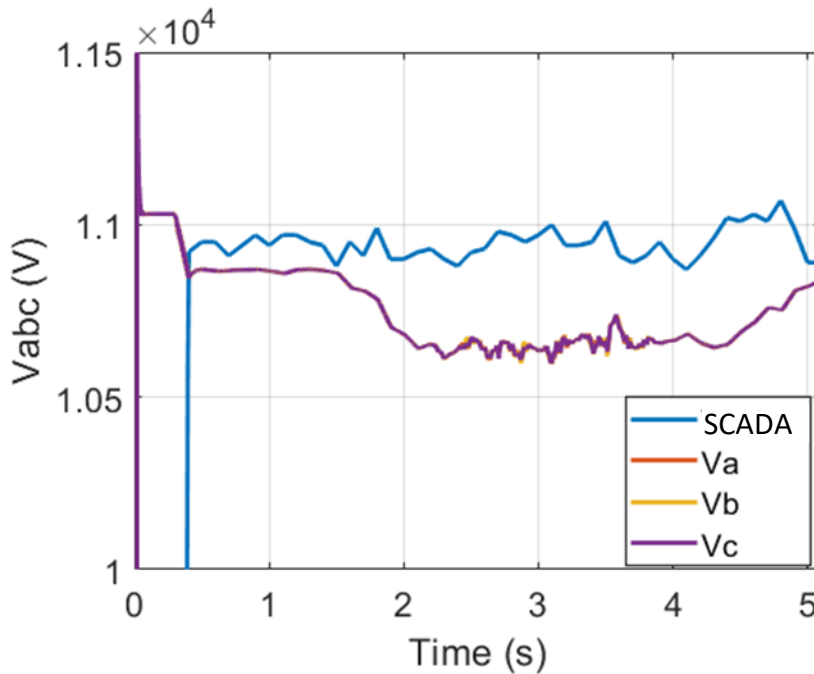


Figure 19: TIVS5 waveforms (top) Three-phase rms voltage. (bottom) Zoomed-in three-phase rms voltage.

3.4.2 TIV3 (BSP) – Analysis of 132/33 transformer tap changer

In order to further assess the source of the discrepancy shown in Figure 19, further investigation was carried out at the TIVE3 busbar, as shown in Figure 20. In the first figure, the voltage rms from the simulation is compared with the voltage rms from the SCADA reading; in the second figure, the load at Tiverton Junction is shown.

It can be seen that between 0.4 s and 1.4 seconds, the two voltage profiles differ by approximately 500 V (1.52%). This difference is attributed to the position of the tap changer at the 132/33 kV substation transformers (upstream to the considered busbar). From 1.5 s, when the load increases, the two waveforms drift more visibly. More specifically, it can be seen that around this time, the active power value at Tiverton Junction starts increasing, while the voltage rms reading from the simulation decreases. The same behaviour is not observed in the SCADA reading, and this is attributed to the tap changer action of the substation transformer. However, the tap positions are not available for the transformers in the Tiverton Network, therefore, the exact tap position is not known.

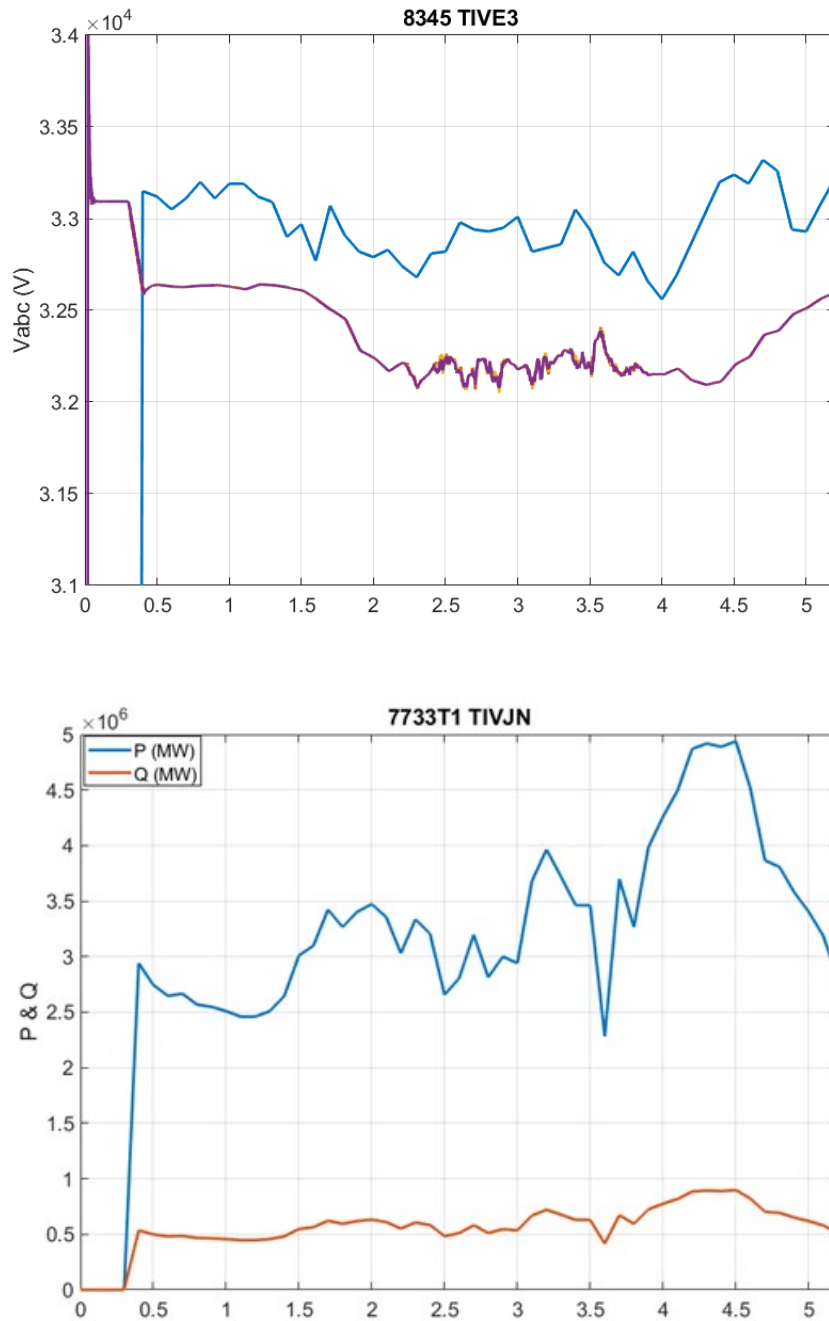


Figure 20 Comparison of simulation results and SCADA readings for the 33 kV voltage rms at TIVE3 busbar with 132/33 kV transformer ratio. The three-phase voltages are overlapped and therefore appear as a single line.

The simulation described above was repeated by modifying the transformer ratio at the 132/33 kV transformers. The results are shown in Figure 21. In this case, the secondary

voltage of both 132/33 kV transformers was set to 33.4125 kV to emulate the first tap action. As a result, in the first seconds of the simulation, the simulation results and the SCADA data are very similar. When the load increases, the two waveforms drift due to the increasing load.

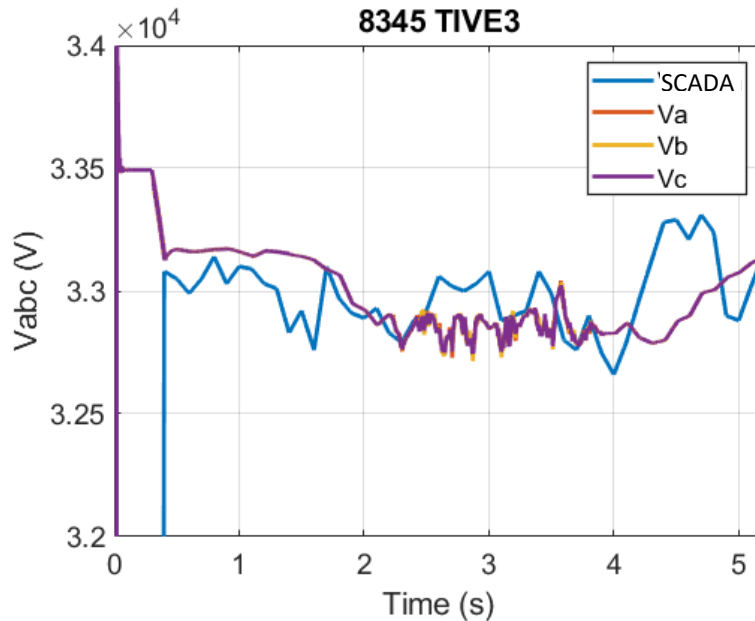


Figure 21: Comparison of simulation results and SCADA readings for the 33 kV voltage rms at TIVE3 busbar with 132/33.4125 transformer ratio.

Figure 22 shows the same results for a longer simulation time, though differences to SCADA values can be seen in the longer term trends.

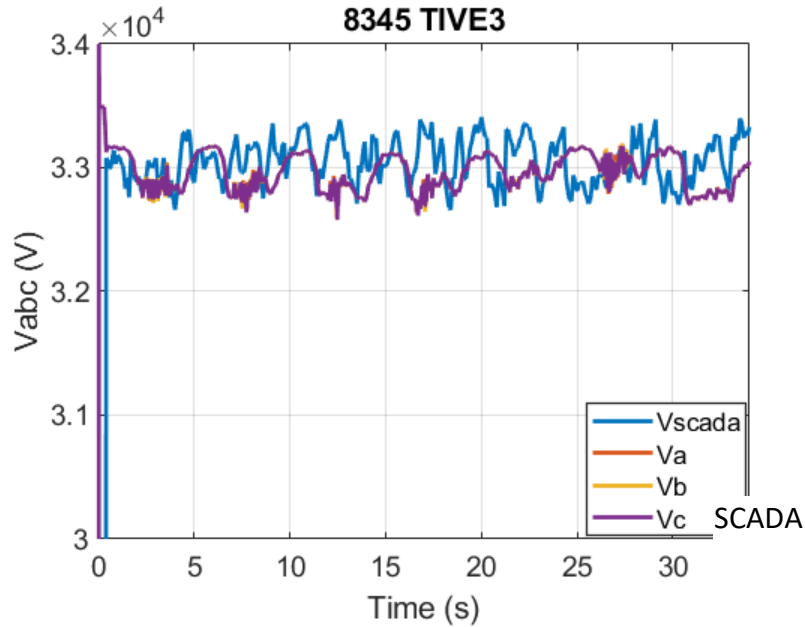


Figure 22: Comparison of simulation results and SCADA readings for the 33 kV voltage rms at TIVE3 busbar with 132/33.4125 transformer ratio for a simulation time corresponding to a week.

To confirm that the simulations were generating reliable voltage indications, further checks were carried out.

Four further point checks were conducted to confirm that the MATLAB/Simulink EMT simulation voltages were similar to those generated by the DigSILENT PowerFactory model. These points were selected to represent points where the system voltage was falling, was rising, was broadly at a lower level, and when the voltage was at a higher level. These checks used data from the first day of simulation (01/10/2020). The voltage rms obtained from the two models are shown in Table 7.

Table 6: Four point checks to compare voltages generated by MATLAB/Simulink and DigSILENT PowerFactory.

Simulation time (s)	TIVE3 voltage pu (from MS – EMT Simulation)	TIVE3 voltage pu (from DP – load flow)
1.5	33.20	33.23
2	32.90	32.98
4	32.87	33.12
4.5	32.90	32.97

These results show a good degree of agreement between the voltages calculated by the EMT simulation, and those calculated by power flow analysis within the DlgSILENT PowerFactory model (using P & Q load/generation data taken from the EMT simulation).

It is therefore concluded that the MATLAB/Simulink EMT simulation voltages are a reliable indication of the system voltages, and that differences to SCADA is due to the absence of tap changer action in the simulation.

3.4.3 CMPV3, STFA3 and AYH3 - Validation of inverter model.

An illustration of basic operation of the modelled output power from the inverter models is shown in Figure 23. For these illustrations, the power reference is kept constant and equal to the maximum value to demonstrate that the inverter output stabilises to a constant value for each PV farm. The different rated powers of the inverters can clearly be seen from the vertical axis. For CMPV3, the total output power of two inverters is included. The initial transient is due to the fact that the inverter switches start to operate at t=0.1 second. At approximately 0.2 seconds, the inverter output stabilises to the rated value. Figure 24 shows a zoomed-in version of the waveforms between 0.5 and 0.6 s.

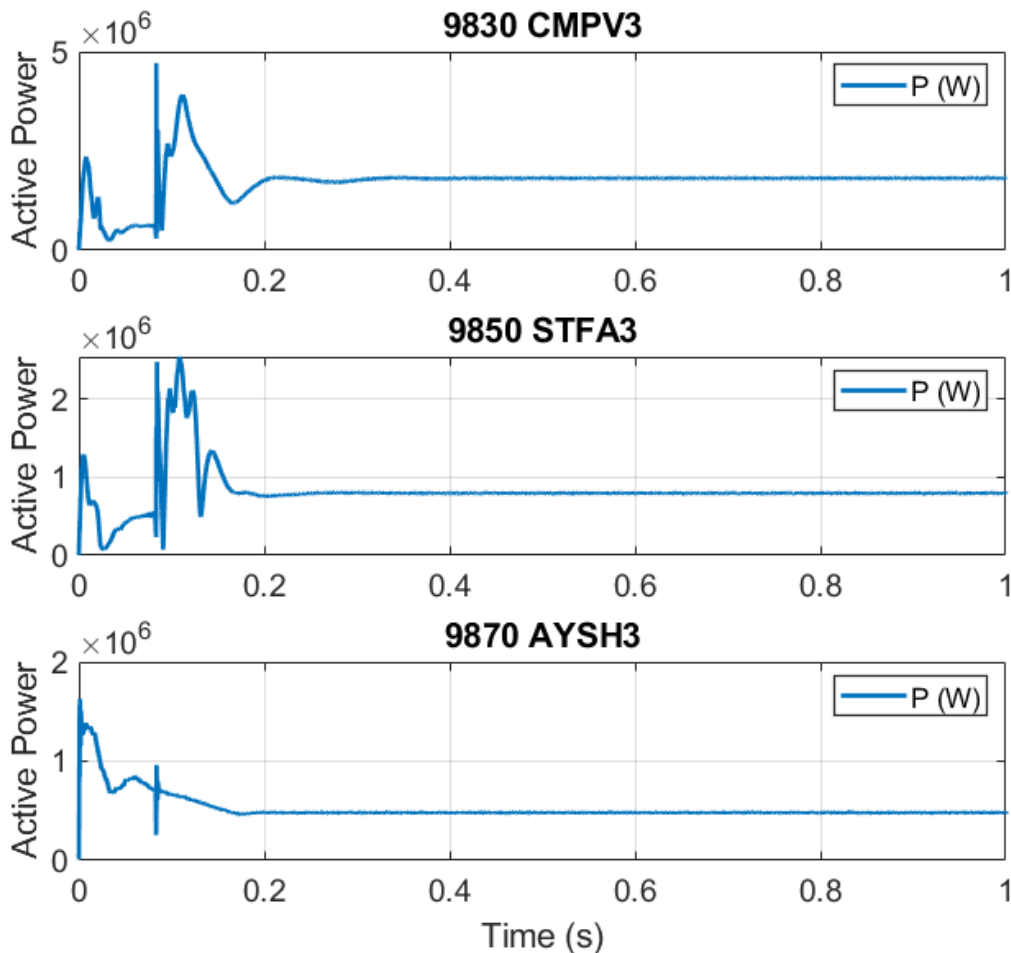


Figure 23: Power output of the three PV farms – from initialisation to 1 second simulation time. For this case, a steady output is considered to show the performance of the three inverters.

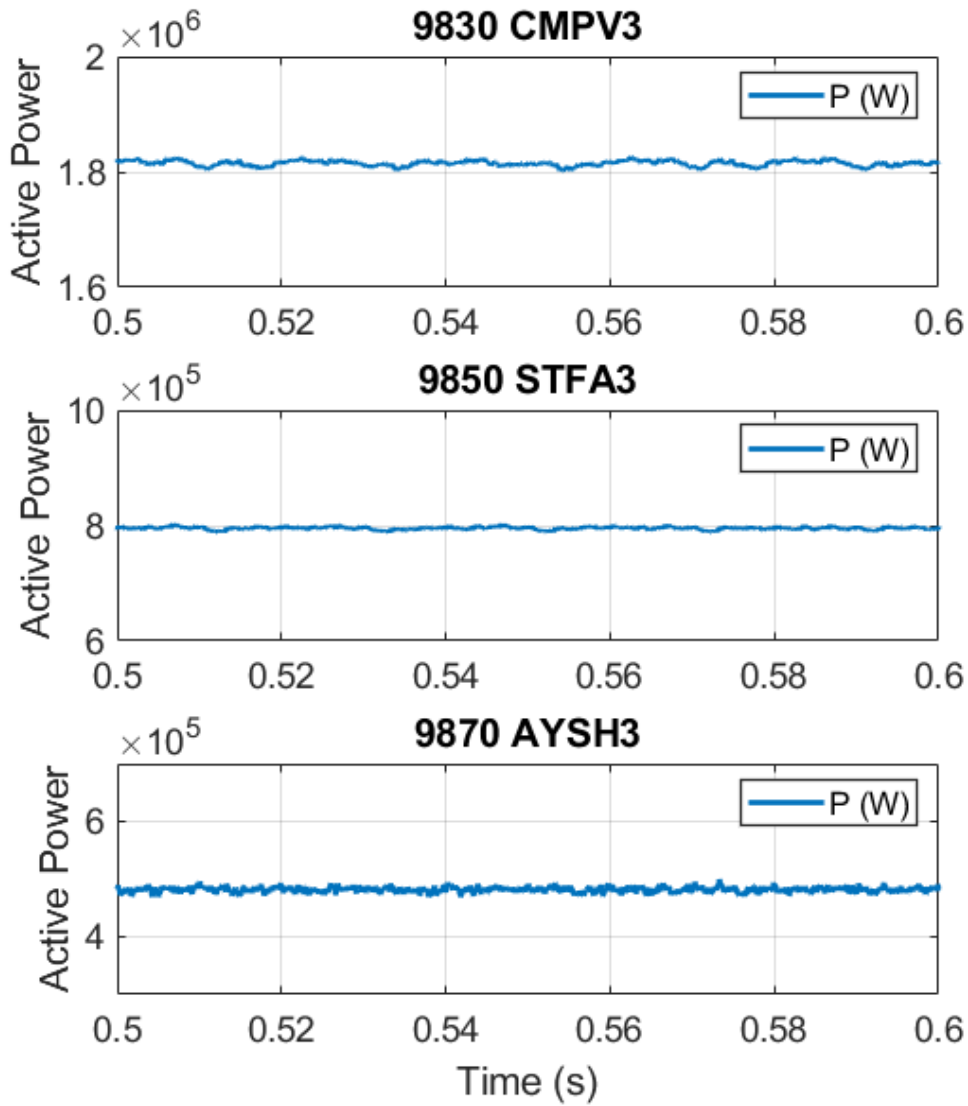


Figure 24: Inverter output power (zoomed-in version for 0.6 s).

The three phase output currents are shown in Figure 25. The inverter output currents are symmetrical and they follow the same fluctuations as the power output during the initial transient. Figure 26 shows a zoomed-in version of the waveforms, between 0.5 and 0.6 s.

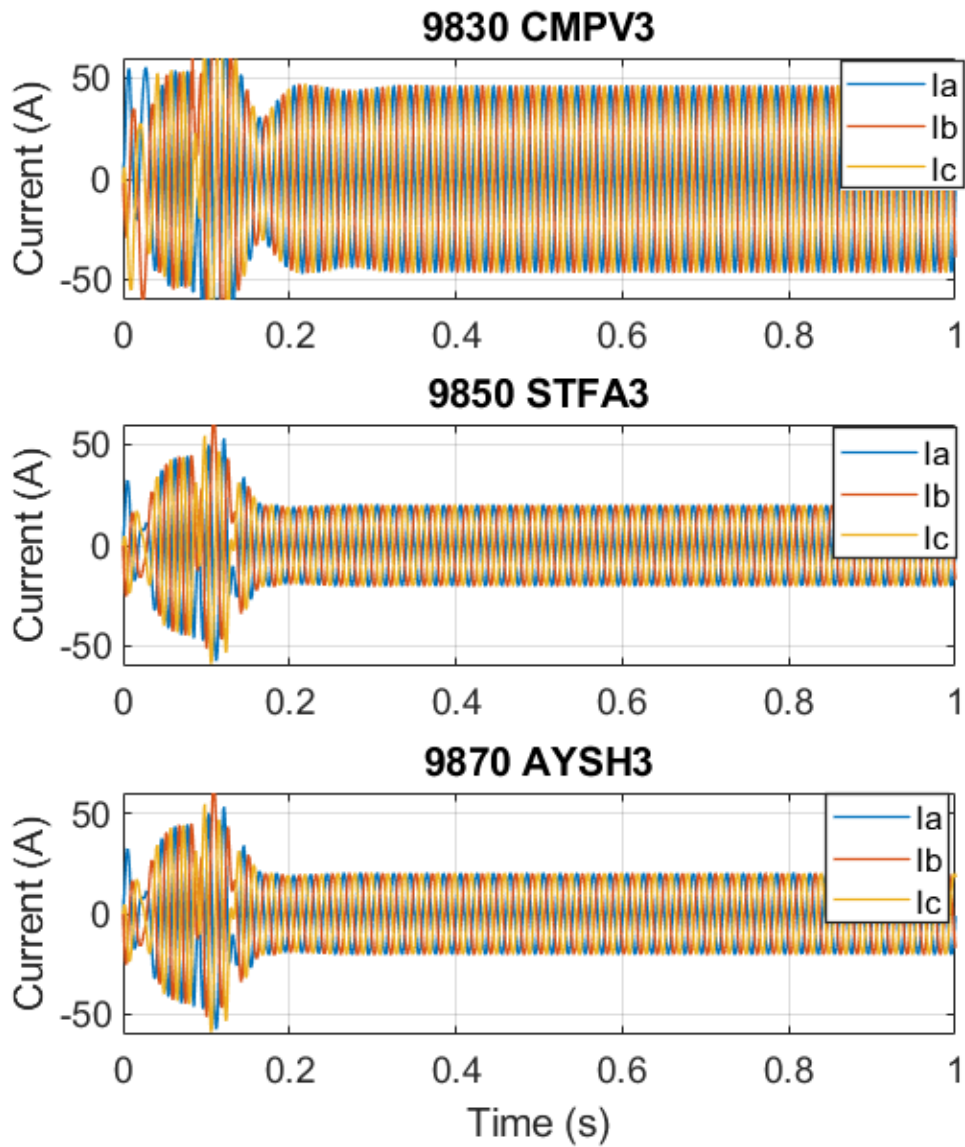


Figure 25: Inverter three-phase output currents for a constant irradiance value.

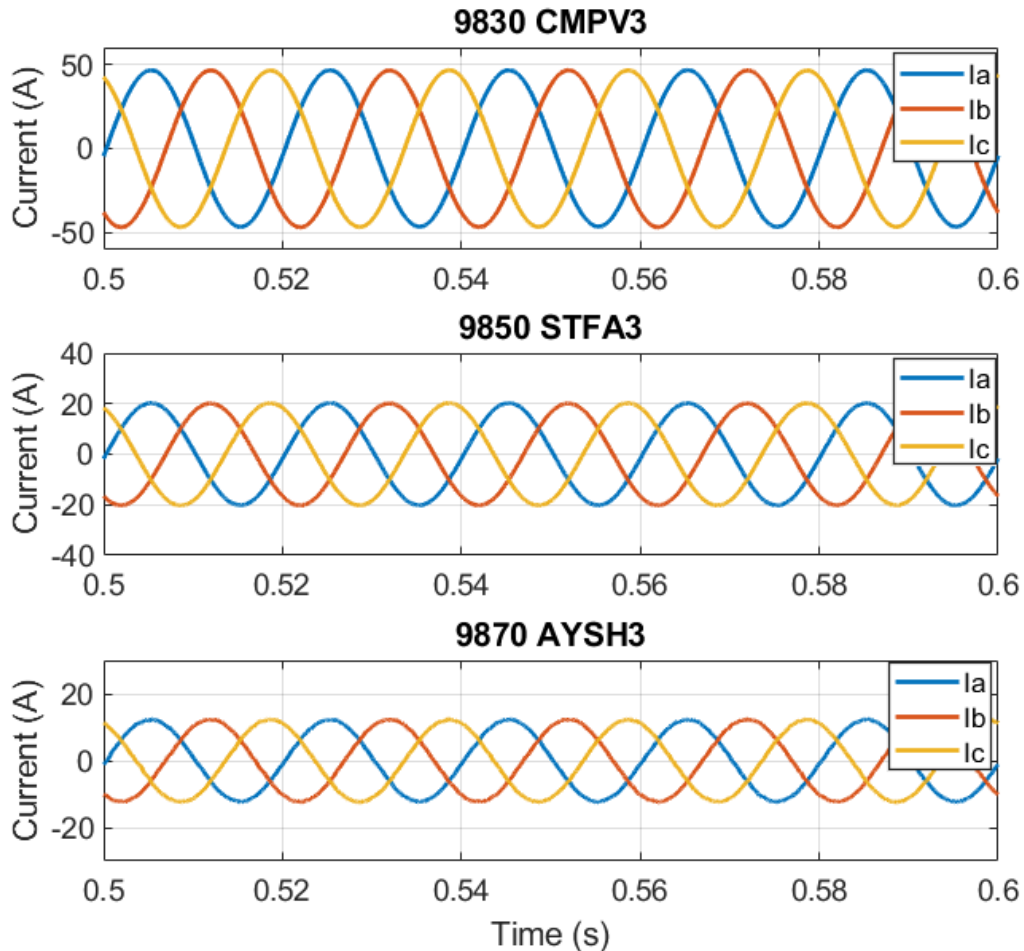


Figure 26: Inverter three-phase output currents (zoomed-in graph for 0.5 to 0.6 seconds).

3.4.4 AYSH3 (PV farm) – Validation of dynamic PV farm model

Figure 27 shows a screenshot from the power quality readings at AYSH3 busbar for October 2nd, 2019 (the recordings for this PV farms starts around mid-day on 1st October 1st, 2019, as indicated in Appendix C2. Therefore, the results for 2nd October are shown in this section to provide results for a full day). This figure shows the current rms value for the three phases: the three readings overlap due to the symmetry of the system, and rapid fluctuations are visible in the output currents, due to rapid variations in irradiance.

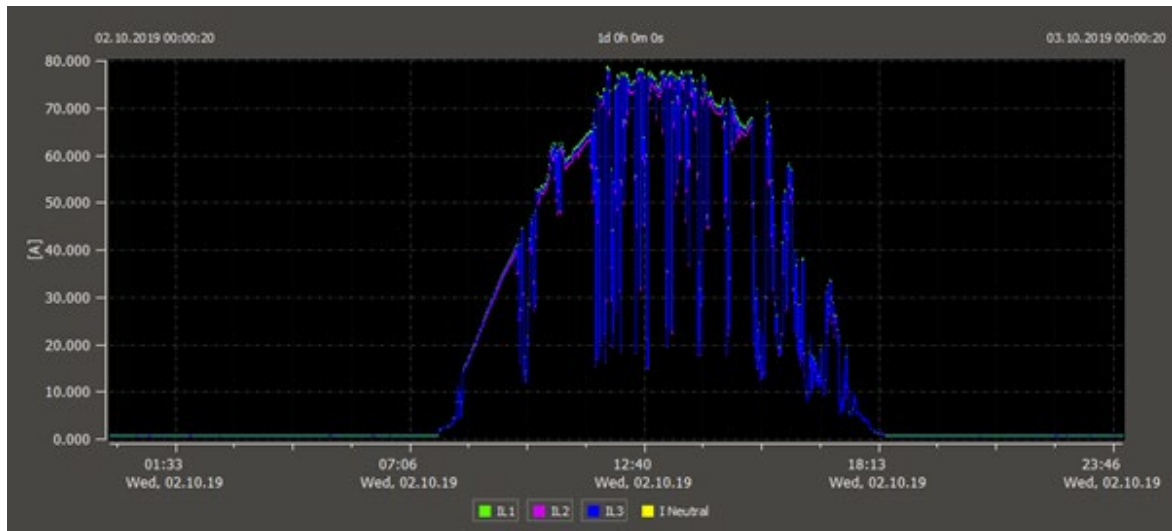


Figure 27: Power quality rms current values for AYSH3 busbar, as displayed in WinPQ-mobile software.

Figure 28 shows the rms current amplitude at Ayshford PV farm used as the input signal to modulate the controlled current sources in the dynamic PV-farm, (model shown in Figure 11).

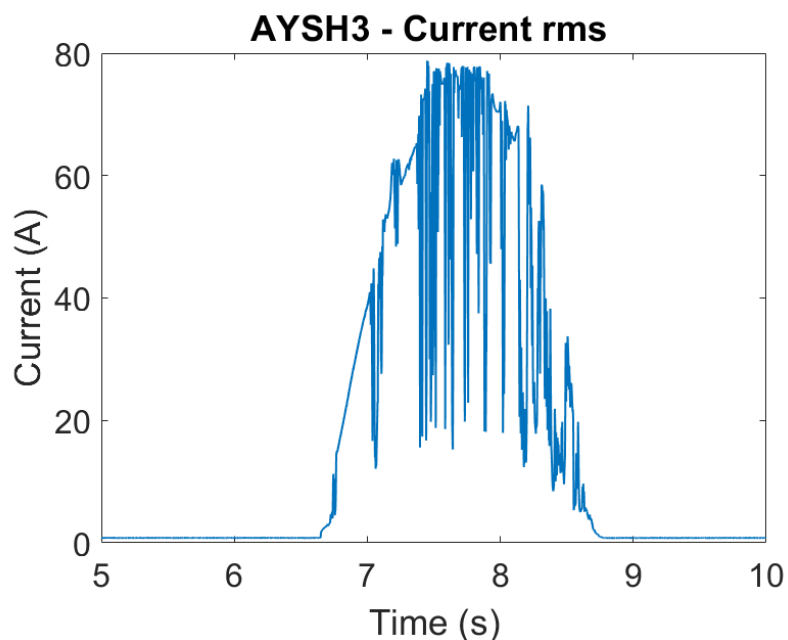


Figure 28: Current rms amplitude measured at Ayshford PV farm, obtained from the PQ data plotted in Figure 27

Comparison of Figure 27 and Figure 28 suggests that the input signal for the PV farm model closely mimics the measured PV site output.

The performance of the composite model is then verified in terms of output power.

Figure 29 shows the power measurement data from the PQ monitor for 2 October 2019 (the negative value is due to the way the meter is connected). Figure 30 shows a graph of active power P generated by Ayshford PV farm for the same day, broken down in three contributions: power generated by the inverter, power generated by the PV farm and total power, compared to the PQ data. It can clearly be seen that the power output from the model matches the measured power output.

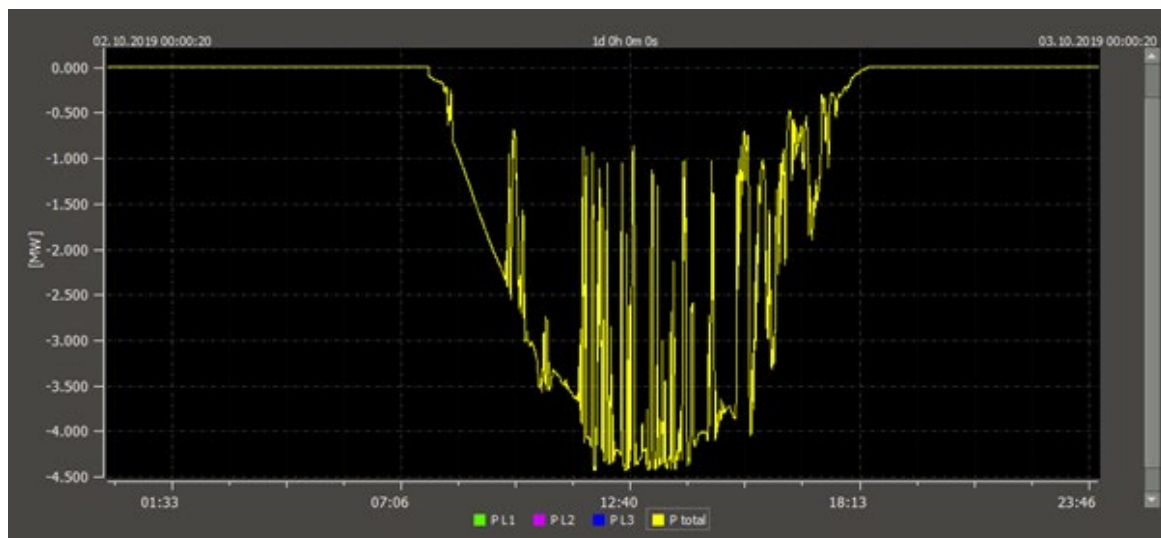


Figure 29: Three-phase power as measured at Ayshford PV farm, obtained from the PQ measurement data.

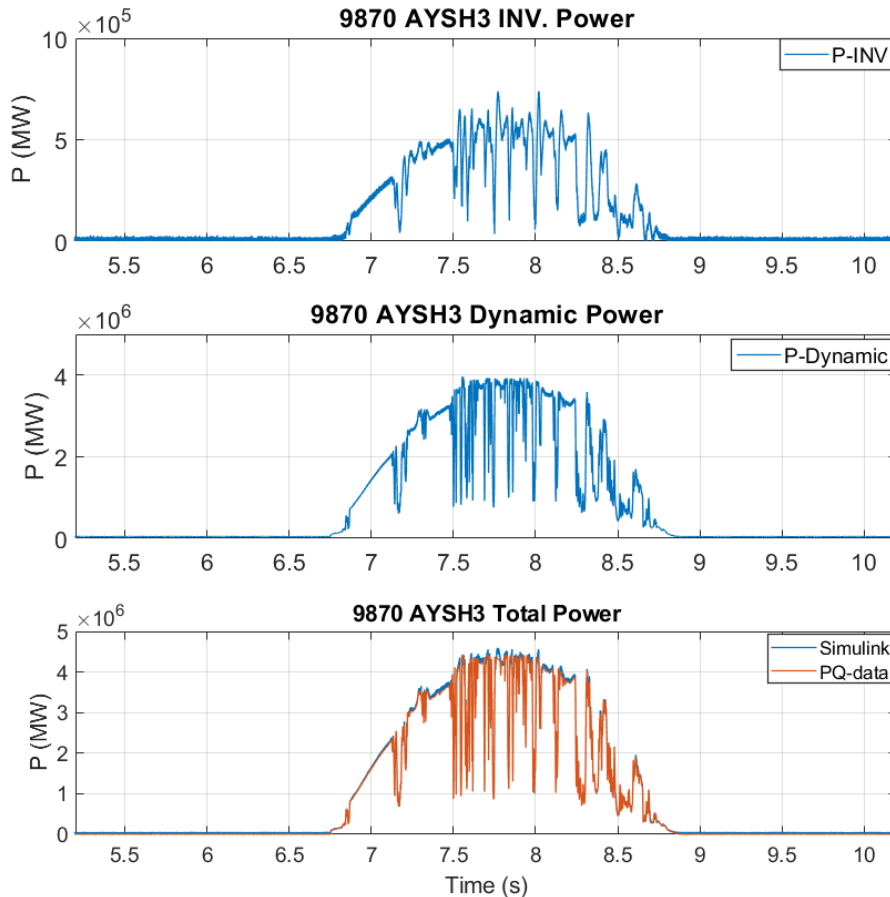


Figure 30: Power Generated from Ayshford Farm on October 2nd, 2019.

3.4.5 EXET1 (System boundary) –Active and Reactive Power Exchange

The last validation pulls together the fundamental P and Q outputs of the model and consists in comparing the power flow for each circuit of the Tiverton Network and at the system boundary with the SCADA data.

The three circuits were defined in Section 2.1 as follows:

- loop 1 (between circuit breakers 1L5 and 4L5);
- loop 2 (between circuit breakers 2L5 and 3L5); and
- feeder 3 (connected via circuit breaker 6L5).

The comparison of active power flow for each circuit is shown in Figure 31. In the first loop there are no PV farms, and therefore there the simulation data and the SCADA data follows

the same pattern. In the second and third loop, the use of PQ data is indicated by the rapid oscillations corresponding to daylight hours. This additional detail is simply not captured by the existing SCADA data. Some minor discrepancies can also be observed in the power values; these are attributed to limitations in the underlying SCADA data (e.g. some of the load busses only report apparent power data, and some suspiciously stable (over time) values have been observed in the SCADA data).

The result at the system boundary is included in Figure 32, and show a close match to the SCADA data, taking into account the limitations already described above.

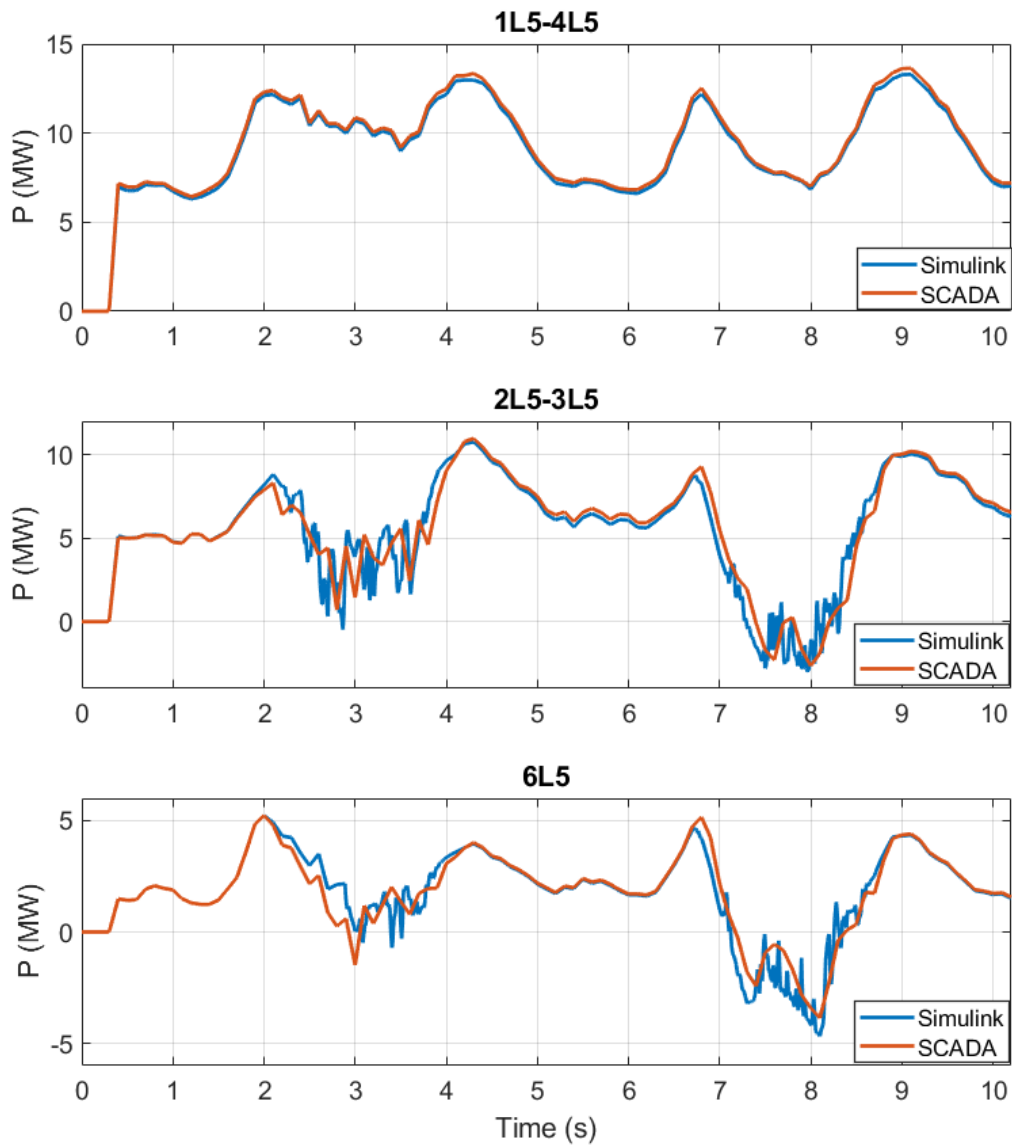


Figure 31: Comparison of active power flow for the three main circuits: loop 1, loop 2 and radial feeder.

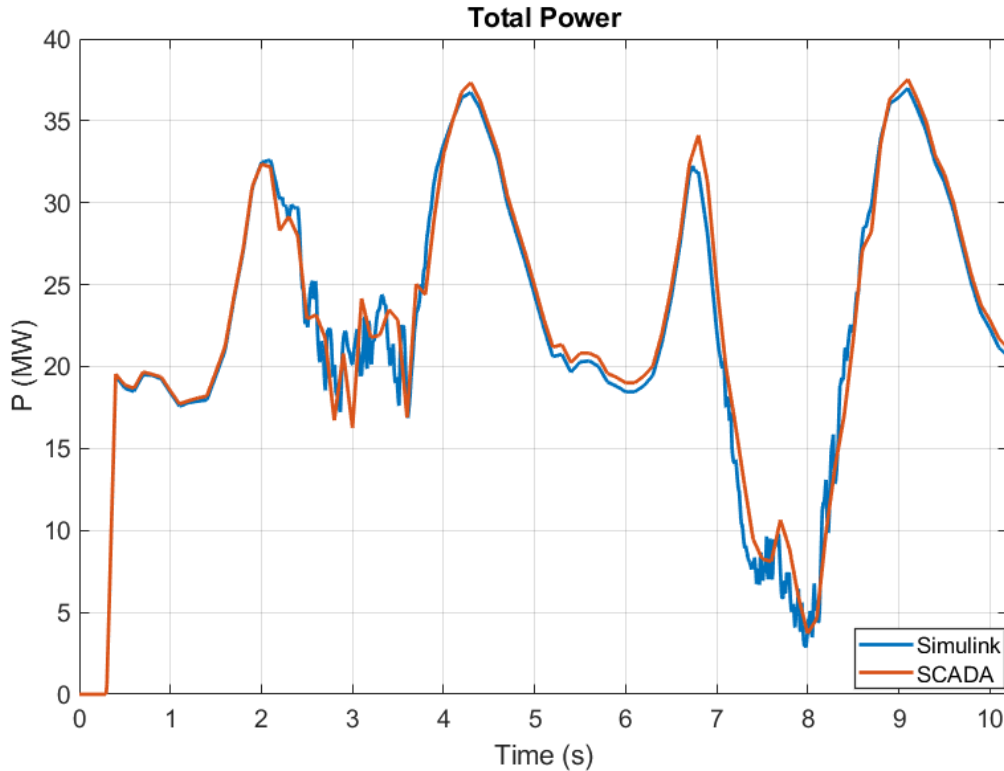


Figure 32: Total active power at EXET1: comparison between simulation results and SCADA data.

The results for the reactive power comparison at each feeder and at the system boundary are shown in Figure 33 and Figure 34, respectively.

The agreement of the reactive power simulation to SCADA is not as close as for active power; however, the reactive power SCADA data is less reliable (e.g. SCADA showing as zero for several consecutive half hour periods on a number of occasions and also apparently not updating as frequently as the active power values). In spite of this, the reactive power trace obtained from the model follows closely the SCADA data during the simulation times corresponding to the day hours. Some discrepancies are observed during the simulation times corresponding to night hours, but overall the two curves display the same trend.

From review of the active and reactive power (EMT) simulations it is concluded that the model shows realistic system behaviour.

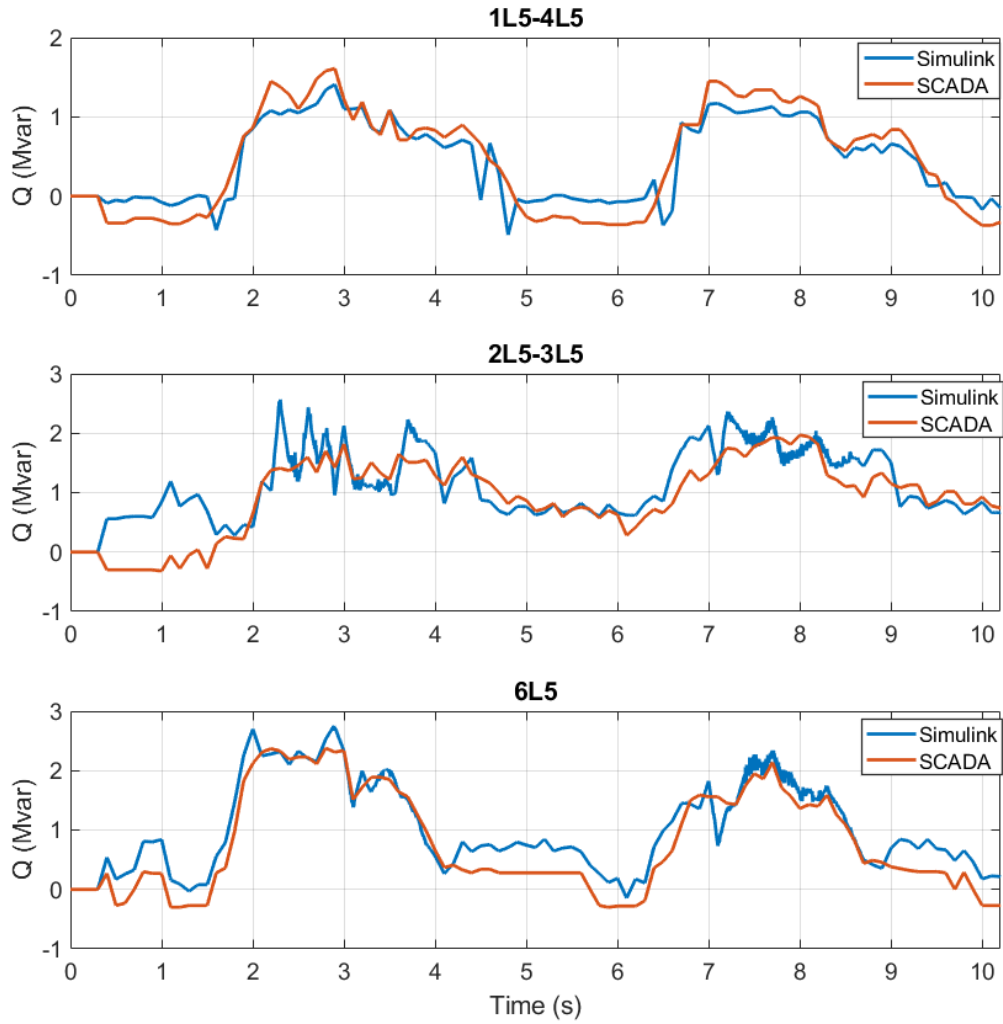


Figure 33: Comparison of reactive power flow for the three main circuits: loop 1, loop 2 and radial feeder.

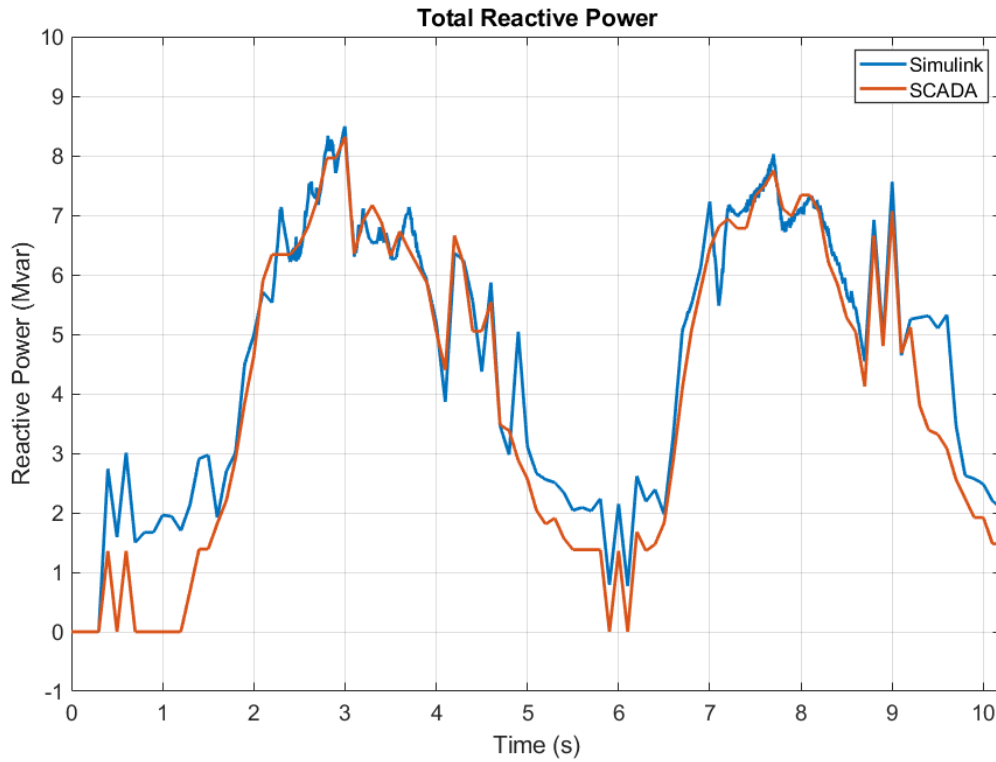


Figure 34: Total reactive power at EXET1: comparison between simulation results and SCADA data.

3.4.6 Conclusions on fundamental frequency results of EMT simulations

MATLAB/Simulink EMT simulations have been performed for a three-week period, based on October 2019.

The fundamental frequency output of the simulation has been compared to:

- SCADA system voltages (both 33 kV and 11 kV) throughout the modelled system; and
- Sample checks of the EMT simulation voltages have been compared to values from the DigSILENT PowerFactory reference model.
- SCADA active and reactive power flows across the system boundary;

Based on these tests, it is concluded that the MATLAB/Simulink EMT simulations provide a realistic model of the fundamental frequency behaviour of the actual network over a three-week time series.

3.5 Harmonic results and validation

Having established that the MATLAB/Simulink EMT simulations provide a realistic model of the fundamental frequency behaviour of the actual network, the final assessment was of the simulation's capability to model harmonic behaviour of the system. This was assessed by:

- Comparing modelled current and voltage harmonics to measured data from temporarily fitted PQ monitors at each of the PV farm sites; and
- Comparing modelled voltage harmonics to PQ monitor data at the BSP 33 kV busbar (TIVE3).

The results from the above comparisons will be shown in Section 3.5.1- 3.5.3.

3.5.1 Harmonic current levels at the PV farms

Figure 35 shows three different components of the Ayshford PV farm model output current: fundamental, harmonic and total.

The upper graph of Figure 35 shows the results for fundamental current. While the current increases linearly in the first part of the graph, a dip in current amplitude on all phases can be observed between 7.05 s and 7.1 s, due to a sudden change in power output recorded from the PQ monitors.

The middle graph of Figure 35 (shows the combined 5th, 7th, 11th and 13th harmonics (i_{ha}) that are injected into the network at AYSH3 bus, where $i_{ha} = i_{h5} + i_{h7} + i_{h11} + i_{h13}$. The magnitude of the injected harmonics can clearly be seen to vary depending on the 50 Hz PV current magnitude shown in the upper chart of Figure 35.

The lower chart of Figure 35 shows the combination of the fundamental current and the modelled harmonic current.

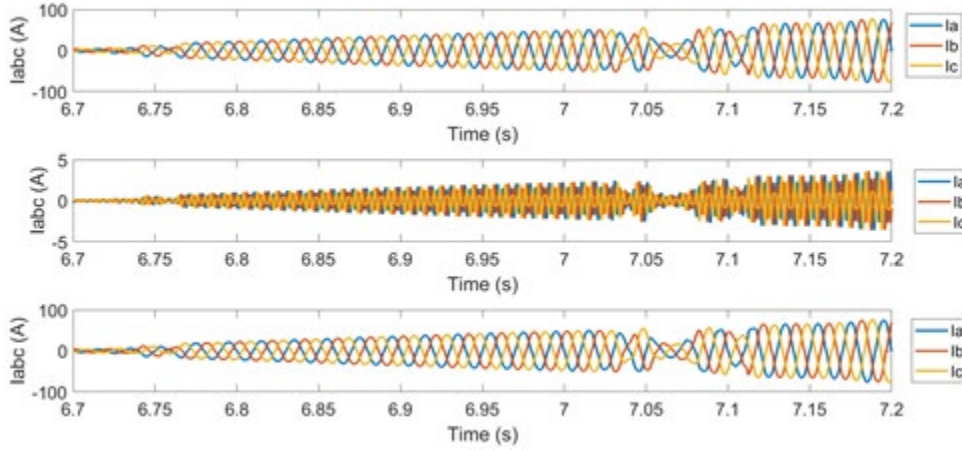


Figure 35: Ayshford PV farm. Three-phase fundamental currents. Three-phase harmonic currents total three-phase currents.

Table 7 - Table 9 show a comparison of measured PQ data with modelled data for current harmonics at the three PV farms. It is noted that the harmonic levels (%) for the four harmonic of interest compare very well to measured values.

Table 7: Ayshford PV farm harmonic currents: comparison of PQ monitoring data and simulation results.

Harmonic order	PQ monitor data			MATLAB model		
	I_{12} (%)	I_{23} (%)	I_{31} (%)	I_{12} (%)	I_{23} (%)	I_{31} (%)
5	1.25	1.32	1.28	1.24	1.31	1.28
7	0.48	0.46	0.47	0.49	0.49	0.51
11	0.17	0.16	0.17	0.16	0.18	0.16
13	0.27	0.26	0.26	0.25	0.28	0.24

Table 8: Cullompton PV farm harmonic currents: comparison of PQ monitoring data and simulation results.

Harmonic order	PQ monitor data			MATLAB model		
	I_{12} (%)	I_{23} (%)	I_{31} (%)	I_{12} (%)	I_{23} (%)	I_{31} (%)
5	1.04	1.17	1.10	1.07	1.20	1.03
7	0.48	0.43	0.45	0.45	0.47	0.43
11	0.10	0.10	0.10	0.09	0.11	0.08
13	0.05	0.05	0.07	0.06	0.08	0.06

Table 9: Stoneshill PV farm harmonic currents: comparison of PQ monitoring data and simulation results.

Harmonic order	PQ monitor data			MATLAB model		
	I_{12} (%)	I_{23} (%)	I_{31} (%)	I_{12} (%)	I_{23} (%)	I_{31} (%)
5	0.83	0.89	0.82	0.79	0.85	0.86
7	0.33	0.30	0.34	0.31	0.32	0.35
11	0.096	0.076	0.073	0.08	0.05	0.08
13	0.04	0.04	0.04	0.06	0.09	0.05

While the variation of harmonic current level between phases is realistic compared to the actual system measurements, this result was not immediately expected, as the model is of a balanced system.

Investigation of the variation of harmonic level between phases identified that the process of creating the PV sites' generation data model necessarily involves the modulation of the magnitude of the current waveforms (to reflect variation in solar irradiance and generation output – the modulating influence shown as purple line in Figure 36). However, this modulation process also introduces small levels of unbalance between the phase waveforms as seen in the phase current traces of Figure 36.

The effect of this process on the PV farm currents is shown in Figure 37 for a longer time scale. This small phase unbalance due to the modelling approach causes the differences in the level of harmonics between phases in Table 7 - Table 9.

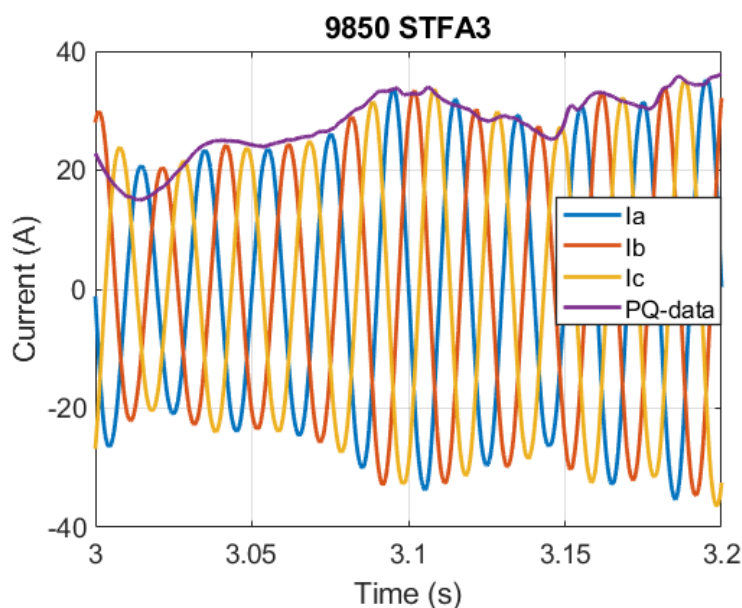


Figure 36: Three-phase currents at Ayshford and current modulation from PQ data.

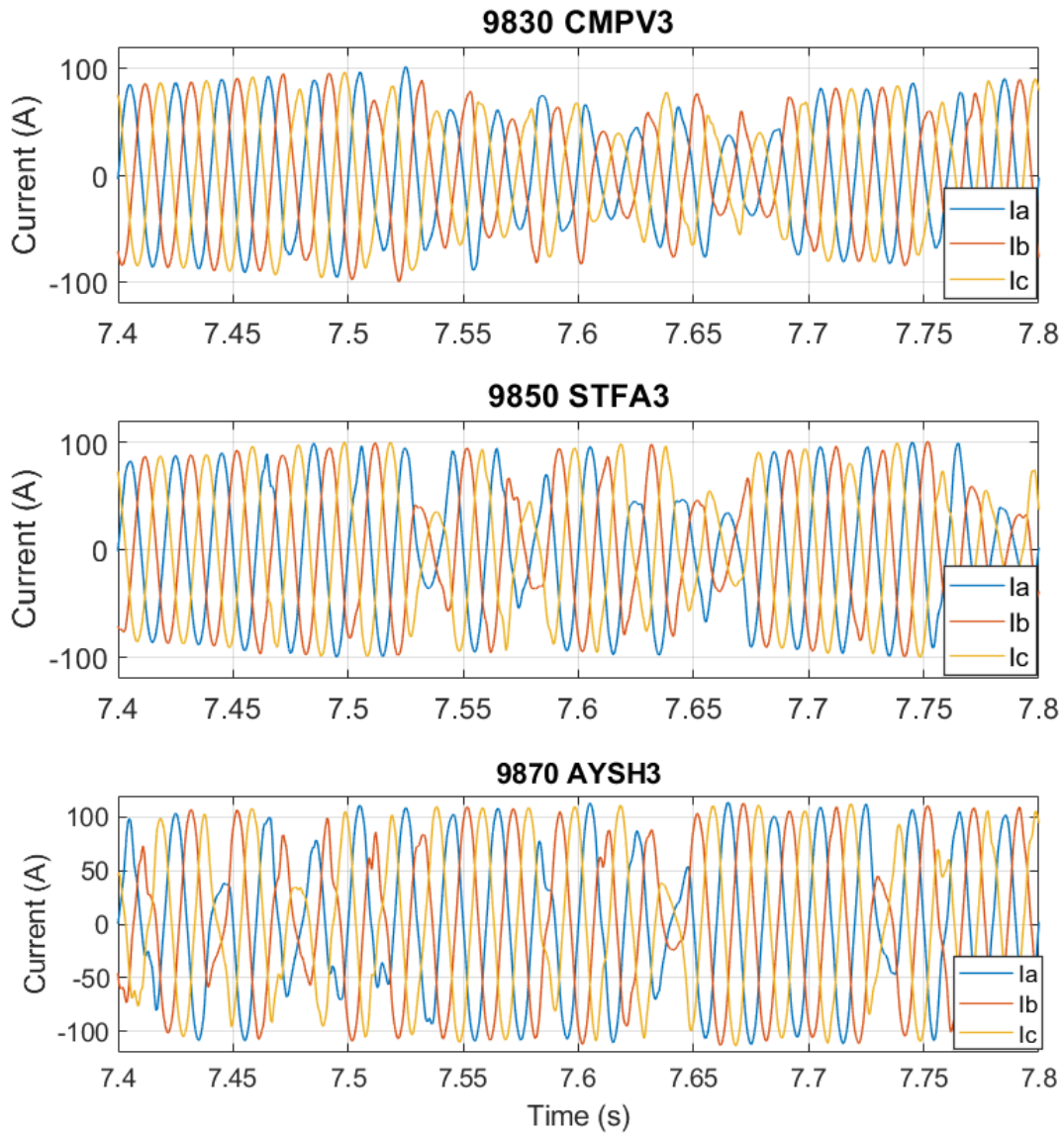


Figure 37: Effect of the modulation on the three PV farms output currents.

As a result of this investigation it was concluded that the between-phase variation seen in the level of current harmonics is a reasonable artefact of the modelling process.

3.5.2 Harmonic voltage levels at the PV farms

The data presented Table 10- Table 12 shows for maximum voltage harmonics at the PV farm sites. Minimum voltage harmonics are shown in Table 13-Table 15.

Table 10: Ayshford PV farm maximum harmonic voltages: comparison of PQ monitoring data and simulation results

Harmonic order	PQ monitor data			MATLAB model		
	V ₁₂ (MAX%)	V ₂₃ (MAX%)	V ₃₁ (MAX%)	V ₁₂ (MAX%)	V ₂₃ (MAX%)	V ₃₁ (MAX%)
5	1.34	1.45	1.23	1.34	1.34	1.34
7	1.04	1.00	1.03	1.03	1.02	1.02
11	0.23	0.23	0.21	0.26	0.26	0.26
13	0.19	0.20	0.20	0.29	0.29	0.29

Table 11: Cullompton PV farm maximum harmonic voltages: comparison of PQ monitoring data and simulation results

Harmonic order	PQ monitor data			MATLAB model		
	V ₁₂ (MAX%)	V ₂₃ (MAX%)	V ₃₁ (MAX%)	V ₁₂ (MAX%)	V ₂₃ (MAX%)	V ₃₁ (MAX%)
5	1.49	1.58	1.41	1.44	1.44	1.44
7	1.04	1.00	1.14	1.15	1.15	1.15
11	0.23	0.24	0.27	0.28	0.28	0.28
13	0.18	0.25	0.28	0.31	0.31	0.31

Table 12: Stoneshill PV farm maximum harmonic voltages: comparison of PQ monitoring data and simulation results

Harmonic order	PQ monitor data			MATLAB model		
	V ₁₂ (MAX%)	V ₂₃ (MAX%)	V ₃₁ (MAX%)	V ₁₂ (MAX%)	V ₂₃ (MAX%)	V ₃₁ (MAX%)
5	1.40	1.51	1.28	1.36	1.36	1.36
7	1.01	1.00	1.00	1.09	1.09	1.09
11	0.19	0.20	0.18	0.27	0.27	0.27
13	0.19	0.26	0.23	0.29	0.29	0.29

Table 13: Ayshford PV farm minimum harmonic voltages: comparison of PQ monitoring data and simulation results

Harmonic order	PQ monitor data			MATLAB model		
	V ₁₂ (MIN%)	V ₂₃ (MIN%)	V ₃₁ (MIN%)	V ₁₂ (MIN%)	V ₂₃ (MIN%)	V ₃₁ (MIN%)
5	0.412	0.446	0.369	0.57	0.57	0.57
7	0.523	0.512	0.510	0.49	0.49	0.49
11	0.010	0.015	0.006	0.12	0.12	0.12
13	0.005	0.004	0.004	0.13	0.13	0.13

Table 14: Cullompton PV farm minimum harmonic voltages: comparison of PQ monitoring data and simulation results

Harmonic order	PQ monitor data			MATLAB model		
	V ₁₂ (MIN%)	V ₂₃ (MIN%)	V ₃₁ (MIN%)	V ₁₂ (MIN%)	V ₂₃ (MIN%)	V ₃₁ (MIN%)
5	0.565	0.614	0.537	0.61	0.61	0.61
7	0.553	0.555	0.553	0.56	0.56	0.56
11	0.003	0.024	0.004	0.13	0.13	0.13
13	0.004	0.003	0.004	0.19	0.19	0.19

Table 15: Stoneshill PV farm minimum harmonic voltages: comparison of PQ monitoring data and simulation results

Harmonic order	PQ monitor data			MATLAB model		
	V ₁₂ (MIN%)	V ₂₃ (MIN%)	V ₃₁ (MIN%)	V ₁₂ (MIN%)	V ₂₃ (MIN%)	V ₃₁ (MIN%)
5	0.506	0.559	0.472	0.56	0.55	0.55
7	0.556	0.538	0.554	0.51	0.51	0.51
11	0.004	0.017	0.005	0.12	0.12	0.12
13	0.003	0.005	0.003	0.09	0.09	0.09

Again, it can be seen that the modelled voltage harmonic levels (%) for the four harmonic of interest compare well to measured values, the exception being that the 13th harmonic levels are modelled as slightly higher than the measured levels.

In addition it was noted that the voltage harmonics (both maximums and minimums) were balanced across phases (in all but one instance), as would be expected if the model had balanced load/generation current harmonics and upstream system voltage harmonics. From the previous review of PV site current harmonics, variation between phases was noted and accepted.

Given that differences between phases were seen in the modelled current harmonics for PV sites, the counter-intuitive lack of variation between phases for voltage harmonics at PV sites was further investigated.

The hypothesised explanation for balance between phases for voltage harmonics (whilst variations exist between phases for the PV farm site current harmonics) was that:

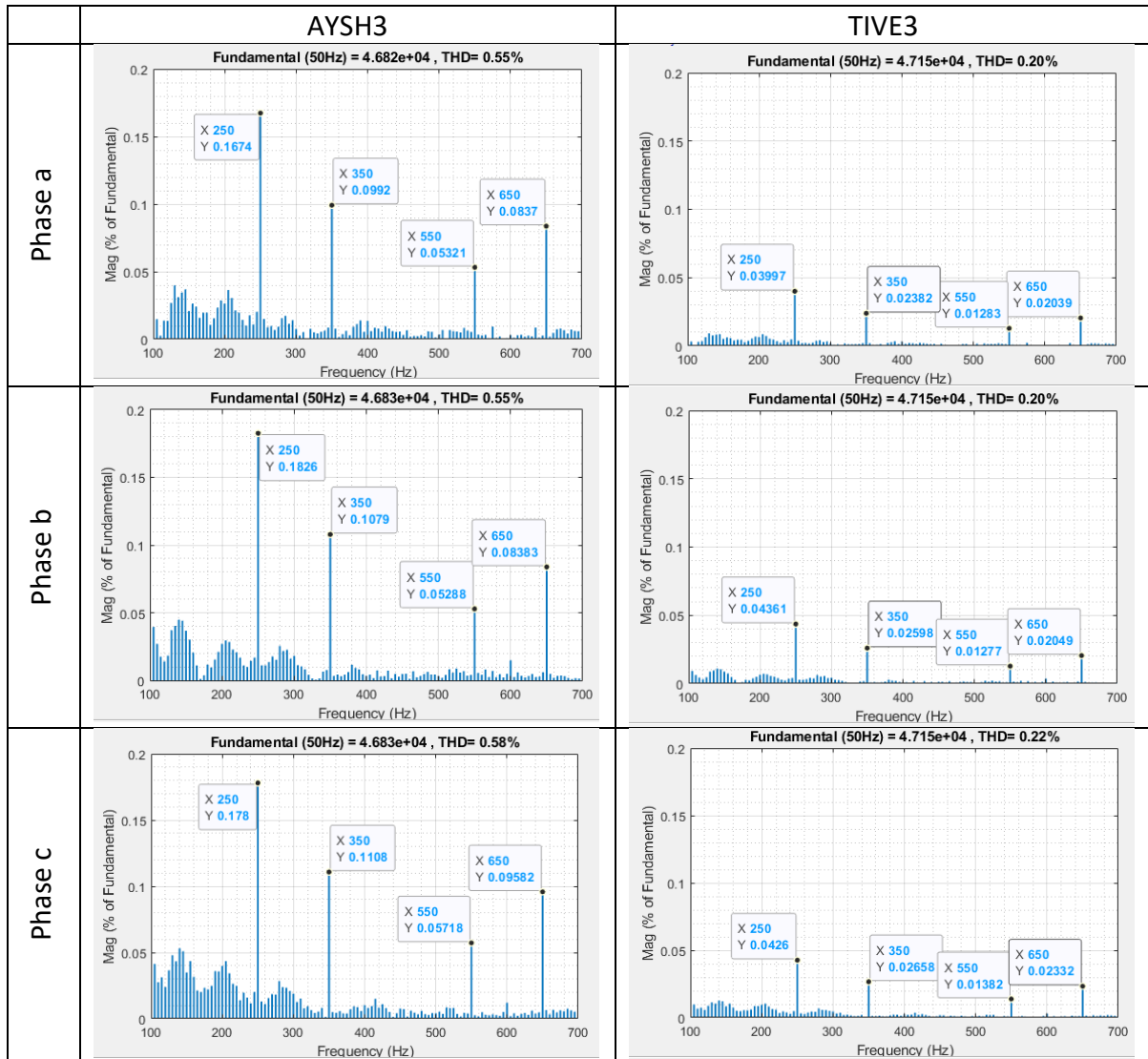
- the PV farms' output would cause variation between phases for voltage harmonics if this was the only load/generation on the system; but
- the balanced harmonic load modelling, plus balanced upstream voltage harmonics, dominated and resulted in balanced voltage harmonics overall.

This hypothesis was tested by retaining only the Ayshford PV site within the model, and investigating the resulting levels of voltage harmonics (both local to the PV site and at the BSP 33 kV busbar).

The results of this investigation are shown in Table 16: the first column shows the voltage FFT at the PV site (AYSH3), the second column at the BSP 33 kV busbar (TIVE3). This data clearly shows unbalance between phases, following the same pattern as the current harmonics for the PV site.

It is concluded that the minor unbalance seen in the current harmonics and the relative balance seen in the voltage harmonics at the PV farm sites from the MATLAB/Simulink EMT simulation are reasonable representations of the actual system.

Table 16: Voltage harmonic spectrum at AYSH3 and TIVE3 when Ayshford PV farms is the only source of harmonics in the model.



3.5.3 TIVE3 - Overall power quality assessment

The main 33 kV busbar at Tiverton (TIVE3) is the BSP of the Tiverton Network and voltage harmonic measurements at this point were made available with temporary monitors. Therefore, after considering harmonic voltage and current levels at the PV sites, the effect of the modelled harmonics at the BSP 33 kV busbar were also assessed.

Visual inspection of the three-phase voltage and current traces at TIVE3 for $4.9 \text{ s} \leq t \leq 1 \text{ s}$ shows no visible impact on the voltage waveform. The effect on current distortion is more visible: this behaviour is quite typical, and it is verified thorough the entire observation period (01-21 October 2020).

Table 16, Table 17 and Table 18 compare the maximum and minimum voltage distortion at TIVE3 and the THD values obtained from the measurements and from the simulation.

The voltage THD is calculated as the rms value of individual harmonic voltages, expressed as a percentage of the fundamental rms [10]:

$$THD = \sqrt{\sum_{h=2}^{h=100} (V_h)^2} \quad (10)$$

where h represents the harmonic order and V_h represents the individual harmonic voltage component (expressed in percent of the fundamental current). An observation window of 200 ms is applied according to [11] [12].

It is noted that overall, the simulated harmonic levels compare very well to measured values.

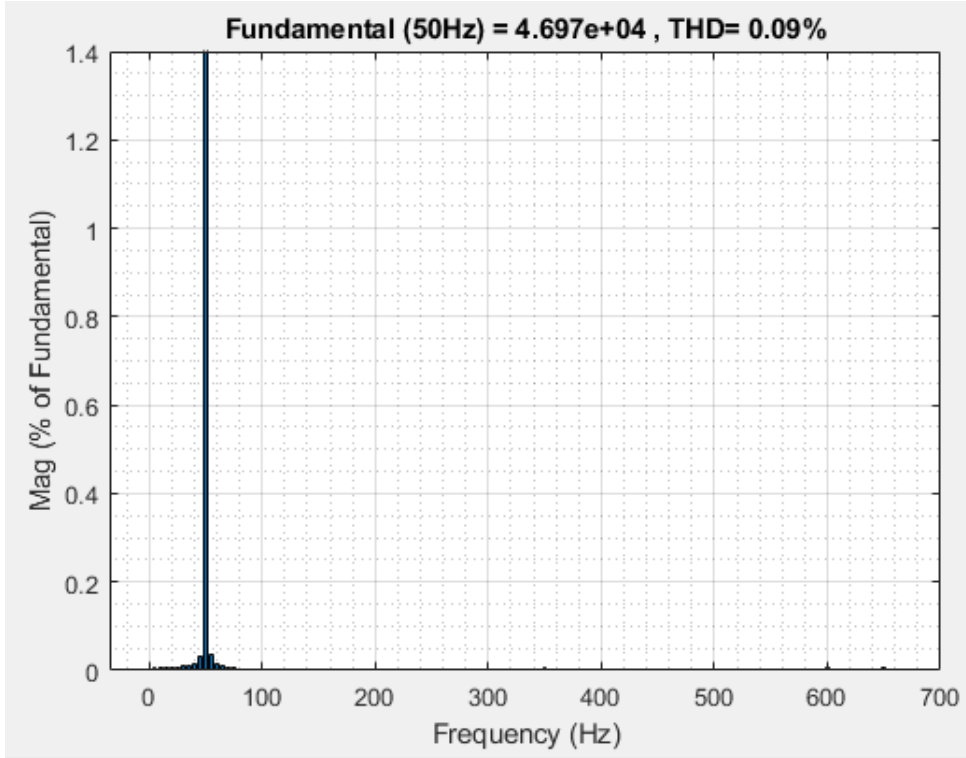
Table 17: TIVE3 maximum harmonic voltage components: comparison between power quality measurements and simulation results.

Harmonic order	PQ monitor data			MATLAB model		
	V ₁₂ (%)	V ₂₃ (%)	V ₃₁ (%)	V ₁₂ (%)	V ₂₃ (%)	V ₃₁ (%)
5	1.32	1.40	1.40	1.31	1.31	1.31
7	1.10	1.06	1.09	1.04	1.04	1.04
11	0.21	0.28	0.26	0.26	0.26	0.26
13	0.22	0.28	0.26	0.28	0.28	0.28
THD	1.60	1.67	1.55	1.73	1.73	1.73

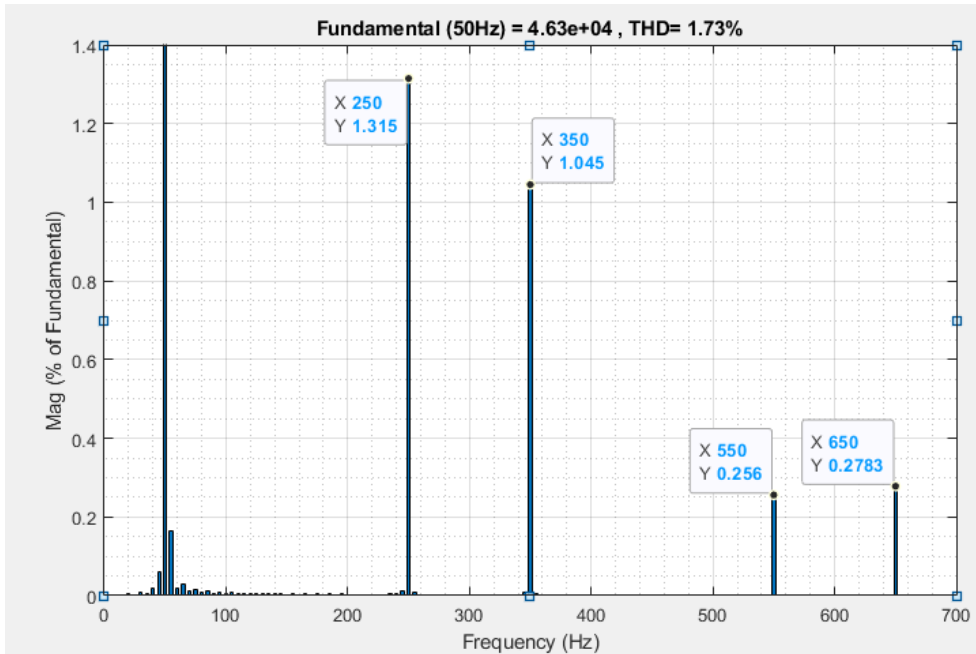
Table 18: TIVE3 minimum harmonic voltage components: comparison between power quality measurements and simulation results.

Harmonic order	PQ monitor data			MATLAB model		
	V ₁₂ (%)	V ₂₃ (%)	V ₃₁ (%)	V ₁₂ (%)	V ₂₃ (%)	V ₃₁ (%)
5	0.470	0.513	0.412	0.52	0.52	0.52
7	0.52	0.521	0.511	0.49	0.49	0.49
11	0.004	0.019	0.005	0.12	0.12	0.12
13	0.003	0.004	0.003	0.10	0.10	0.10
THD	0.67	0.75	0.66	0.73	0.73	0.73

In Figure 38, harmonic distortion results are shown for three different simulation times: $t = 1$ s and $t = 9$ s. The observation window is 10 cycles/200 ms. As expected, before harmonic injection into the model (i.e. $t=1$ s), the THD is zero. After harmonic injection, the THD is increased, and the 5th, 7th, 11th and 13th harmonic components are visible. The values shown in Figure 38



(a) FFT analysis at t=1 s.



(b) FFT analysis at t=9 s.

Figure 38: Tiverton 33 kV THD voltage calculation and THD analysis at three different simulation times.

3.5.4 Conclusions on harmonic aspects of EMT simulations

MATLAB/Simulink EMT simulations have been performed for a three-week period, based on October 2019, incorporating both fundamental and harmonic frequencies.

The output of the simulation has been compared to data from temporarily installed PQ monitors, at the three PV farm sites and at the BSP 33 kV busbar.

Minor levels of unexpected unbalance between phases were observed in the simulation data for PV site current harmonics, accompanied by arguably counter-intuitive balanced voltage harmonics at the PV sites. The unbalanced current harmonics were investigated and accepted as a reasonable artefact of the generation modelling process, and that the resulting balanced harmonics were accepted as being due to dominance of the remainder of the balanced system load and balanced upstream influence, over the minor current phase unbalance at the PV sites.

Based on the results and analysis presented, it is concluded that the MATLAB/Simulink EMT simulations provide a realistic model of the harmonic behaviour of the actual network over a three-week time series.

4 WP1 Conclusions

The aims of Work Package 1 included to establish an appropriate modelling environment in which an active filter algorithm added to existing solar inverters can be developed and tested.

A modelling environment to achieve this has been established in MATLAB/Simulink.

The underlying network model and component parameters have been assessed by undertaking a series of power flow studies and frequency response checks and comparing the results with those from a WPD DigSILENT PowerFactory model, and, where appropriate, to SCADA data. Good agreement has been found between the results for these tests from the two models and to SCADA, and it is concluded that the MATLAB/Simulink model provides a satisfactory representation of the system under study.

The capability of the developed environment to perform EMT simulation has been assessed by:

- i) comparing fundamental frequency simulation outputs (P, Q & V) to available SCADA data; and
- ii) comparing harmonic frequency simulation outputs to temporarily installed PQ monitor data.

Points of note were recognised in the simulation results, and were investigated and found to be valid. Based on the results and analysis undertaken, it is concluded that the MATLAB/Simulink EMT simulations provide a realistic model of the fundamental and harmonic behaviour of the actual network over a three-week time series.

Overall, it is concluded that the established MATLAB/Simulink modelling environment provides a realistic representation of the actual network for the purpose of developing and testing harmonic mitigation algorithms to be overlaid on already included PV inverter models.

5 Lessons learned

- It has been shown that MATLAB/Simulink software can be used to model both the 50 Hz behaviour and the harmonic behaviour of the Tiverton Network accurately. The modelling of the 50 Hz components is straightforward as identical component blocks are present in MATLAB/Simulink and DigSILENT PowerFactory. For harmonic analysis, MATLAB/Simulink showed some limitations. For example, it is not possible to model frequency-dependency of components, however, these limitations were overcome by modelling these components separately.
- Further difficulties were observed with numerical stability of the time domain solver and these were resolved by the introduction of large shunt resistors such that they have no (or absolute minimum) impact on the simulation results. For example, it was established that multiple current sources cannot be connected to the same node, unless shunt resistors are used. The dynamic model used for loads also require a large resistance connected in parallel. The resistances used in the model are greater than $10^4 \Omega$.
- The largest time-step that can be used with the current Simulink model is $8 \mu\text{s}$, due to the presence of short lines modelled using distributed parameters but this small time-step will be equally required for the active filter algorithms in the later stages. As a result, running an EMT simulation for the Tiverton Network is computationally intensive. Running one day data set takes about 20 min, using a 32 GB RAM, SSD, 1 TB Desktop PC with i-7 processor. Running a time domain simulation for one week takes slightly above 2 hrs. The size of the data generated for a week simulation is about 8 GB. To limit the size of data generated, a one-month study will be run using four different simulations, by feeding different SCADA and power quality data set to the same network model.
- Both the power quality monitor data and the SCADA data are used to develop dynamic models, However, they present a significantly different time resolution. Therefore, appropriate scaling needs to be applied when the data are imported to ensure that the PV farms and the load models are temporally aligned.

6 Bibliography

- [1] Mathworks Technical Documentation, “Simulink Product Page,” [Online]. Available: <https://www.mathworks.com/products/simulink.html>. [Accessed 12 05 2020].
- [2] OPAL-RT Technologies, “RT-LAB real time simulation software,” [Online]. Available: <https://www.opal-rt.com/software-rt-lab/>. [Accessed 12 05 2020].
- [3] DigSILENT Power Factory Technical Reference Documentation, “General Load,” 2019.
- [4] J. Arrilaga and C. Arnold, Computer analysis of power systems, John Wiley & Sons, Ltd., 1990.
- [5] J. Martinez-Velasco, Introduction to Electromagnetic Transient Analysis of Power Systems, John Wiley and Sons , 2014.
- [6] MathWorks Help Center, “ode23tb,” [Online]. Available: <https://uk.mathworks.com/help/matlab/ref/ode23tb.html>. [Accessed 11 05 2020].
- [7] H. Akagi, Y. Kanazawa and A. Nabae, “Instantaneous Reactive Power Compensators Comprising Switching Devices without Energy Storage Components,” *IEEE Transactions on Industry Applications*, Vols. IA-20, no. 3, pp. 625-630, May 1984.
- [8] R. Park, “Two reaction theory of synchronous machine,” *AIEE Transection*, bol 48, pp 716-730, 1929.
- [9] The Energy Networks Association, “Engineering Recommendation G5/5: Planning Levels for Harmonic Voltage Distortion and the Connection of Non-Linear Equipment to Transmission Systems and Distribution Networks in the United Kingdom,” 2020.
- [10] International Electrotechnical Commission, “IEC 61000-4-7, Electromagnetic compatibility (EMC) - Part 4-7: Testing and measurement techniques –General guide on harmonics and interharmonics measurements and instrumentation, for power supply systems and equipment connected thereto,” 2002.
- [11] International Electrotechnical Commission, “IEC 61000-4-30, Electromagnetic compatibility (EMC) - Part 4-7: Testing and measurement techniques –Power quality measurements methods,” 2003.
- [12] a-eberle, “Power Quality Analyser PQ box 100,” [Online]. [Accessed 13 05 2020].
- [13] DigSILENT GmbH, “Technical reference documentation for models,” 2019.

- [14] A. Hariri and M. Faruque, "Impacts of distributed generation on power quality," in *North American Power Symposium (NAPS)*, Pullman, WA, 2014.

Appendix A Literature Review - Executive Summary

This literature review addresses how distribution network connected inverters associated with renewable energy sources may provide harmonic compensation as an additional, or “ancillary service”. In other words, how inverters may be used as Active Filters while simultaneously delivering fundamental power.

Current harmonics are caused by nonlinear devices connected to the power grid as they draw or inject non-sinusoidal currents when supplied with a sinusoidal voltage. These current harmonics interact with the power grid’s impedance to create voltage distortion that can adversely affect the distribution system’s equipment, and customer equipment that is connected to the system. Power quality standards have been developed for the UK system (currently G5/4-1, with G5/5 expected to be implemented during 2020) that define voltage distortion planning levels. Newly connected equipment is expected to be compliant.

Mitigation of harmonics produced by connected non-linear equipment, loads or generation, can be achieved by installing either Passive Filters (combinations of inductive, capacitive and resistive components that sink the harmonic currents) or Active Filters (power converters controlled to inject current harmonics with opposing phase angles). Active Filters can either be standalone systems, or can be implemented as additional control algorithms placed within an existing power converter (the focus of this WPD innovation project).

The main functional blocks required within an Active Filter controller are: harmonic current or voltage extraction to establish harmonic levels; a current loop controller to establish the required level of intervention; and gate signal generation to implement the required electrical intervention. This review details different implementations for each of these main functional blocks, together with advantages and disadvantages of each implementation.

The review also identifies previous work that has investigated power converter controller implementations that deliver both fundamental power and harmonic mitigation. In these cases, active filtering is performed as an ‘ancillary service’. Three specific implementation examples are described in detail, together with simulation results. Each simulation shows the feasibility of mitigating harmonics and also illustrates: (i) the requirement to limit harmonic mitigation in coordination with fundamental power output, to operate the power converter within equipment ratings; and (ii) the ability of mitigating time-varying harmonics.

Results from hardware implementations of Active Filter operation within multi-functional inverters are not very common in the literature, partly due to the novelty of this approach. However, two examples are presented that again show successful mitigation of harmonics (one with additional phase balancing functionality, and one for a hybrid wind–PV system). One further example is also presented where harmonic mitigation functionality was added to a STATCOM operating in south-west Scotland on a system that was experiencing voltage total harmonic distortion (THD) of up to 3.3%. With active filter functionality enabled, voltage THD was successfully reduced to around 1%.

This literature review has provided a detailed summary of previous research and development that can beneficially be built upon in the work Swansea University are

undertaking to develop an algorithm that can improve the network's harmonic levels by controlling existing Distributed Generation inverters, acting individually or as a coordinated group.

Appendix B Description of the Tiverton Network

An overview of the area to be included in the model is shown in Figure 39. The main busbar at Tiverton is rated 33 kV and the substation is supplied by two 132/33 kV transformers. The main busbar supplies eight 11 kV busbars (anticlockwise listing):

- Tiverton Moorhays (bus 7735, TIVM5)
- Tiverton South (bus 7737, TIVS5)
- Bridge Mills (bus 7117, BRIM5)
- Cullompton (bus 7236, CULL5)
- Dunkeswell (bus 7271, DUNK5)
- Hemyock (bus 7367, HEMY5)
- Burlescombe (bus 7136, BURL5)
- Tiverton Junction (bus 7733, TIVE5)

The network includes: one radial feeder (Tiverton 33kV, Ayshford Court, Burlescombe, Hemyock, Dunkeswell); two ring circuits (Tiverton 33 kV, Tiverton Moorhays, Tiverton South and Tiverton 33kV), (Tiverton 33 kV, Cullompton Solar Park, Bridge Mills, Cullompton, Stoneshill SP, and Tiverton 33kV); plus Tiverton Junction, directly connected to the Tiverton 33kV bus.

Three solar farms exist within the 33 kV system: Ayshford Court (bus 9370, AYSH3), Stoneshill farm (bus 9850, STFA3) and Cullompton (bus 9830, CMPV3). The main characteristics of the three PV farms are as follows:

Ayshford:

- Connection agreement: Export capacity = 4,550 kva; import capacity = 50 kva
- The PV farm includes nine 500 kVA 33/0.4 kV transformers; each transformer connecting to four junction boxes; each junction box connecting up to 7 Siemens Sinvert PVM20 inverters

Cullompton:

- Connection agreement: Export capacity = 4,082 kva; import capacity = 60 kva
- The PV farm includes two 2000 kVA 33/0.4 kV transformers; each transformer connecting to one HEC Fresun 1800 KVA inverter

Stoneshill:

- Connection agreement: Export capacity = 4,000 kva; import capacity = 50 kva
- The PV farm includes five 33/0.38 kV transformers; each transformer connecting to one 800 kVA inverter.

Harmonic Mitigation Work Package One – Model Development

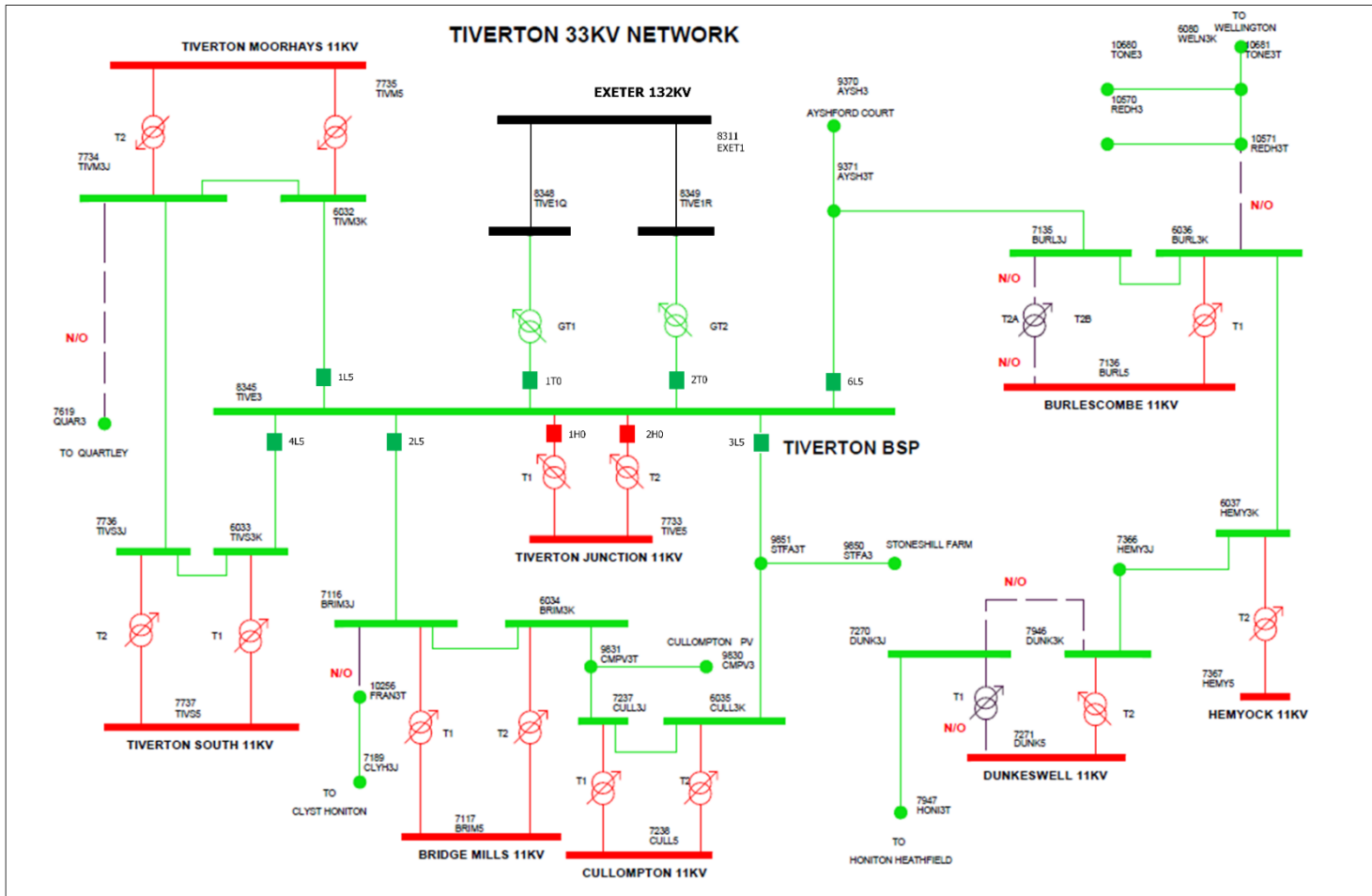


Figure 39: Overview of the Tiverton Network.

Appendix C Description of the data files provided by WPD

C.1 SCADA data

Swansea University received from WPD a detailed set of load flow data on December 19th, 2019. These data covered all Tiverton Network for the period of December 2018 – October 2019. A summary of the data included in this set is provided in Table 19.

The SCADA data consists in half-hour samples for each one of the quantities shown in the table.

Table 19: Overview of the data provided by WPD for Tiverton 33 kV network on December 19th, 2019.

Site	Measurement point	S	P	Q	V (33 kV)	V (11 kV)
Tiverton BSP (2 Tx site)	Tiverton 33 kV CB 1T0	X	✓	✓	X	
	Tiverton 33 kV CB 2T0	X	✓	✓	X	-
	Tiverton 33 kV CB 1L5	X	✓	✓	X	-
	Tiverton 33 kV CB 2L5	X	✓	✓	X	-
	Tiverton 33 kV CB 3L5	X	✓	✓	X	-
	Tiverton 33 kV CB 4L5	X	✓	✓	X	-
	Tiverton 33 kV CB 6L5	X	✓	✓	✓	-
Tiverton South (2 Tx site)	Tiverton South (33/11 kV) T1	X	✓	✓	X	✓
	Tiverton South (33/11 kV) T2	X	✓	✓	X	-
	Tiverton South VT2	X	X	X	✓	
Tiverton Moorhayes (2 Tx site)	Tiverton MHayes (33/11 kV) T1	X	✓	✓	X	✓
	Tiverton MHayes (33/11 kV) T2	X	✓	✓	X	
	Tiverton Moorhayes 1S0	X	X	X	X	X
Tiverton Junction (2 Tx site)	Tiverton Jun (33/11 kV) T1	✓	X	X	X	✓
	Tiverton Jun (33/11 kV) T2	✓	X	X	X	✓
Ayshford	Ayshford solar park	X	✓	✓	✓	-
Stoneshill	Stoneshill solar park 1L5	X	✓	✓	✓	-
Cullompton	Cullompton solar park CB 1L5	X	✓	✓	✓	-
Cullompton (2 Tx site)	Cullompton(33/11 kV) T1	X	✓	✓	X	✓
	Cullompton (33/11 kV) T2	X	✓	✓	X	
	Cullompton VT2	X	X	X	✓	X
Bridge Mills (2 Tx site)	Bridge Mills (33/11 kV) T1	X	✓	✓	X	✓
	Bridge Mills (33/11 kV) T2	X	✓	✓	X	
	Bridge Mills 1S0	X	X	X	✓	X
Burlescombe (2 Tx site)	Burlescombe (33/11 kV) T1	✓	X	X	X	✓
	Burlescombe(33/11 kV) T2	✓	X	X	X	✓
	Burlescombe 33 kV CB 1H0	X	X	X	✓	X
Dunkeswell	Dunkeswell(33/11 kV) T2	X	✓	✓	X	✓

(2 TX site)	Dunkeswell 33 kV, VT2	X	X	X	✓	X
Hemyock (1 Tx site)	Hemyock (33/11 kV) T2	X	✓	✓	X	✓
	Hemyock 33kV 1S0	X	X	X	✓	X

C.2 Power Quality (PQ) data

During the months of September and October 2019, WPD performed harmonic measurements at a four busbars of the Tiverton Network, with the aim to provide Swansea University information about the harmonic levels in the system and aid model development. Ultimately, the harmonic measurements carried out in October 2019 were used because the readings taken in September 2019 used protection CT secondary wiring and contained high-frequency harmonic components that were considered not reliable.

The power quality meters used were PQ-Box 100 [13]. The readings are taken every 10 s.

With reference to the network diagram shown in Appendix B, the following busbars were monitored for harmonic assessment:

1. Tiverton BSP (8345/TIVE3) - Voltage only measurements
2. Ayshford Court (9370/AYSH3) - voltage and current
3. Stonehill Farm (9850/STFA3) – voltage and current
4. Cullompton (7238/CULL5) – voltage and current

For Tiverton 33 kV busbar the data included voltage magnitude, harmonic levels, and THD. For the three solar farms, additional information is provided in terms of fundamental and harmonic current, active, reactive and apparent powers.

C.3 Modelling of the data for EMT simulations

An overview of the time scale for the SCADA data and the power quality data provided by WPD for October 2019 is presented in Table 20. Each row shows the period of where SCADA and power quality data are available. For each power quality recording, a different row is provided as the readings start and stop at different times

Harmonic Mitigation Work Package One – Model Development

Table 20: Overview of the SCADA data and power quality data provided by WPD for October 2019, and corresponding simulation time.

		01.10. 2019				02.10. 2019				...	21.10. 2019	25.10. 2019	31.10. 2019	
		24/00 AM	06 AM	12 PM	18 PM	24/00 AM	06 AM	12 PM	18 PM	24/00 AM				
SCADA Data	All network	0:00											24:00	
PQ-DATA	AYSH32 files			12:57							05:37			
	CULL53 files			09:39								09:33		
	STFA33 files			10:47								08:52		
	TIVE31 file			8:22								08:27		
Simulation time (sec)		0.3	1.5	2.7	3.9	5.1	6.3	7.5	8.9	9.9	149.1

As explained in Section 3.1, each SCADA data point is modelled with 0.1 second interval. Therefore, modelling one day of SCADA data requires 4.8 s simulation time.

The power quality data was measured with a higher resolution of 10 s time interval. Therefore, the number of data points in 24 h of real time is equal to 8640, i.e. 6 samples * 60 minutes * 24 hours. These data points must equally distributed in 4.8 s of Simulink time in order to match the SCADA data. Hence, by dividing the simulation time of one day by the number of data points (4.8 s/ 8640), an interval of 0.556 ms corresponds to each data point from the power quality meters.

To convert the time of any data point from SCADA measurements to the corresponding simulation time then the following formula can be used:

$$T_{sim,S} = [(4.8 i - 4.8) + 0.4] + 0.2 * h \quad (\text{sec})$$

where $T_{sim,S}$ is the simulation time, i is the SCADA day number, h is the SCADA time in hours (using 24 h system). For example, if the SCADA data point is on 2nd of October at 16:30, then this data point ($i=2, h=16.5$) will appear at $T_{sim,S} = 8.5$ s.

For the PQ data, the formula is as follows:

$$T_{sim,PQ} = [(4.8 i - 4.8) + 0.4] + 0.2 * h + 0.003336 * m + 55.6 * 10^{-6} * s \quad (\text{sec})$$

where $T_{sim,PQ}$ is the simulation time, i is the PQ day number, h is the PQ time in hours (using 24 h system), m is PQ time in minutes, and s PQ time in seconds.

For example, if the PQ-data point is on 2nd of October at 16:30:50, then this data point ($i=2, h=16, m=30, s=50$) will appear at $T_{sim} = 8.50286$ s. If the PQ-data point is on 4th of October at 12:45:00, then this data point ($i=4, h=12, m=45, s=0$) will appear at $T_{sim,PQ} = 17.35012$ s.

From Table 20:

- The data recorded at Ayshford PV farm started on 1/10/19 at 12:58 which gives the starting simulation time at $T_{sim,PQ}=2.990$ s
- The data recorded at Cullompton PV farm started on 1/10/19 at 09:39 which gives a starting simulation time at $T_{sim,PQ}=2.333$ s
- The data recorded at Stoneshill PV farm started on 1/10/19 at 10:48 which gives a starting simulation time at $T_{sim,PQ}=2.560$ s

Appendix D Validation of frequency sweep results within MATLAB/Simulink

The impedance of any electrical systems is a function of the frequency and it depends on the values of individual components resistance, inductance and capacitance and of their connection. For the Tiverton Network, the harmonic impedance is the result of the interaction of the network components as well as of the interaction with the upstream network.

This section of the report explains the process implemented to validate the harmonic impedance model in MATLAB and explain any discrepancies with the DigSILENT PowerFactory model provided.

D.1 Frequency dependence of upstream system

For the power frequency studies shown so far, an equivalent upstream system model equal to the short-circuit contribution was utilised. For harmonic studies it is important to capture the frequency dependency of the upstream network and hence a frequency dependent equivalent model is required. In a dedicated power system analysis tool performing simulation in frequency domain, this can be simply provided as a tabular data or by means of equations approximating the frequency dependency. MATLAB circuit components do not support modelling of frequency dependency in a tabular format as in DigSILENT PowerFactory. This was, confirmed with Mathworks technical support, though this feature may become available in future releases of the software.

As a result, for this project, an alternative solution was developed. Parallel resonant blocks have been connected to represent the frequency dependency of the equivalent upstream network. These components have been chosen to mimic the different resonance conditions of the upstream system. The visualization of this model is shown in Figure 40, while the values of resistance, inductance and capacitance for each block are shown in Table 21.

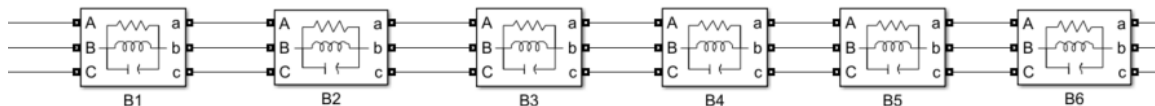


Figure 40: Representation of the frequency dependency.

Table 21: Values of the components Figure 40.

	B1	B2	B3	B4	B5	B6
R (Ω)	68	94	14	9	4	10
L (mH)	10.3	6.7	3.3	0.397	9.573	2.255
C (μ F)	35	32	340	140	240	200

A comparison between the frequency responses of the upstream network in Simulink and in DlgSILENT PowerFactory at the Exeter 132kV bus is shown in Figure 41. This graph has been obtained by disconnecting the system downstream of EXET1 in both simulation models. This figure shows that the two representations are very close, and demonstrates that the ‘cascaded’ model approach implemented in MATLAB/Simulink provides a good representation the network frequency dependency shown in DlgSILENT PowerFactory.

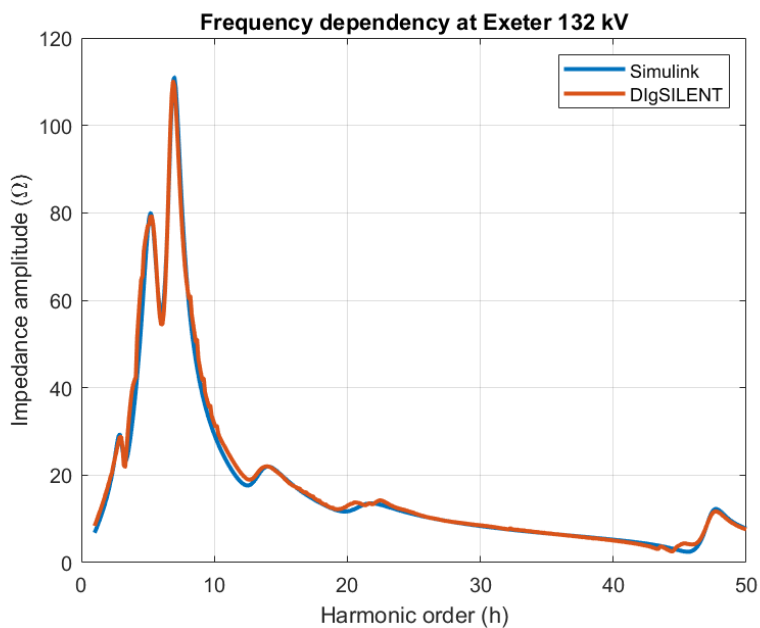


Figure 41: Comparison for frequency response of the upstream network.

D.2 Harmonic frequency scans

While carrying out the harmonic impedance analysis on the Tiverton Network it became apparent that the initial frequency scans led to some discrepancies between results from the DlgSILENT PowerFactory and MATLAB models.

Therefore, to explain these differences, Swansea University built smaller models of the system and worked closely with Mathworks support to validate the impedance model.

In all these models, the stray capacitances of the transformers were disconnected and ignored, as they make the model more complex without affecting significantly the frequency response. Additionally, as observed in earlier work, these stray capacitances seemed to create instability for the dynamic model.

Validation 1 – 132 kV Distributed parameters line

Initially the frequency response of the distributed parameter line between bus TIVE1Q and bus EXET1 (where the equivalent system is connected) was calculated. A screenshot showing this component, the impedance measurement block and the main parameters in Simulink is shown in Figure 42. The block labelled as 'Z' is responsible for calculating the impedance frequency response. The same line was studied in DgSILENT PowerFactory.

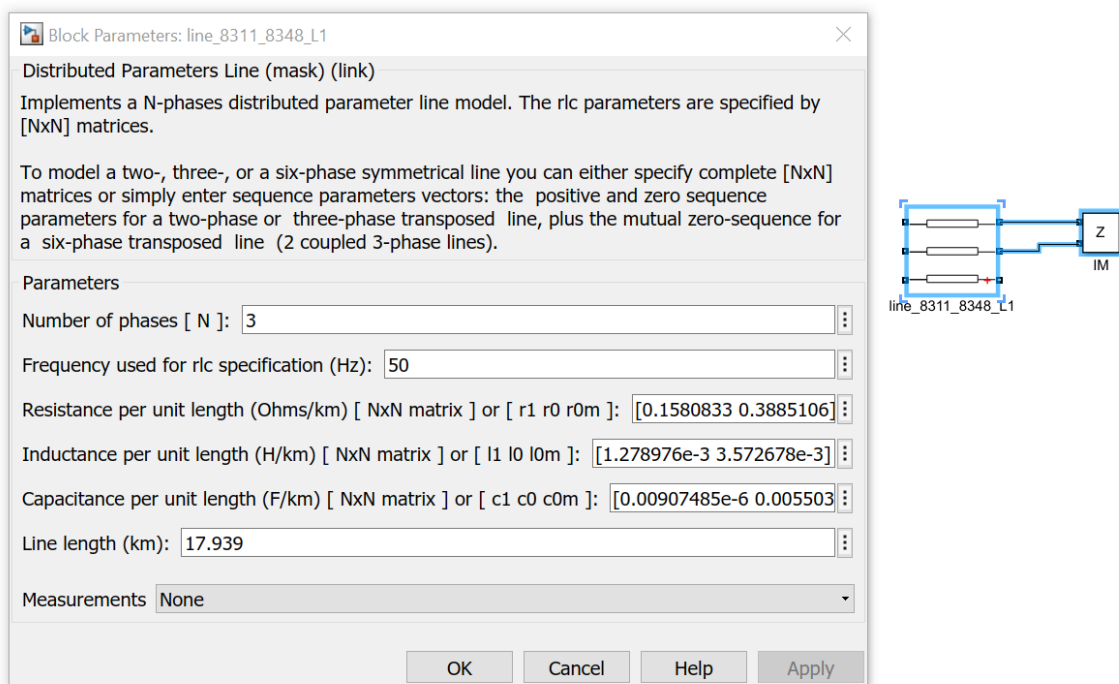


Figure 42: Distributed line model block in Simulink, main parameters and block used to calculate impedance.

To further validate the two models, a script was composed to calculate the frequency response in MATLAB. The script calculates the distributed line parameters taking into account the characteristic impedance and the propagation constant, as well as the hyperbolic correction factors [7]. As a result, the impedance and admittance of the line are:

$$\mathbf{Z} = \mathbf{Z}_c' \cdot l \cdot \frac{\sinh \boldsymbol{\gamma} \cdot l}{\boldsymbol{\gamma} \cdot l} \quad (5)$$

$$\mathbf{Y} = \frac{1}{2} \cdot \mathbf{Y}_c' \cdot l \cdot \frac{\tanh (\boldsymbol{\gamma} \cdot l/2)}{\boldsymbol{\gamma} \cdot l/2} \quad (6)$$

where l is the line length, $\boldsymbol{\gamma}$ is the propagation constant, \mathbf{Z}_c' is the characteristic impedance per unit length, \mathbf{Y}_c' the characteristic admittance per unit length, defined as:

$$\boldsymbol{\gamma} = \sqrt{\mathbf{z}\mathbf{y}} \quad (7)$$

$$\mathbf{Z}_c' = \sqrt{\mathbf{z}/\mathbf{y}} \quad (8)$$

$$\mathbf{Y}_c' = 1/\mathbf{Z}_c' \quad (9)$$

where \mathbf{z} and \mathbf{y} indicate the per-unit length impedance and admittance (all the quantities using bold fonts are complex numbers).

The comparison of the frequency response using the script, the Simulink and DigSILENT PowerFactory is shown in Figure 43. Frequencies up to the 200th order are shown because the first resonant frequency for this line is around 160th harmonic order. The graph indicates a good agreement between the models, thus giving confidence that the frequency response for distributed lines in Simulink is the same as in DigSILENT PowerFactory.

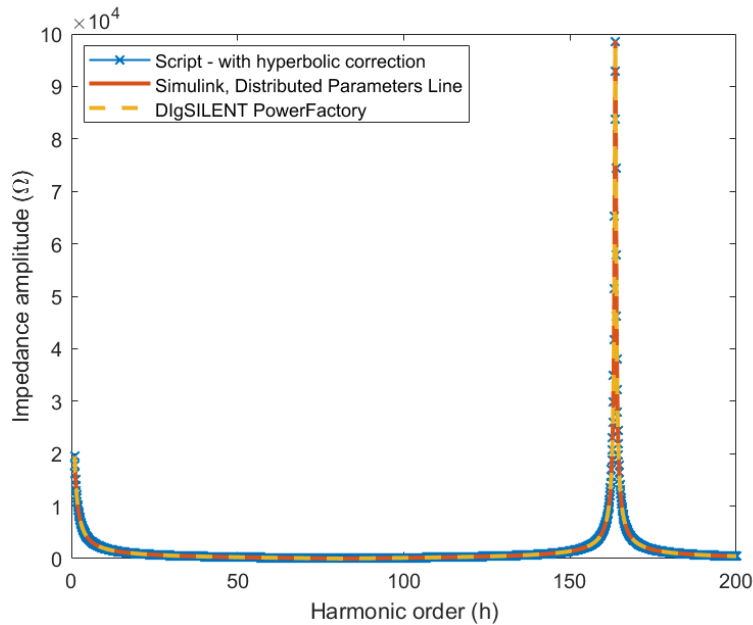


Figure 43: Validation 1 - Comparison between script, Simulink and DigSILENT PowerFactory.

Validation 2 – 132 kV Distributed parameters line and upstream equivalent source

A second validation test was carried out to verify the correctness of the equivalent source model. In this case, the equivalent source at Exeter 132 kV was connected to the cable model – to achieve a valid comparison, the frequency dependency capability within PowerFactory of the upstream network was disabled, due to the Simulink environment not having this function.

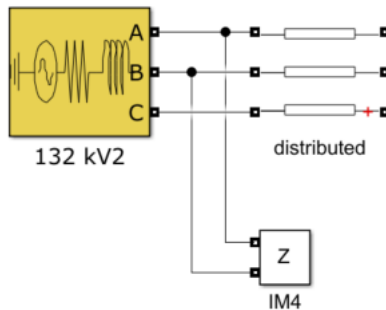


Figure 44: System built for Validation case 2.

The equivalent impedance of this system is calculated also using a script. Essentially, the total impedance seen by the impedance measurement block is obtained as the parallel of the line

impedance and of the source impedance, for various frequencies. The hyperbolic correction factors are taken into account.

A comparison between the script, the Simulink and the DigSILENT PowerFactory model is shown in Figure 45. Given the high degree of match between the three graphs, it can be concluded that the equivalent source and the combined line model in Simulink replicate accurately the DigSILENT PowerFactory frequency response.

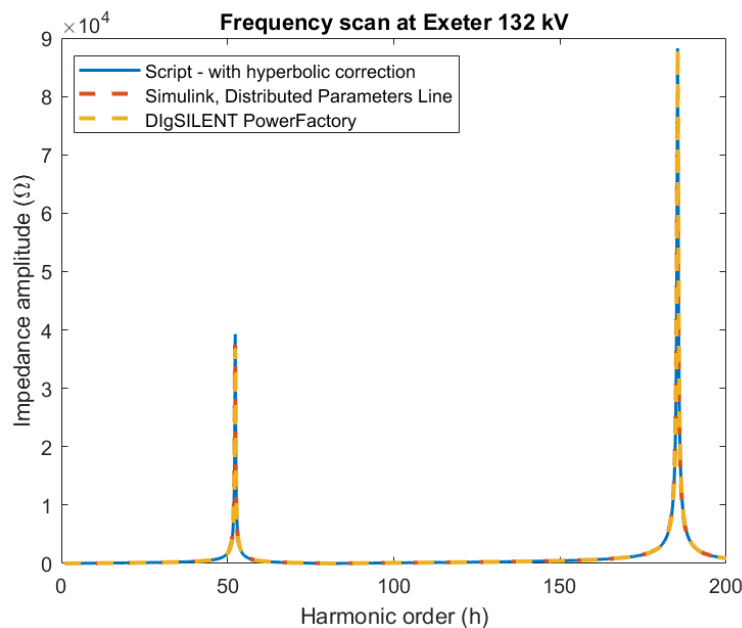


Figure 45: Validation 2 - Comparison between script, Simulink and DigSILENT PowerFactory.

Validation 3

The third validation experiment consisted in adding one of the Tiverton 132/33 kV transformers and allowed validation of the transformer model. The model in this case therefore includes the 50 Hz the equivalent source (as in Validation 2), one line section and one transformer, and the three elements are connected in series. For this test, it is possible to calculate the equivalent impedance at both sides of the transformer (transformer secondary side left open).

These two results are shown in Figure 46 and Figure 47 for the 132 kV and the 33 kV bus, respectively. While the results at the 132 kV bus match quite well, one can notice an increasing difference between the two models for frequencies above the 100th harmonic at the 33 kV bus.

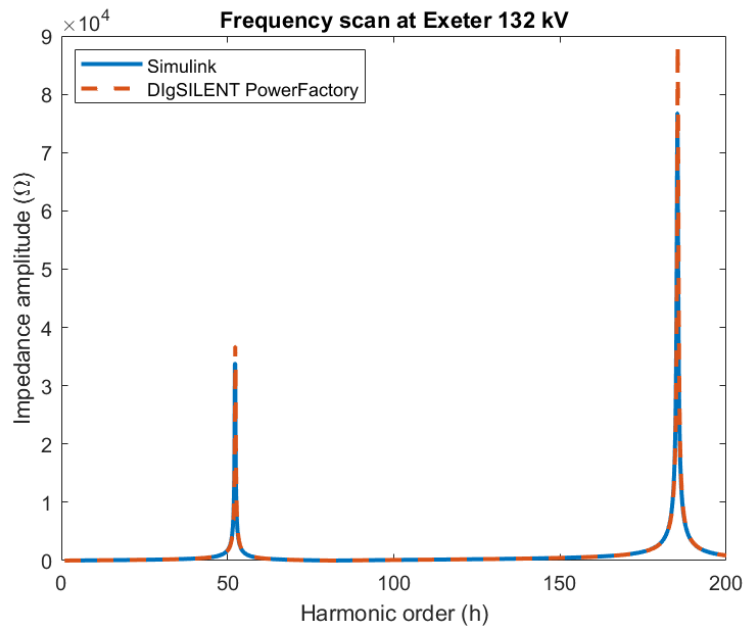


Figure 46: Validation 3a - Comparison between Simulink and DlgSILENT PowerFactory when eddy current-/copper losses ratio is 0.1.

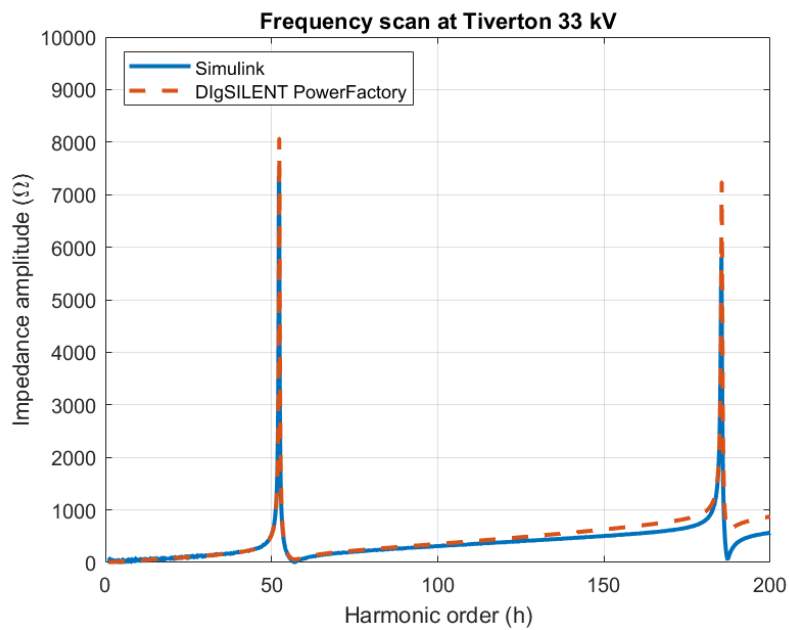


Figure 47: Validation 3a - Comparison between Simulink and DlgSILENT PowerFactory at TIVE3 with eddy current-/copper losses ratio set to 0.1.

Even if this region is above the frequencies of interest for this project, the cause of this difference was still worth investigating because it could affect the frequency response when a high number of components was connected.

After ensuring that all components were modelled and connected correctly, it was observed that the DlgSILENT PowerFactory model includes the magnetisation branch of the transformer and one parameter that is used to express the ratio of eddy current-/copper losses in the transformer.

For the Tiverton 132/33 kV transformers, the value used in the DlgSILENT PowerFactory model provided by WPD was 0.1, as shown in Figure 48⁸.

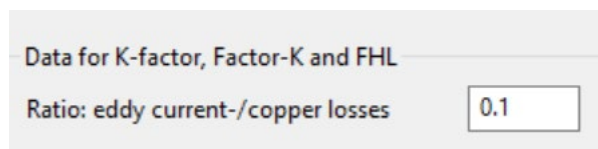


Figure 48 Transformer K-factor in DlgSILENT PowerFactory for the 132/33 kV transformers.

After discussion with Mathworks technical support, it was concluded that this value cannot be modelled in Simulink. Therefore, the eddy current-/copper losses value was changed to zero in DlgSILENT PowerFactory and the scans were repeated. The results obtained after implementing this change are included in Figure 49 and Figure 50 for the 132 kV and 33 kV busbar, and they show a good overlap between the two models. This result confirms that the mismatch in the modelling basis (as seen in Figure 49) was causing a discrepancy between Simulink and DlgSILENT PowerFactory.

⁸ According to the DlgSILENT PowerFactory documentation, 0.1 is the 'default' value [7]. After discussion with the DlgSILENT PowerFactory technical support, it has been clarified that the 'eddy current-/copper losses' ratio models the stray losses in the windings and is not related to core losses.

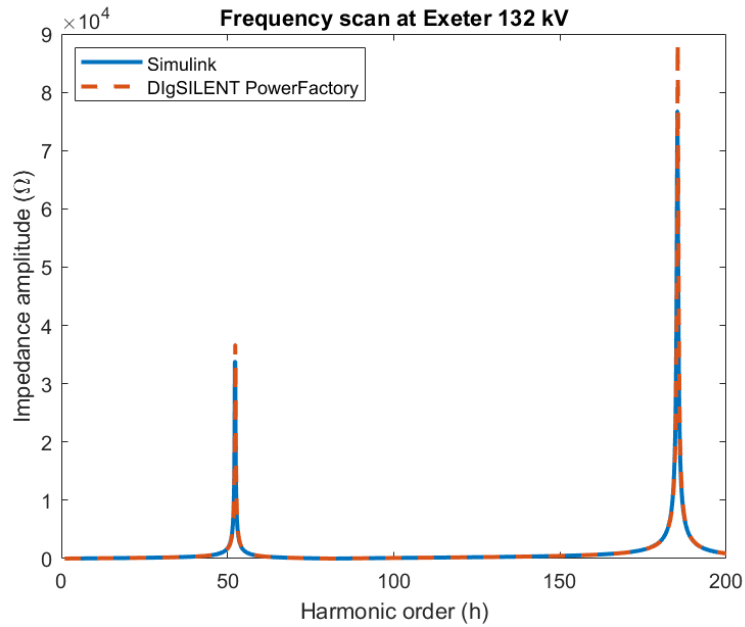


Figure 49: Validation 3b - Comparison between Simulink and DlgSILENT PowerFactory at EXET1 after modifying the ratio eddy current-/copper losses to zero.

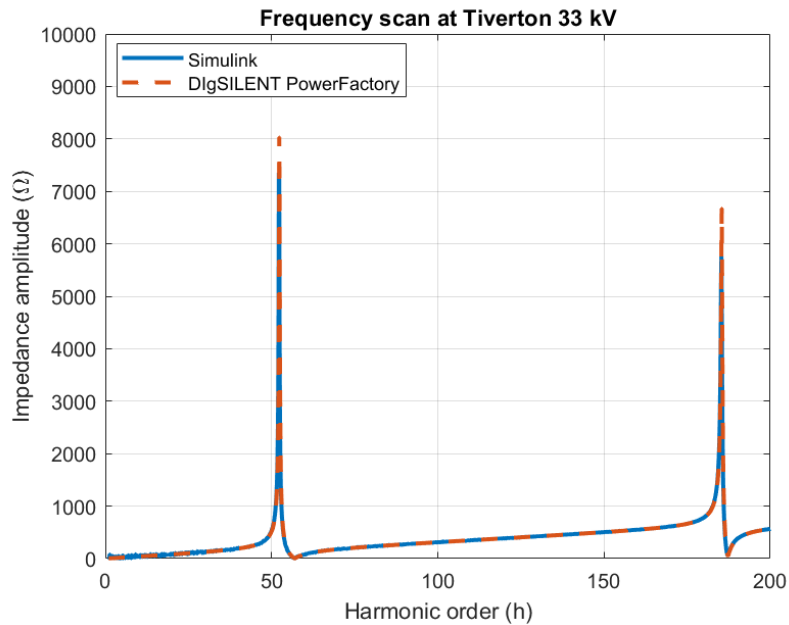


Figure 50: Validation 3b - Comparison between Simulink and DlgSILENT PowerFactory at TIVE3 after modifying the eddy current-/copper losses ratio to zero.

Radial feeder

After modifying the ‘eddy losses-/copper losses’ ratio to a value of zero, more components were added in Simulink including the radial network up to Hemyock. During this process, a good match was observed except when the load at Hemyock was added. For the case considered in this section (Summer Maximum Load Minimum Generation), the load at Hemyock is a mix of a resistive and a capacitive component (positive active power and negative reactive power).

In the DigSILENT PowerFactory model provided by WPD, all loads are modelled using load type ‘Model 1’. The input to the model are active and reactive power values, and then the PowerFactory software automatically calculates the corresponding circuit components. For the purpose of calculating the frequency scan in PowerFactory, the load is modelled as series-connect resistance and inductance (R and L) when the reactive power is positive, and as a parallel-connected resistance and capacitance (R and C) when the reactive power is negative [3]. These two representations are shown in Figure 51.

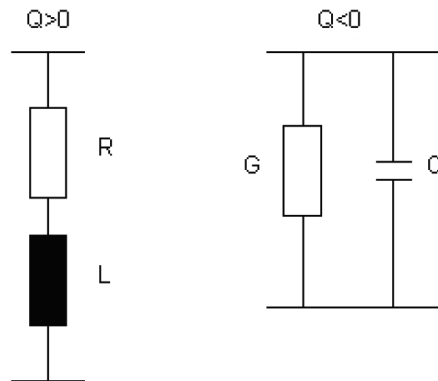


Figure 51: Equivalent load representation used for positive and negative reactive power – image extracted from DigSILENT PowerFactory load model documentation [3].

Initially a series representation of R and C components was adopted for the load model in the Simulink model, however, this was leading to discrepancy in the frequency scans between Simulink and PowerFactory. Therefore, the load was changed to a parallel representation in Simulink. Figure 52 and Figure 53 show the resulting frequency scans obtained for three cases:

1. DlgSILENT PowerFactory;
2. Simulink with parallel representation; and
3. Simulink with series representation.

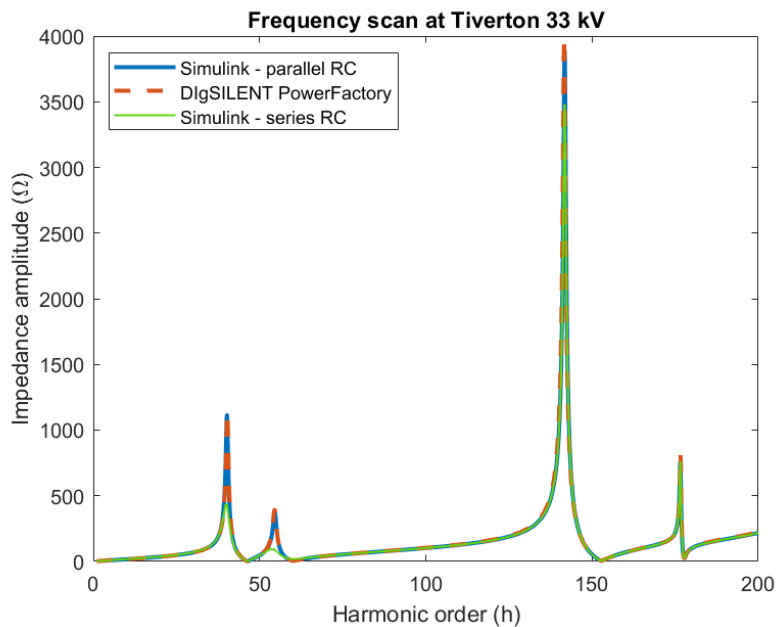


Figure 52: Comparison between Simulink and DlgSILENT PowerFactory at the TIVE3 bus for changing load representation at HEMY5.

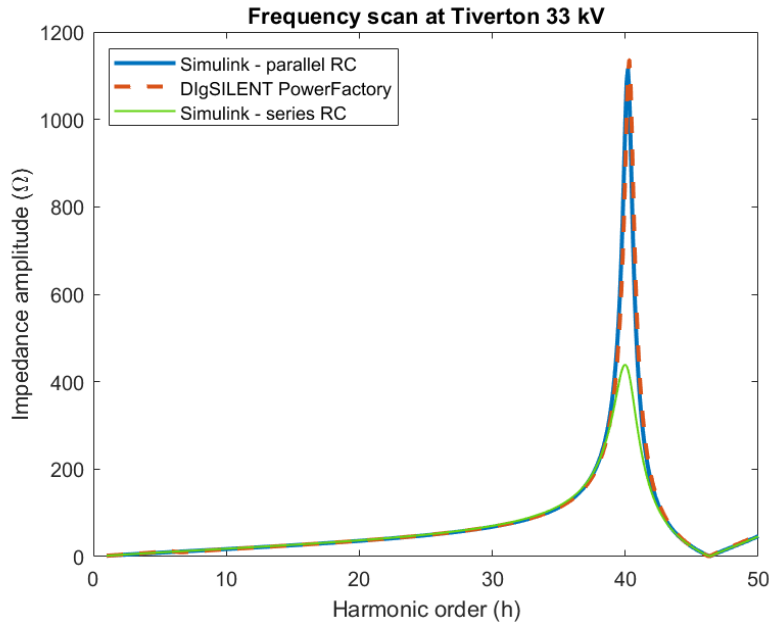


Figure 53: Comparison between Simulink and DlgSILENT PowerFactory at the TIVE3 bus for changing load representation at HEMY5 – zoomed in representation for harmonic orders up to the 50th.

It is evident that changing the load representation has a large impact on the frequency scan results: while the resonant frequencies are the same in the three cases, the damping is less pronounced with the parallel RC model within Simulink. This phenomenon is particularly visible in Figure 53. On the contrary, the parallel RC model representation shows results that match PowerFactory.

Complete network

Following on completion of the analysis on the radial feeder. More components were added to build the complete network. While carrying out this process, other minor discrepancies between the two models were identified. For example, in DlgSILENT PowerFactory the capacitance of the line connecting StonesHill PV farm to the system is equal to zero. Initially, an attempt was made to include small capacitances for these lines in Simulink, as this software does not accept zero values. However, it was observed that these capacitances, although small, had an impact in the high-frequency ranges (around the 140th harmonic). Therefore, it was decided to model these lines as series branches consisting of lumped R and L components, as this representation does not require a capacitance value. By making this change, the match between the response of the two models was found to be very close for all cases studied.

The frequency scans for the complete network are shown in Figure 3, Figure 4 and Figure 5. All figures are obtained with the PowerFactory eddy current-/copper losses ratio equal to zero. The only capacitive load included in the network for this case is shown in the one connected at HEMY5, while all other loads are inductive and therefore a series representation is used.

The graphs show that the Simulink model and the DlgSILENT PowerFactory model have the same behaviour in terms of harmonic impedance. More specifically, the two models exhibit series and parallel resonances at the same frequencies, and with the same amplitude.

These results confirm that the Simulink model is able to duplicate the basic harmonic behaviour of the DlgSILENT PowerFactory model thus reasonably allowing correct modelling of harmonic propagation through the Tiverton Network.

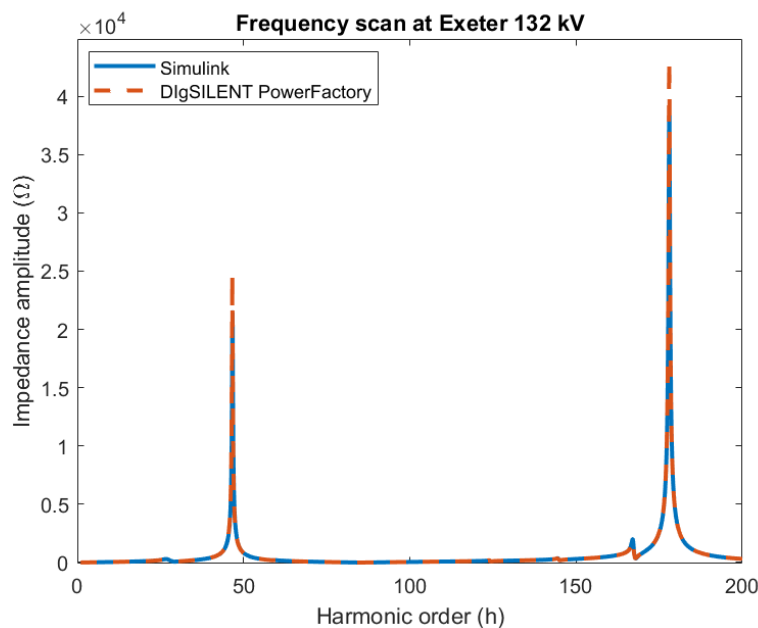


Figure 54: Comparison between Simulink and DlgSILENT PowerFactory – EXET1 bus.

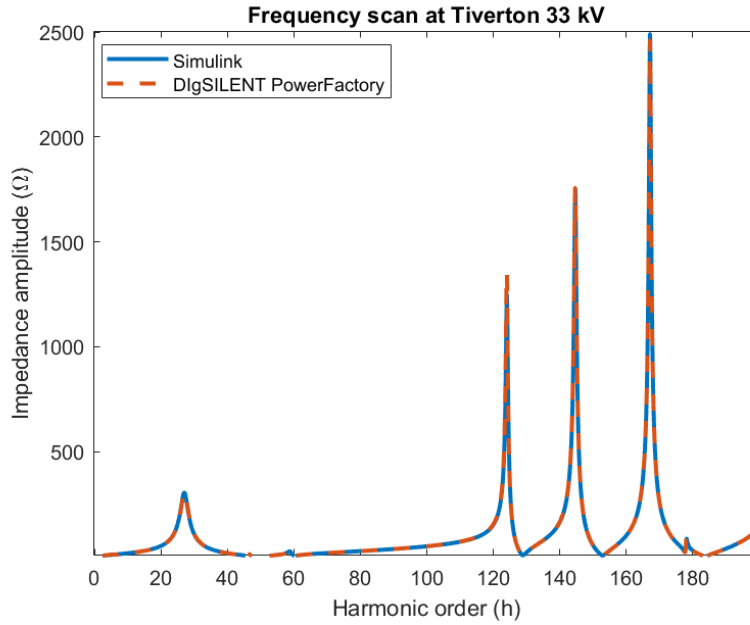


Figure 55: Comparison between Simulink and DlgSILENT PowerFactory for the complete network – TIVE3 bus.

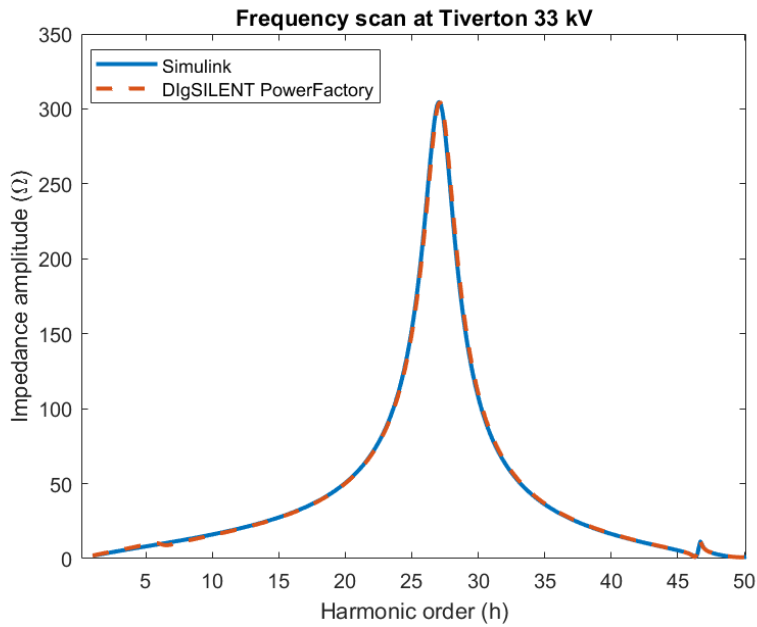
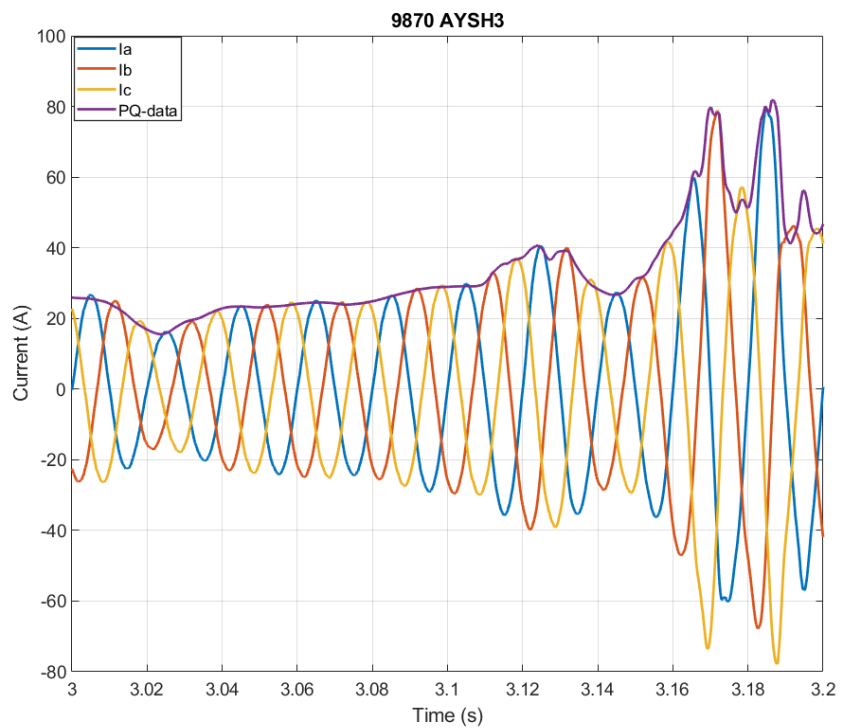
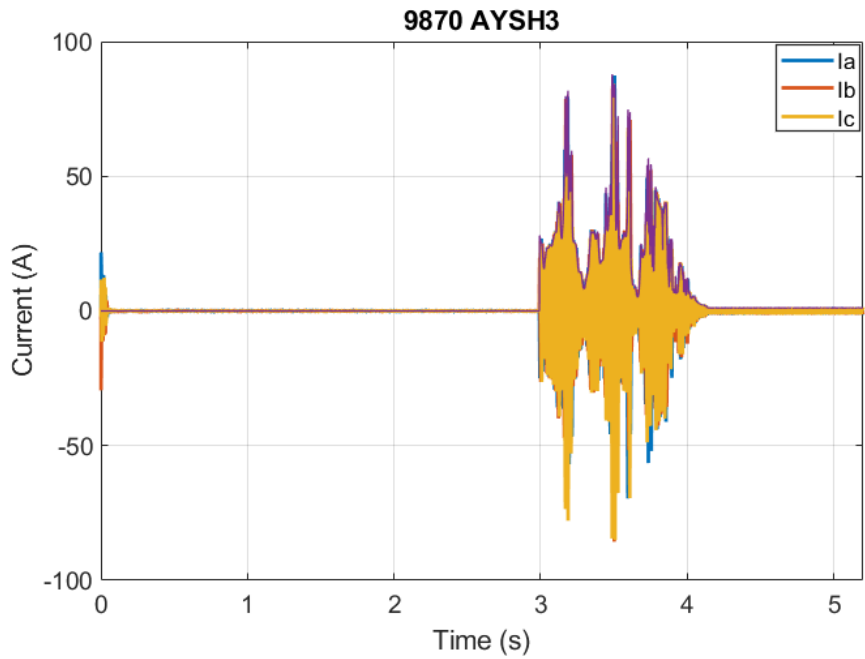
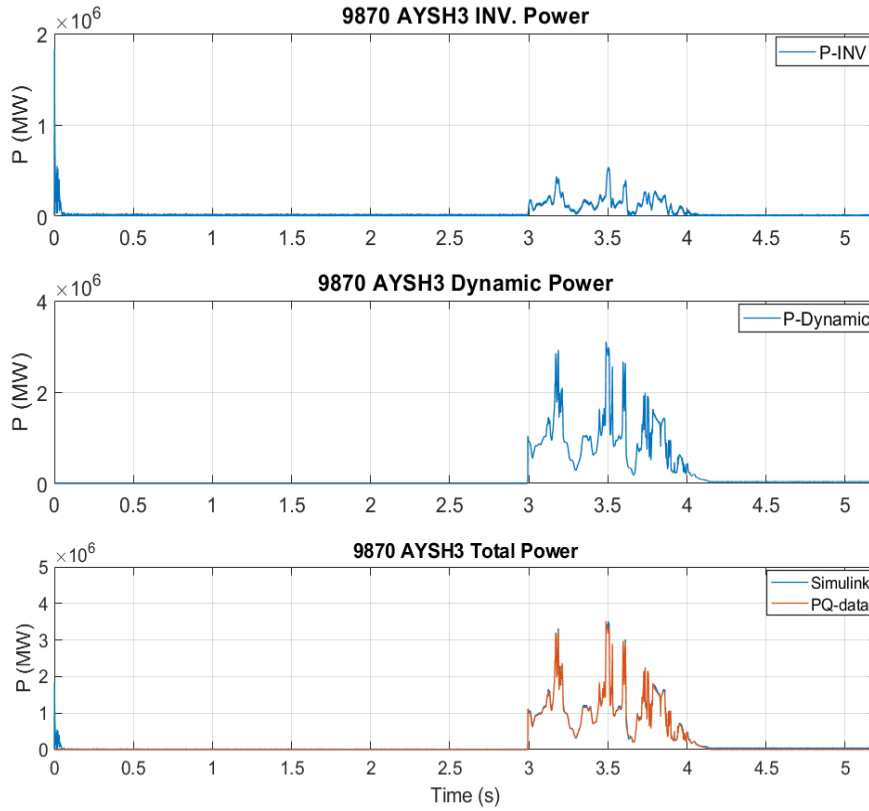


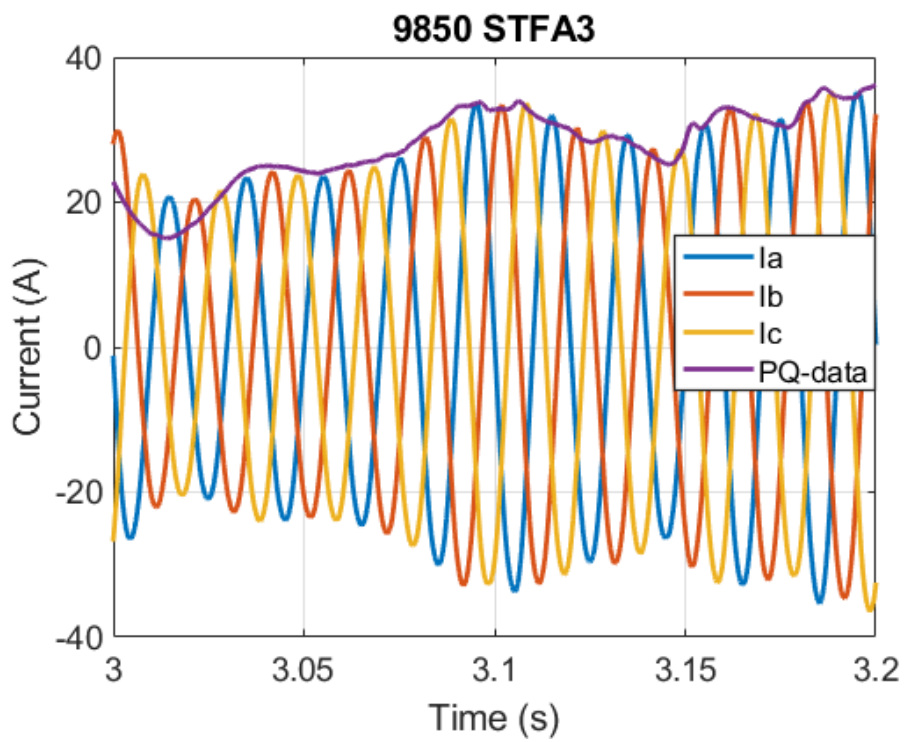
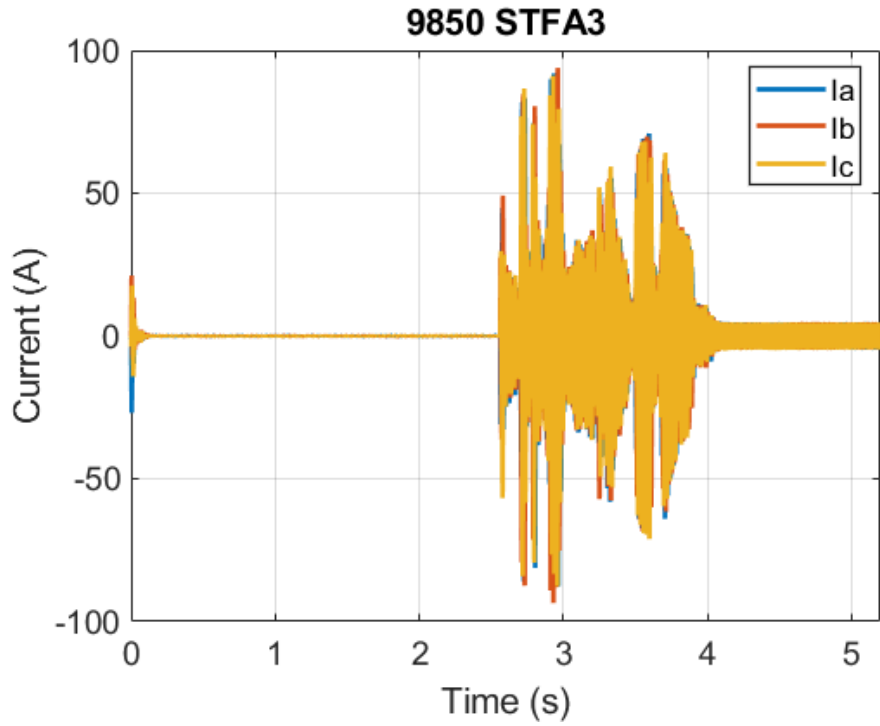
Figure 56: Comparison between Simulink and DlgSILENT PowerFactory for the complete network – TIVE3 bus, zoomed in version.

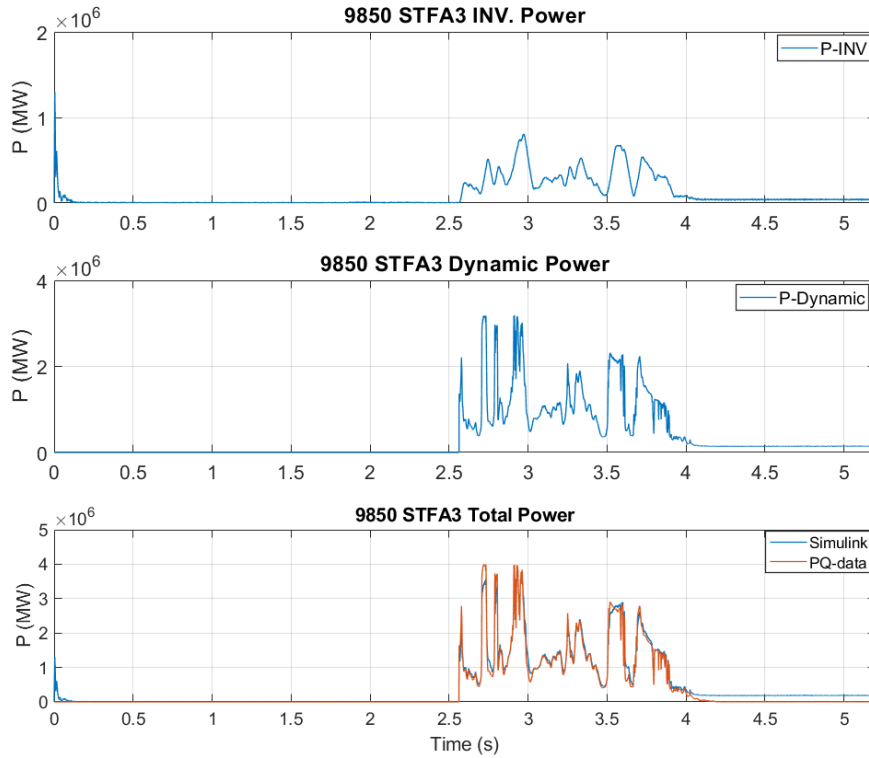
Appendix E Dynamic simulation results for 1 October 2019

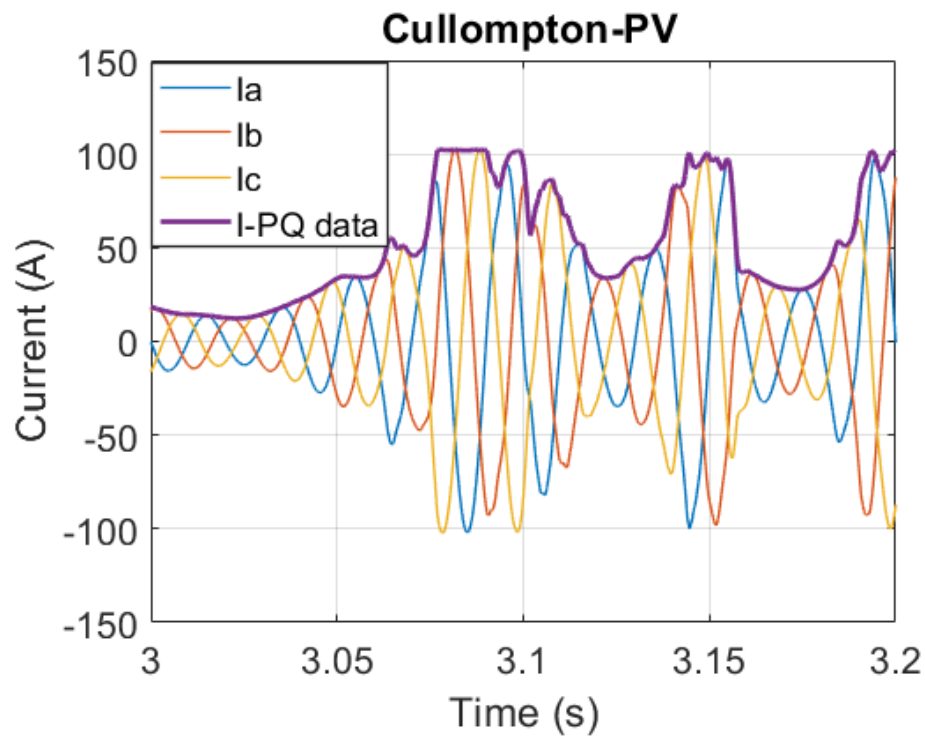
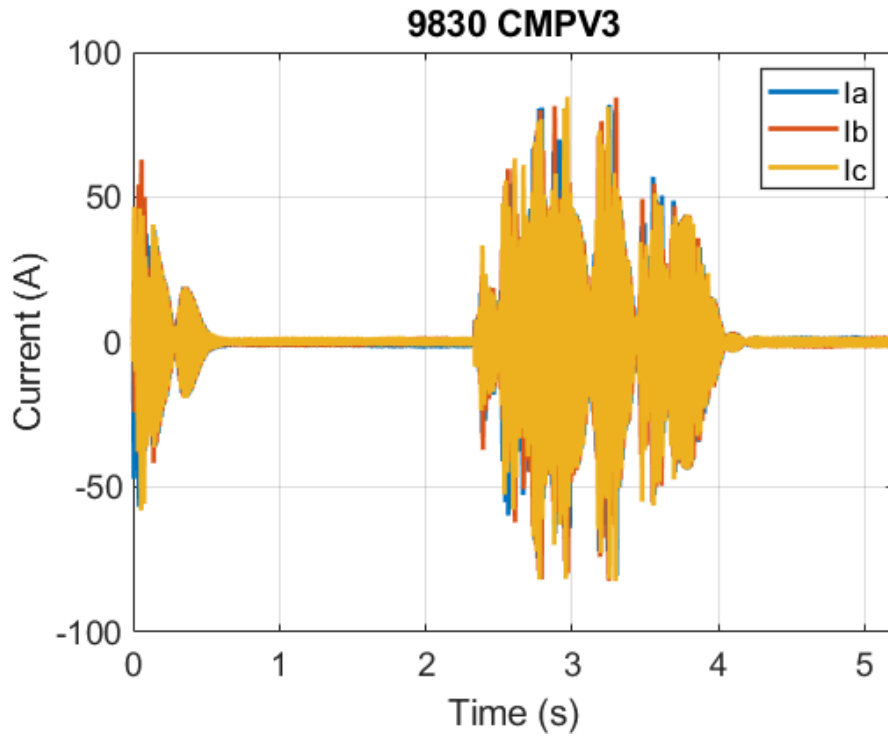
E.1 Results for PV farms

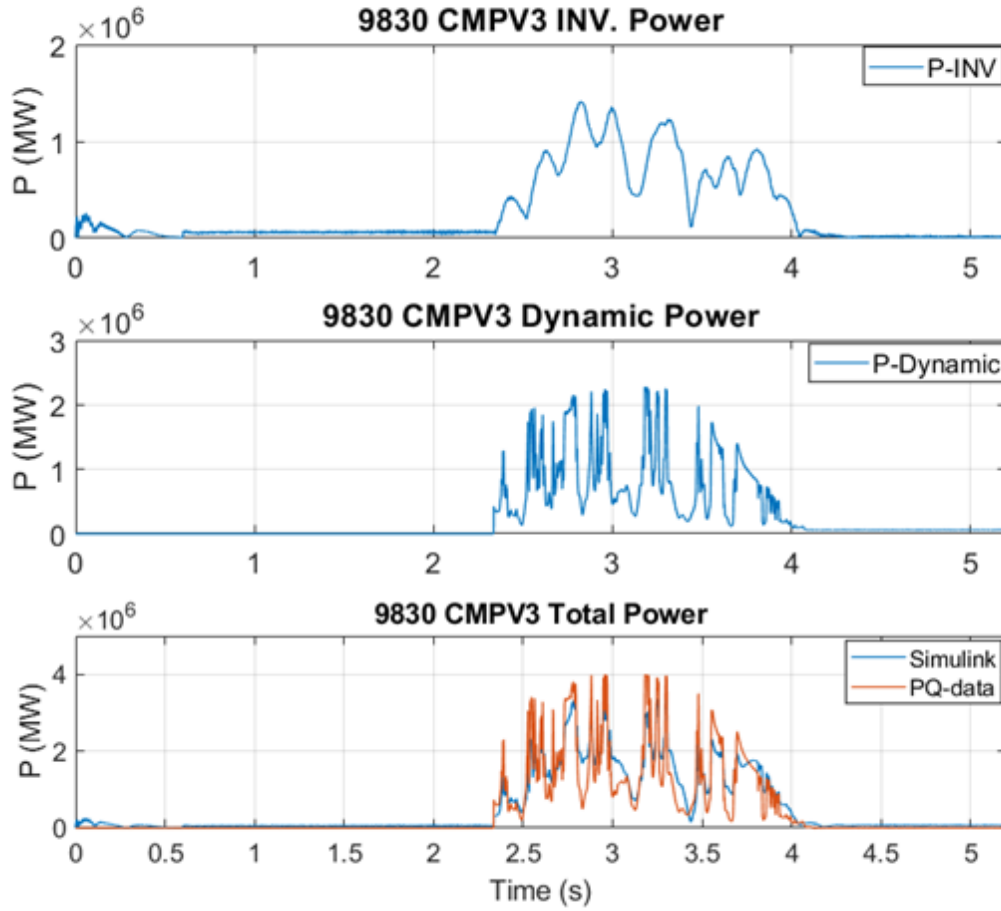




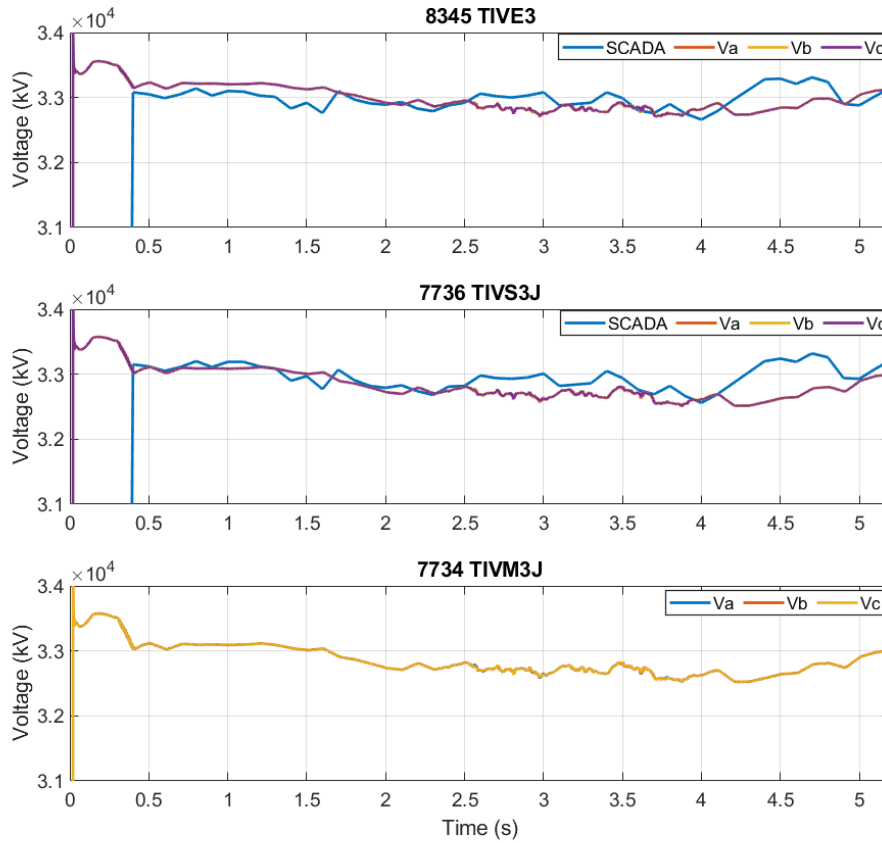




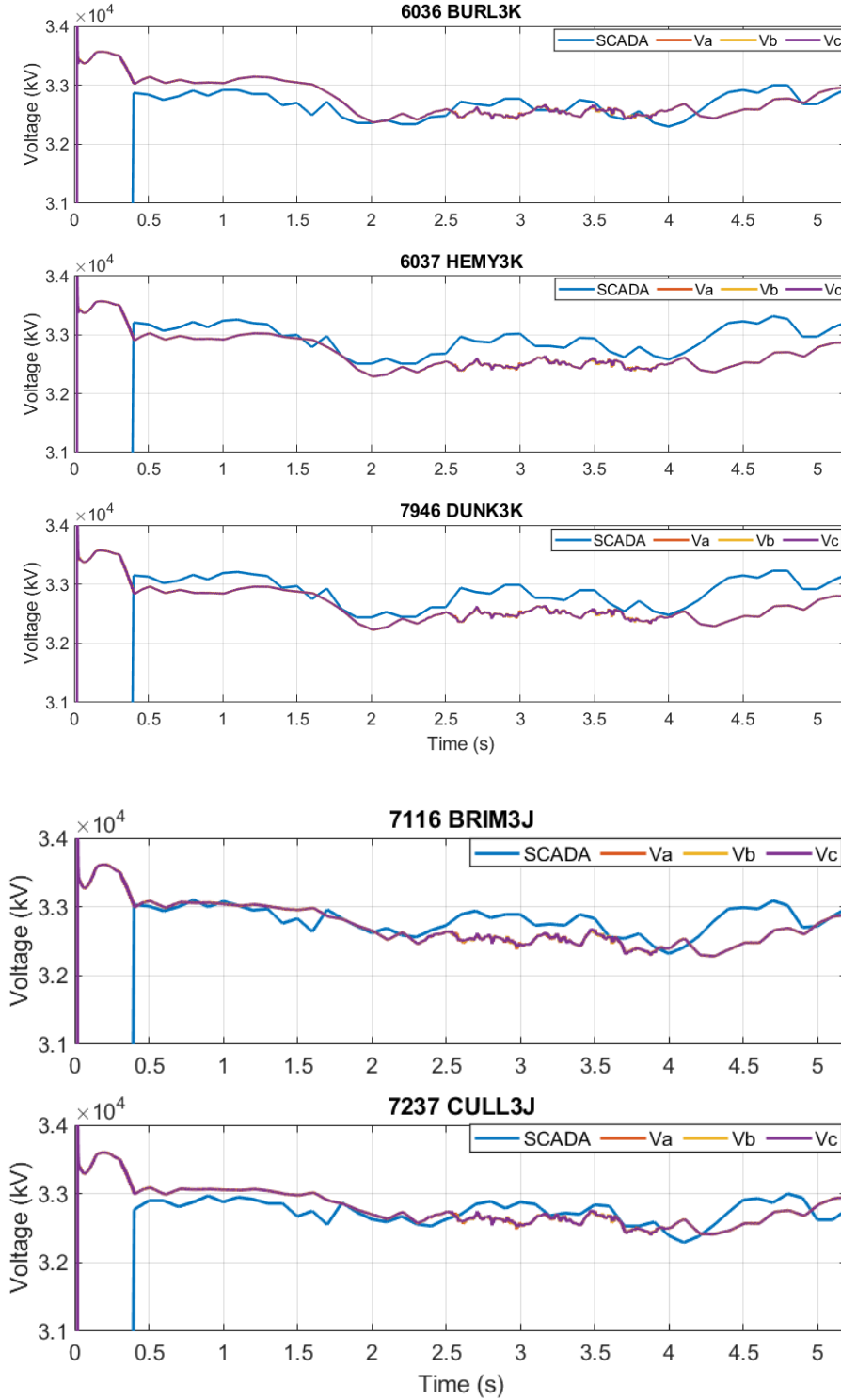


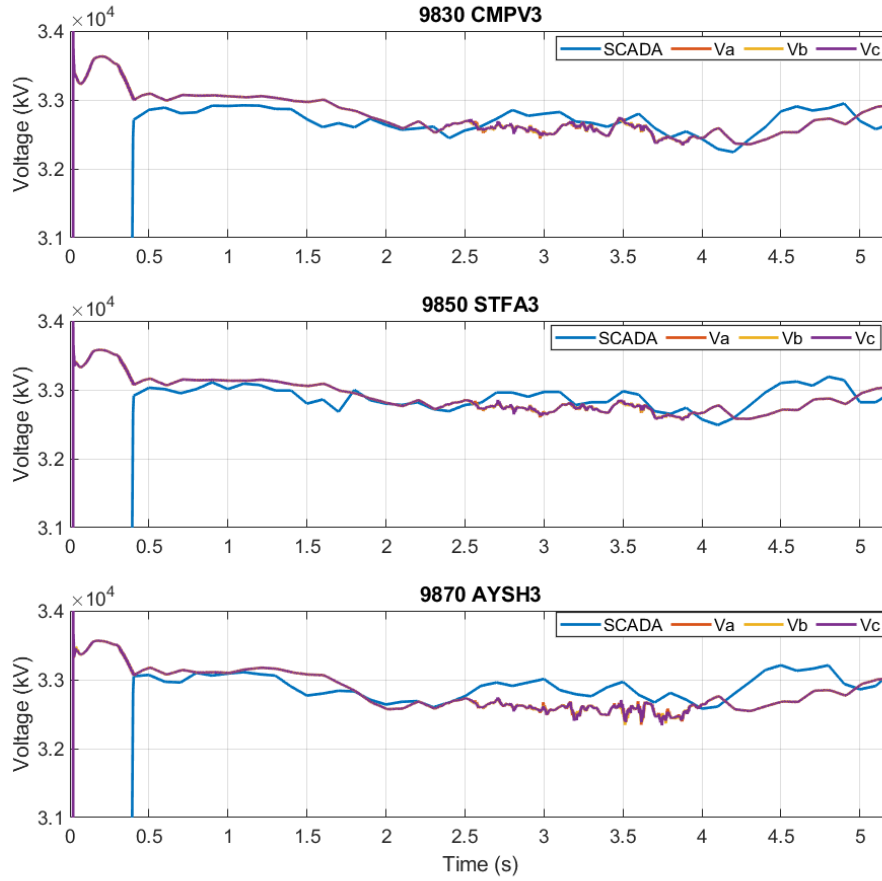


E.2 Results for 33 kV buses – voltage rms

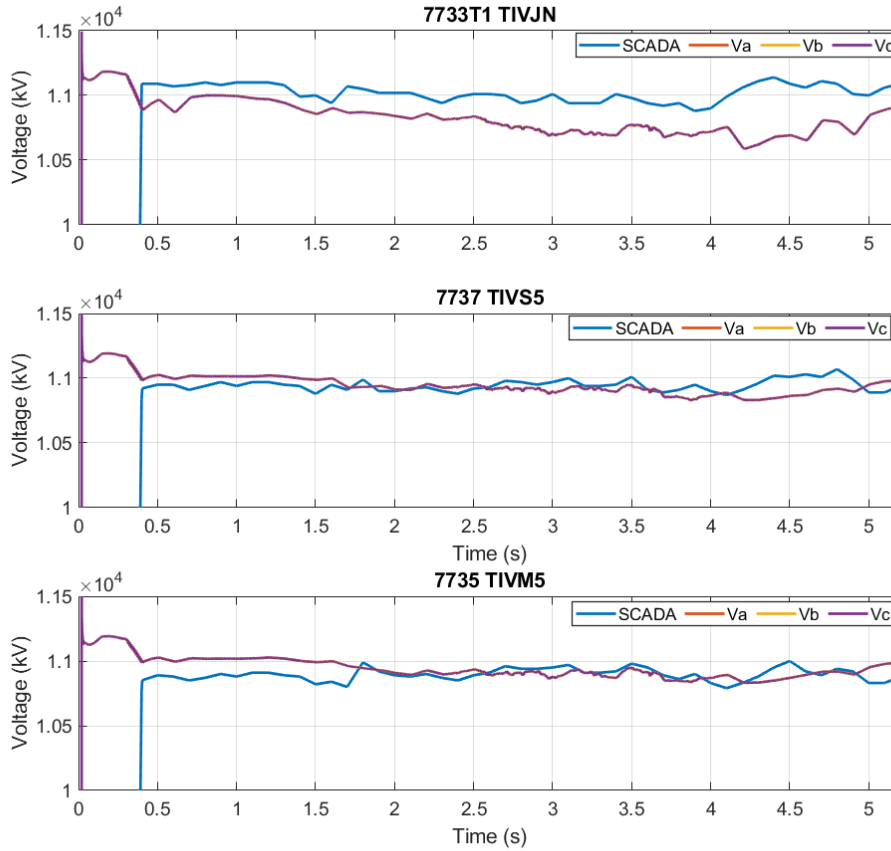


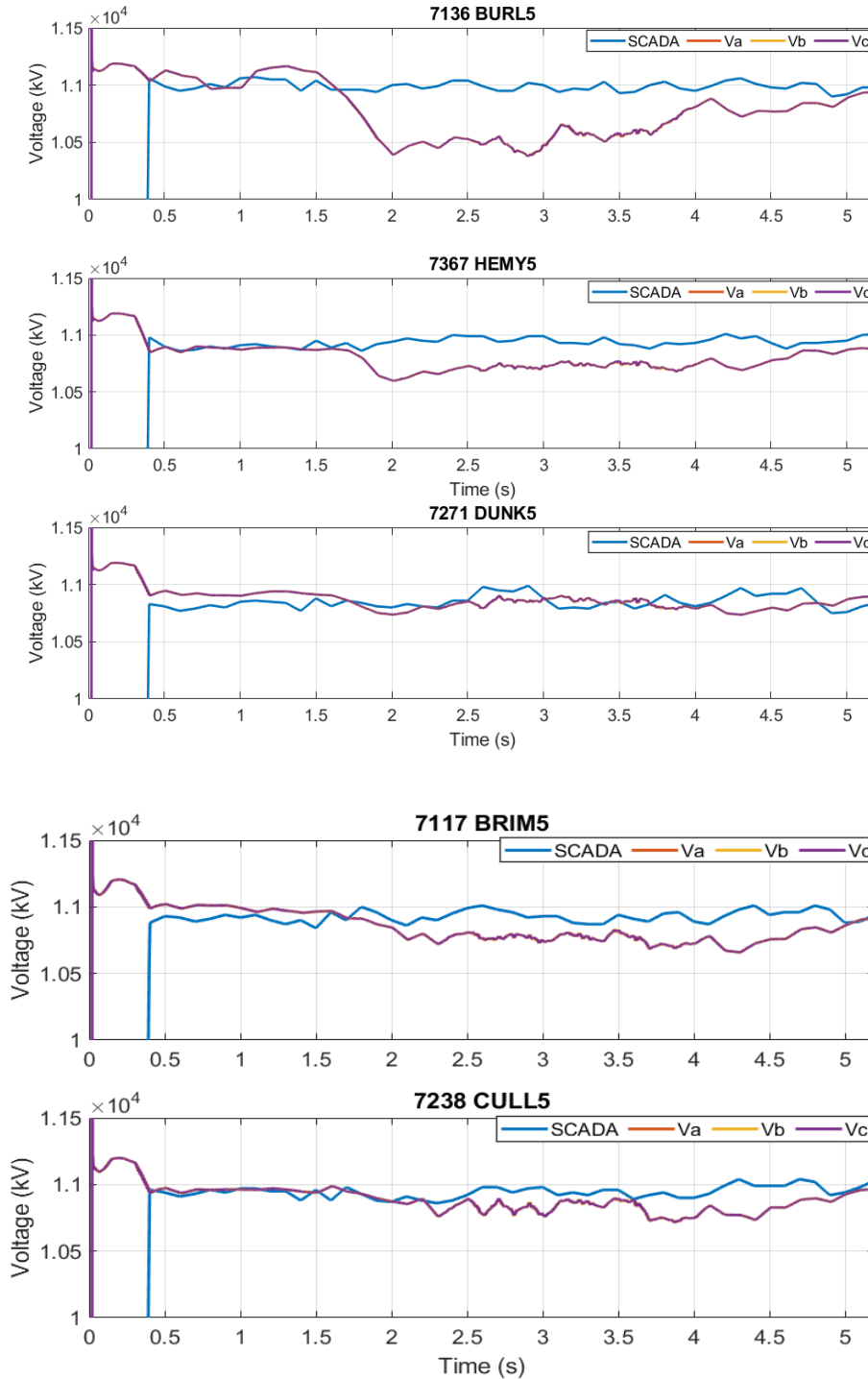
Note: No SCADA data available for TIVM.



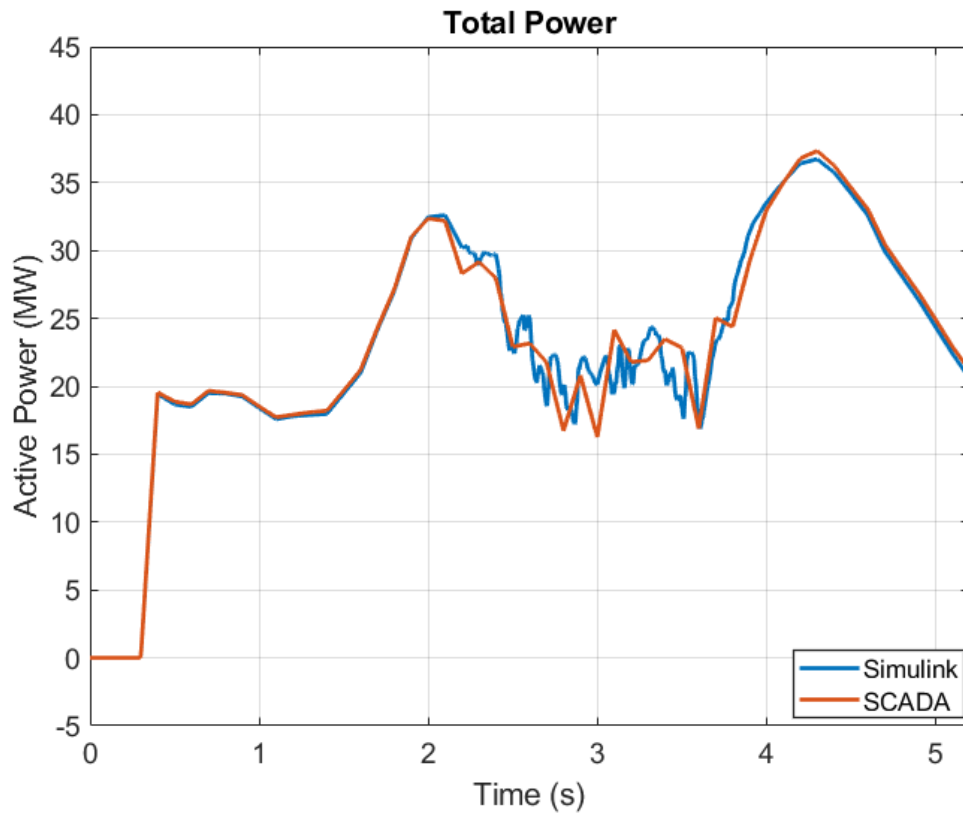


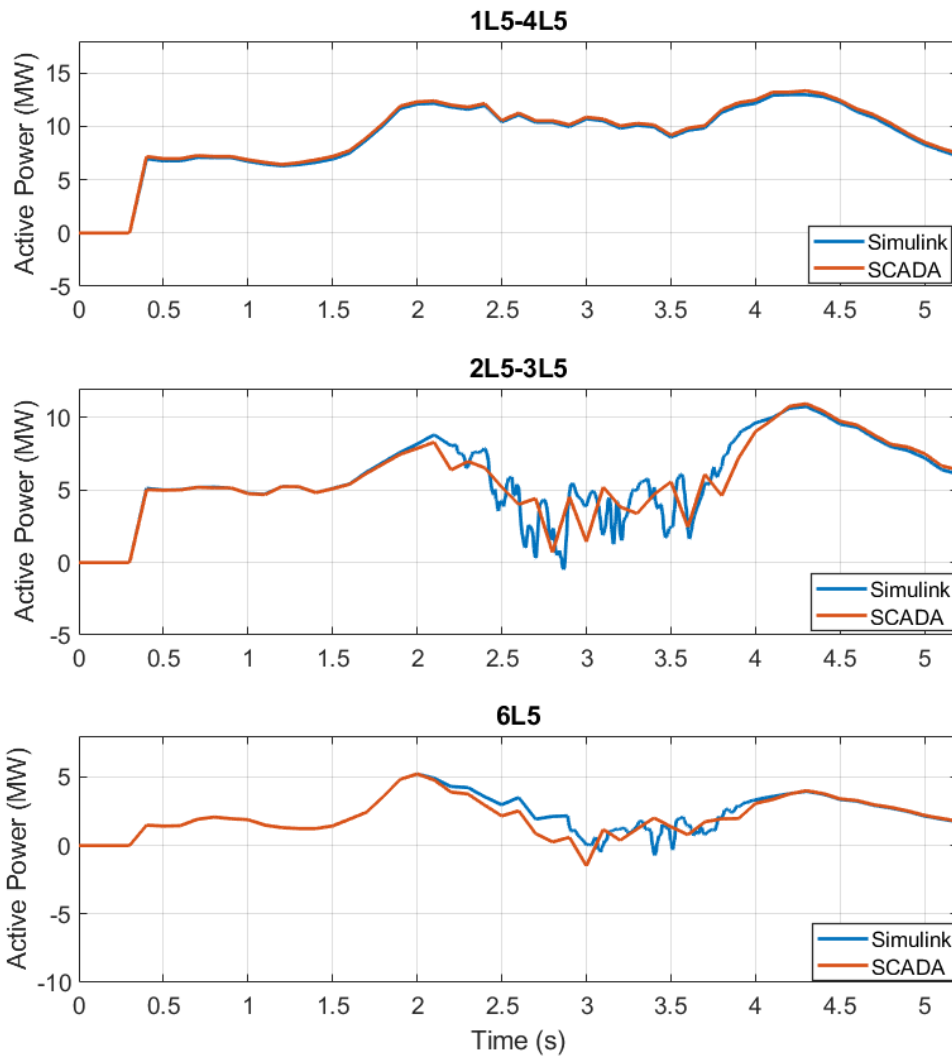
E.3 Results for 11 kV buses – voltage rms (with tap changing)

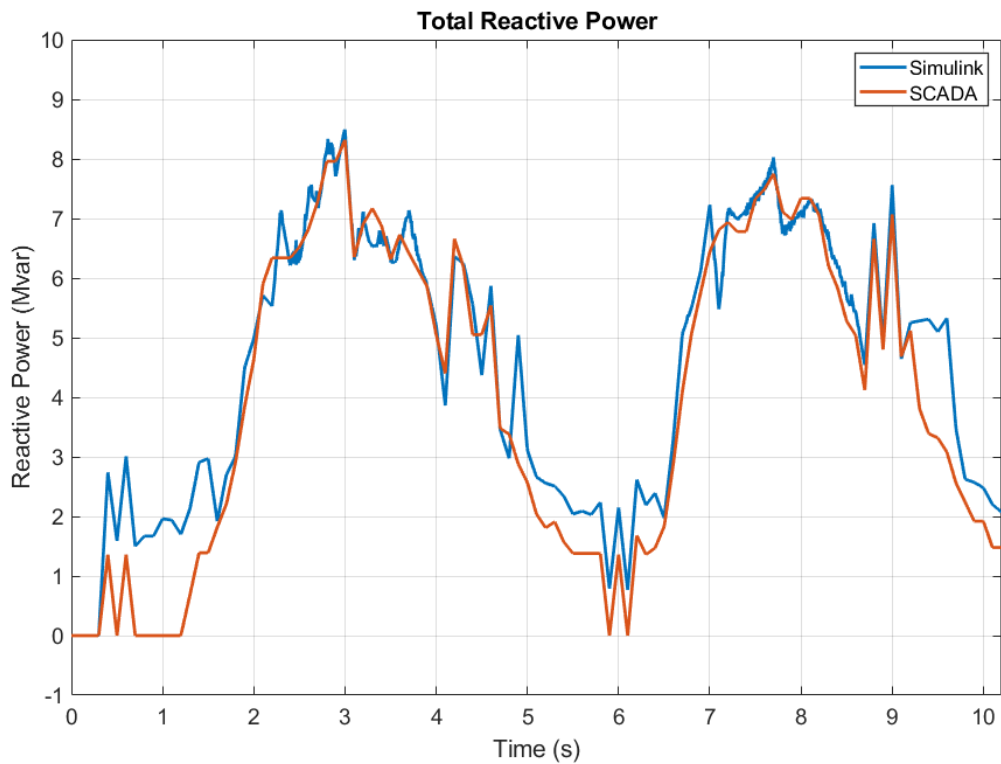
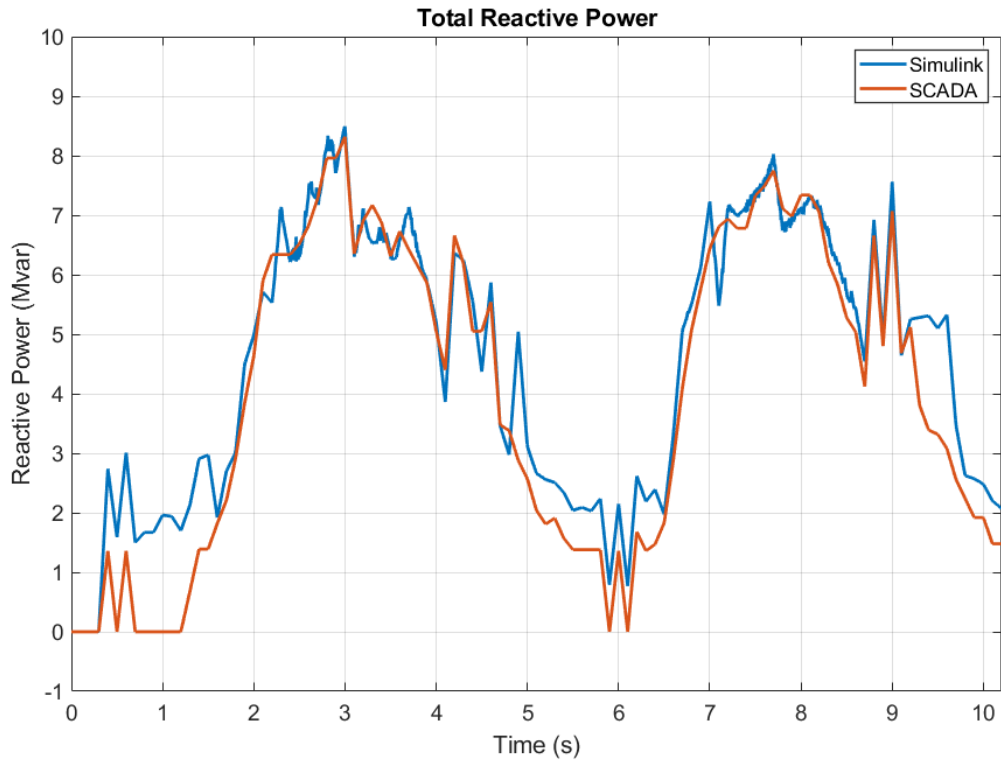




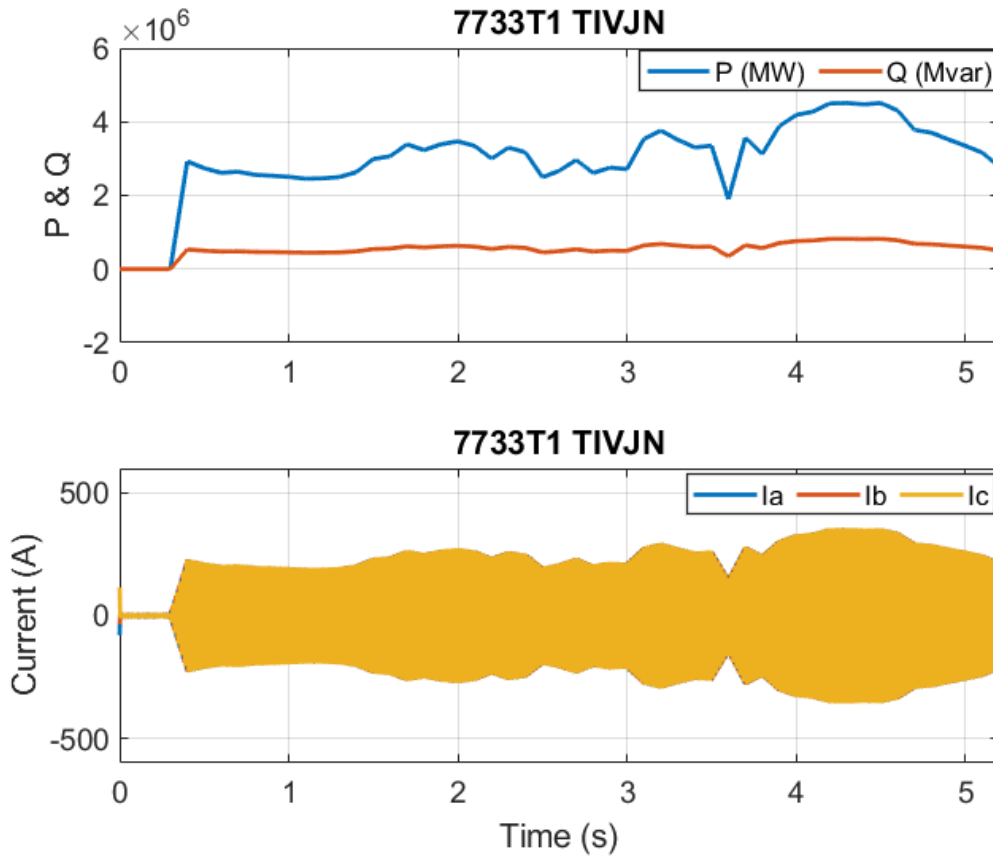
E.4 Results for system boundary

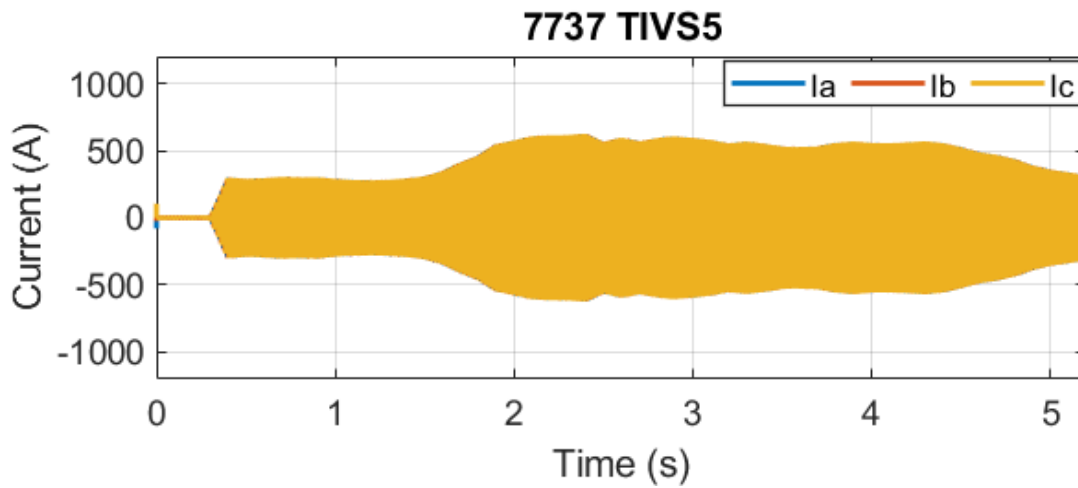
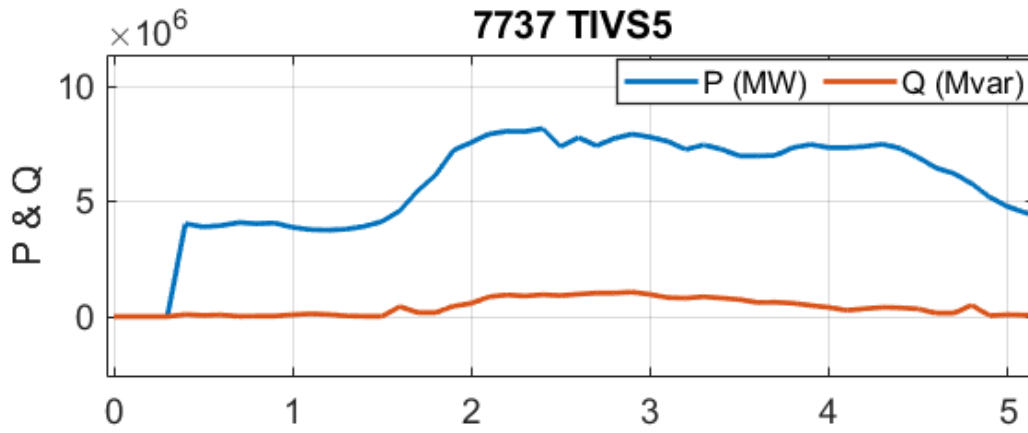


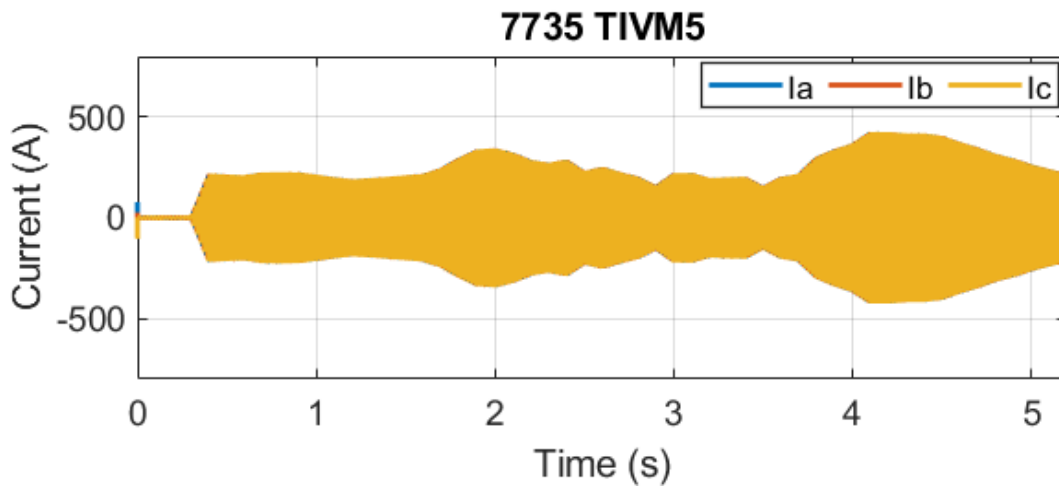
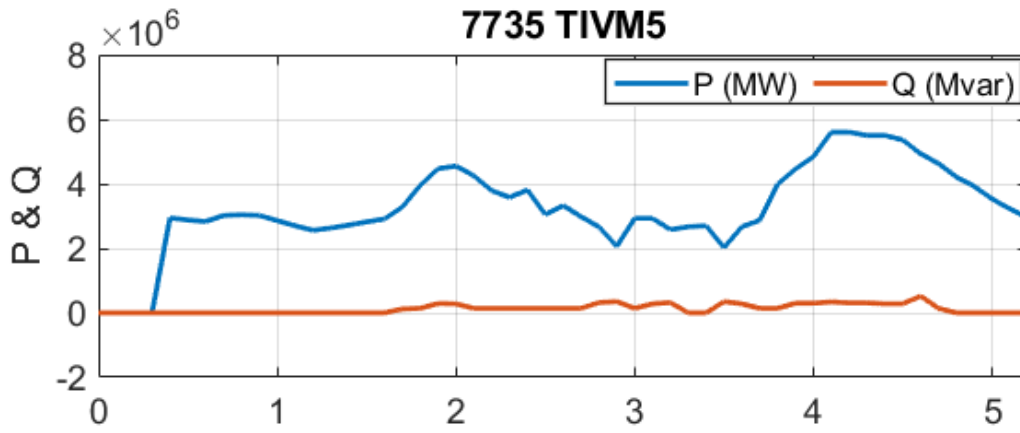


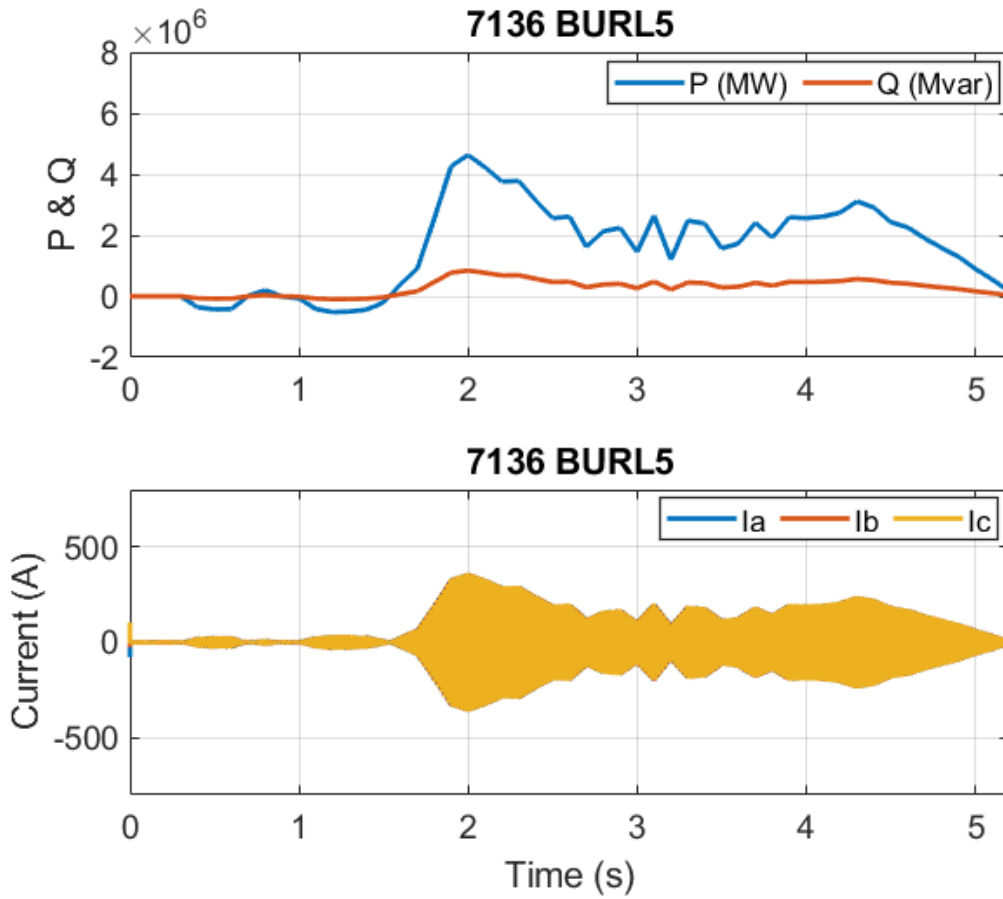


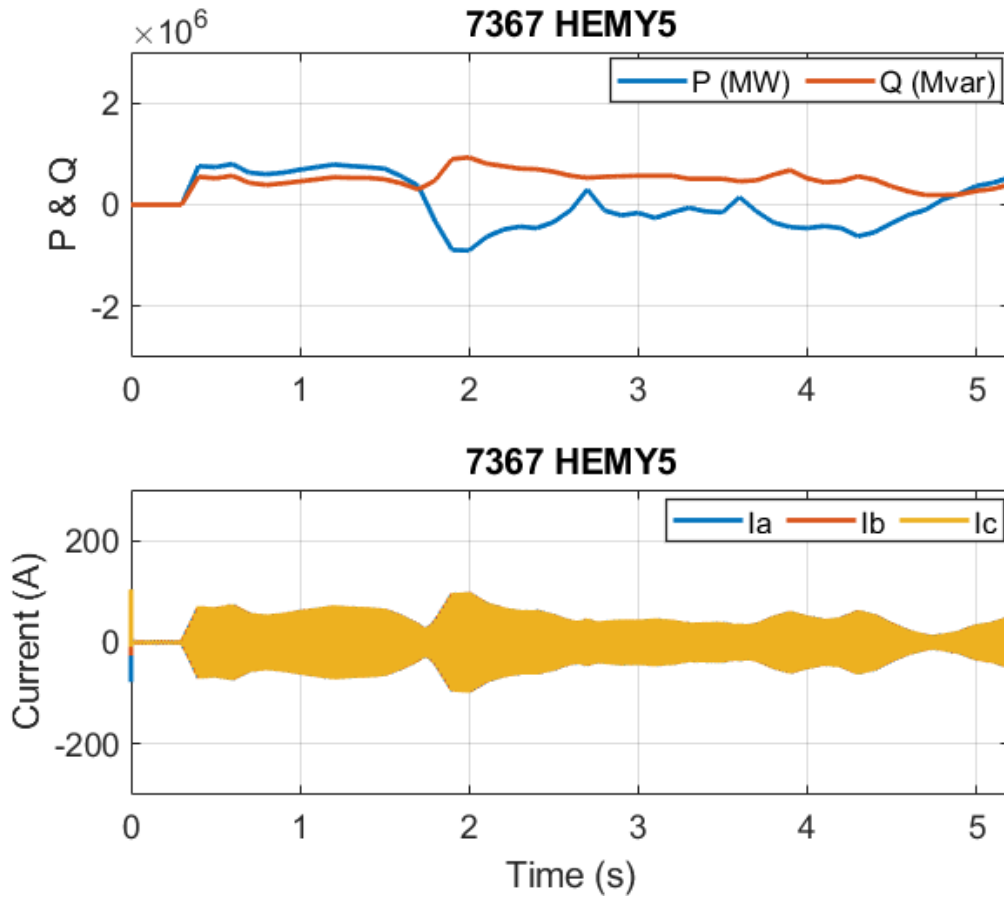
E.5 Results for 11 kV buses - Load active and reactive power, and current

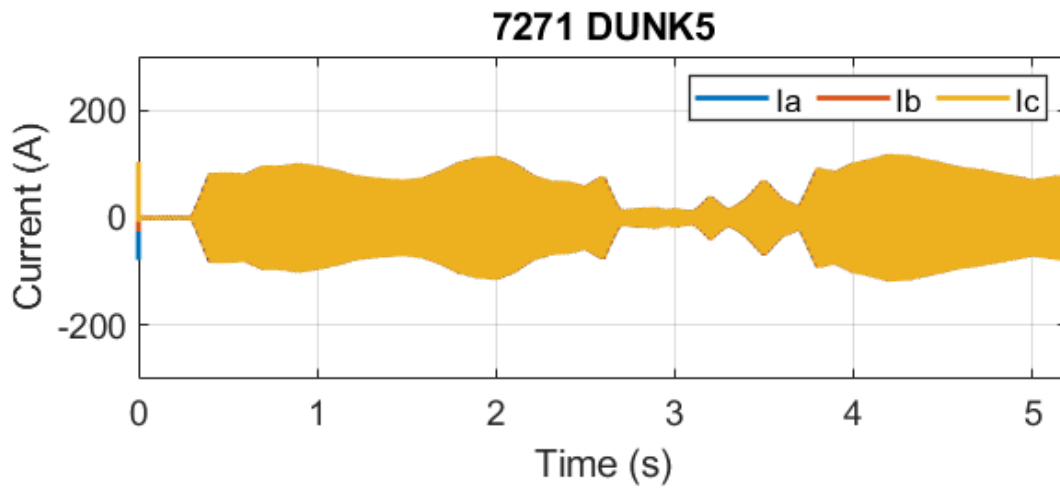
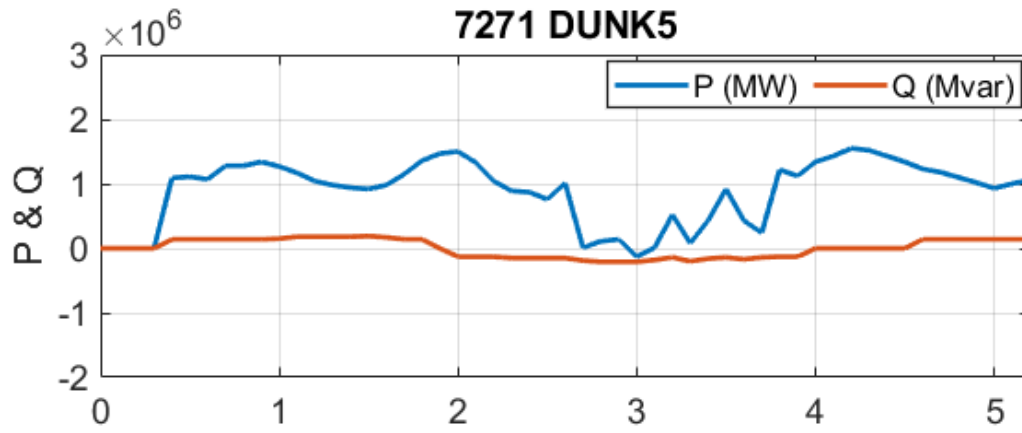


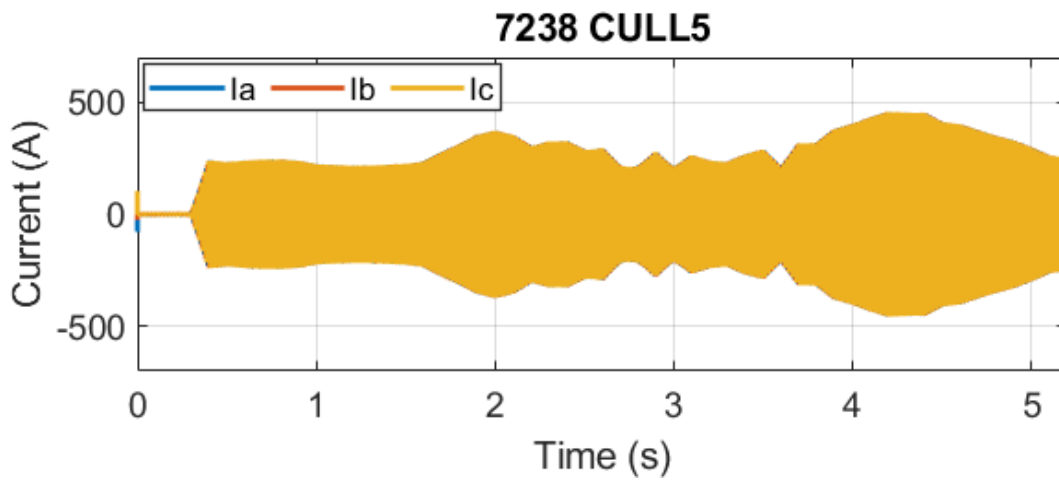
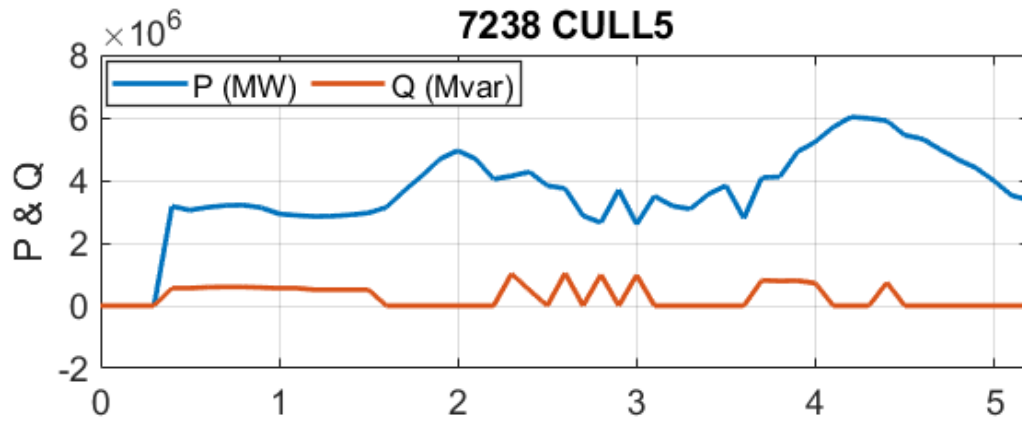


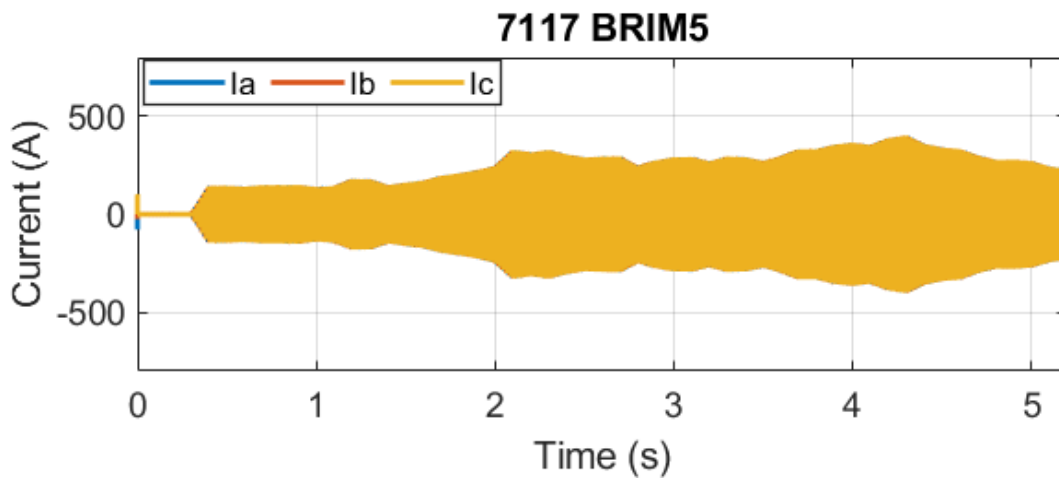
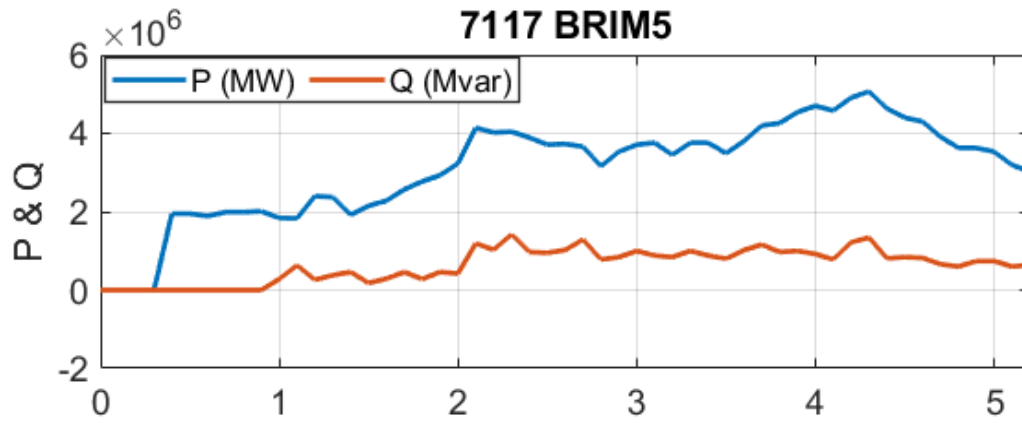












Appendix F Dynamic simulation results for 1-21 October 2019.

The simulation time for three weeks is 101.2 s: 0.4 seconds are used for initialisation, and then 4.8 seconds for each week day. The comparison between the simulation time and the real time is shown in Figure 57.

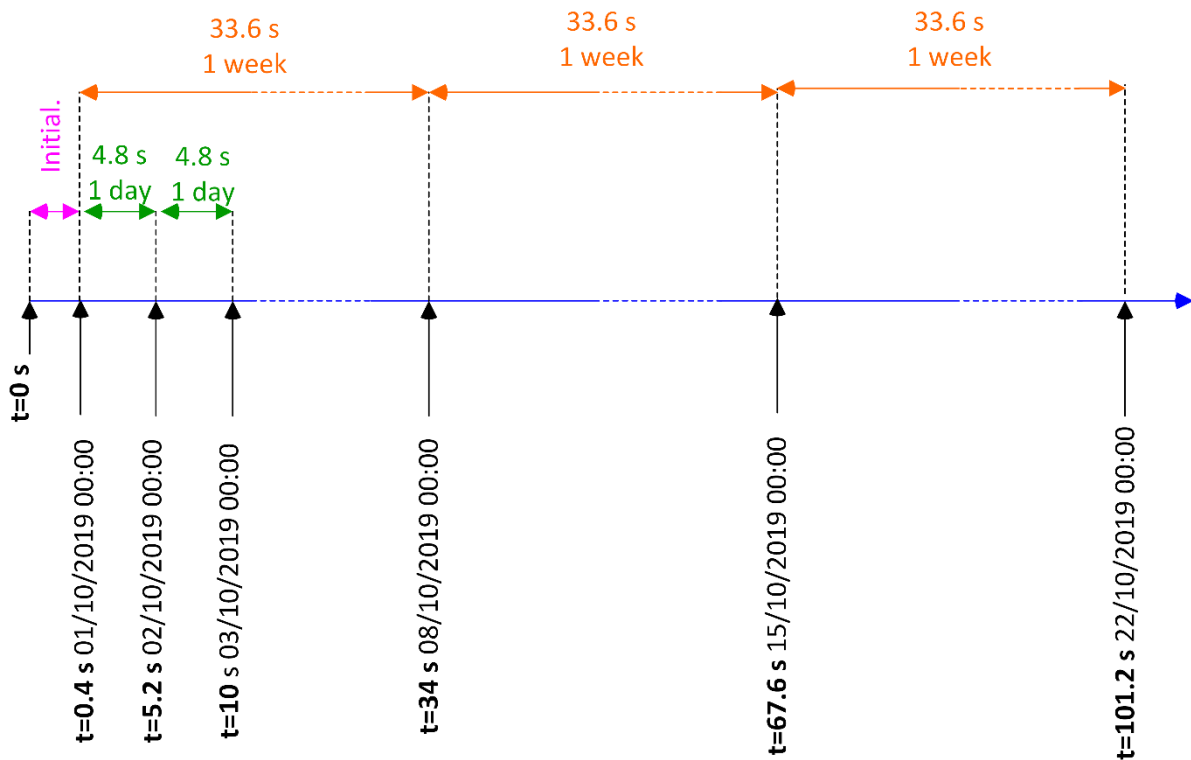
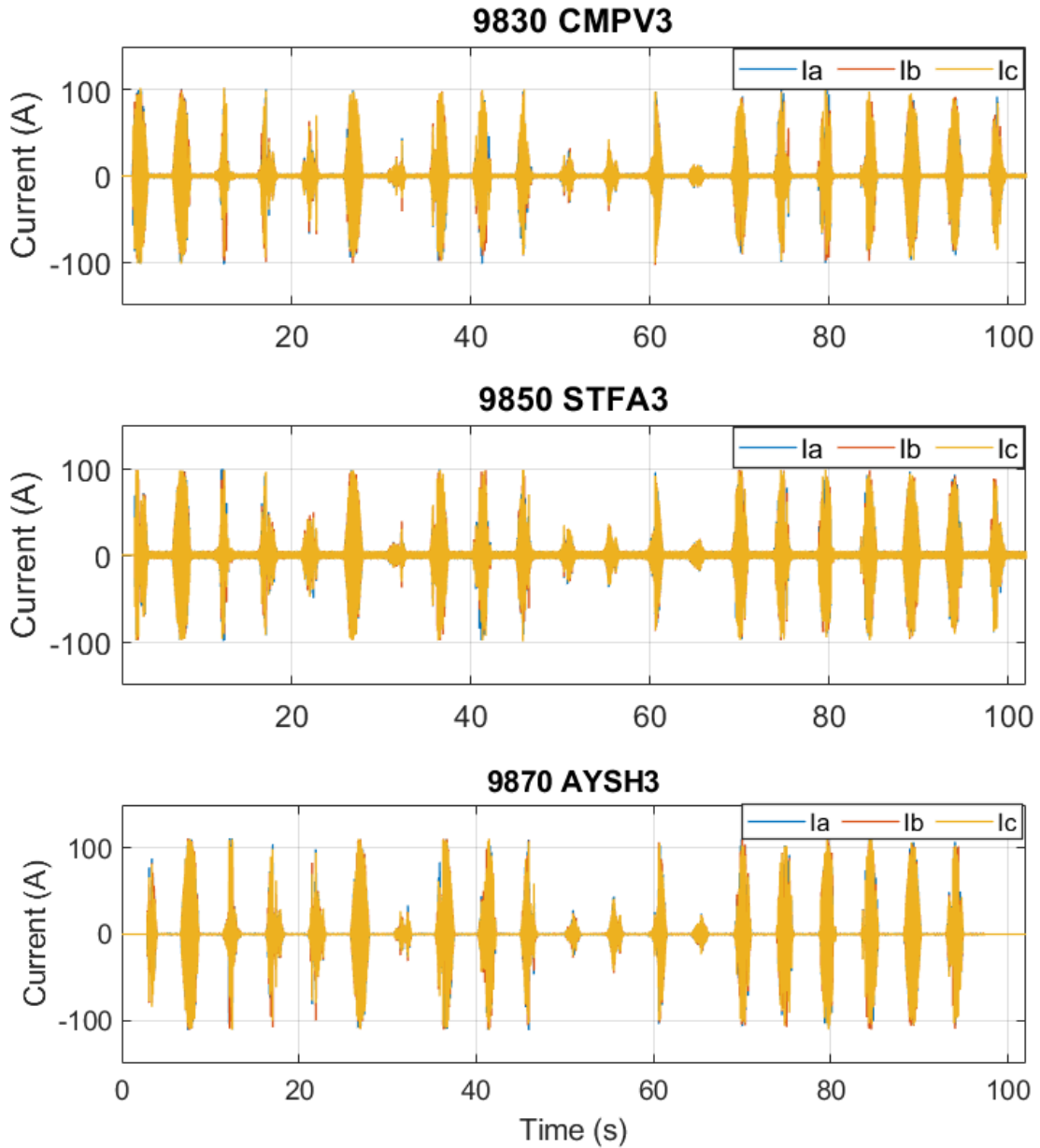
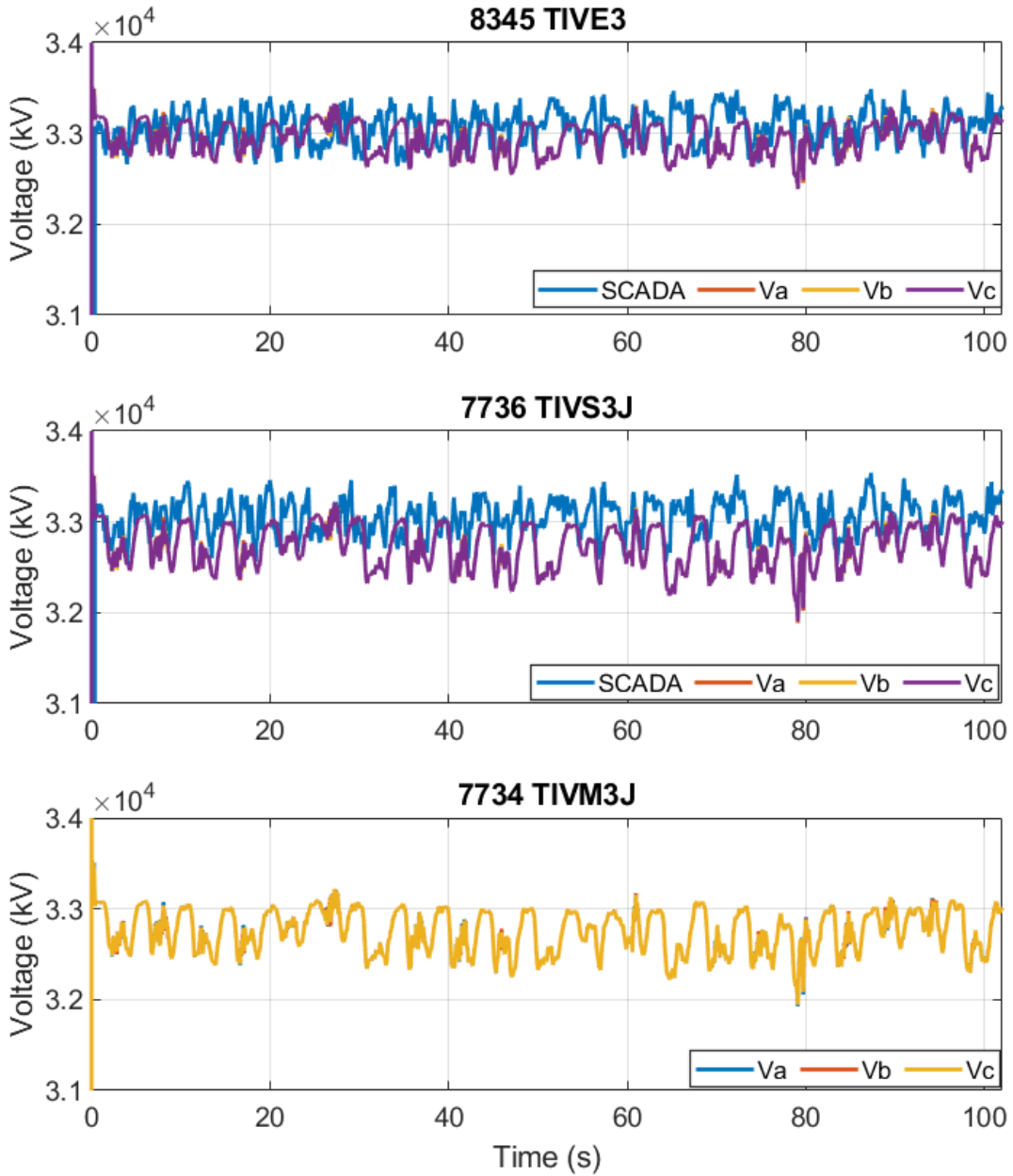


Figure 57: Comparison between simulation time and real time for the results presented in Appendix E.

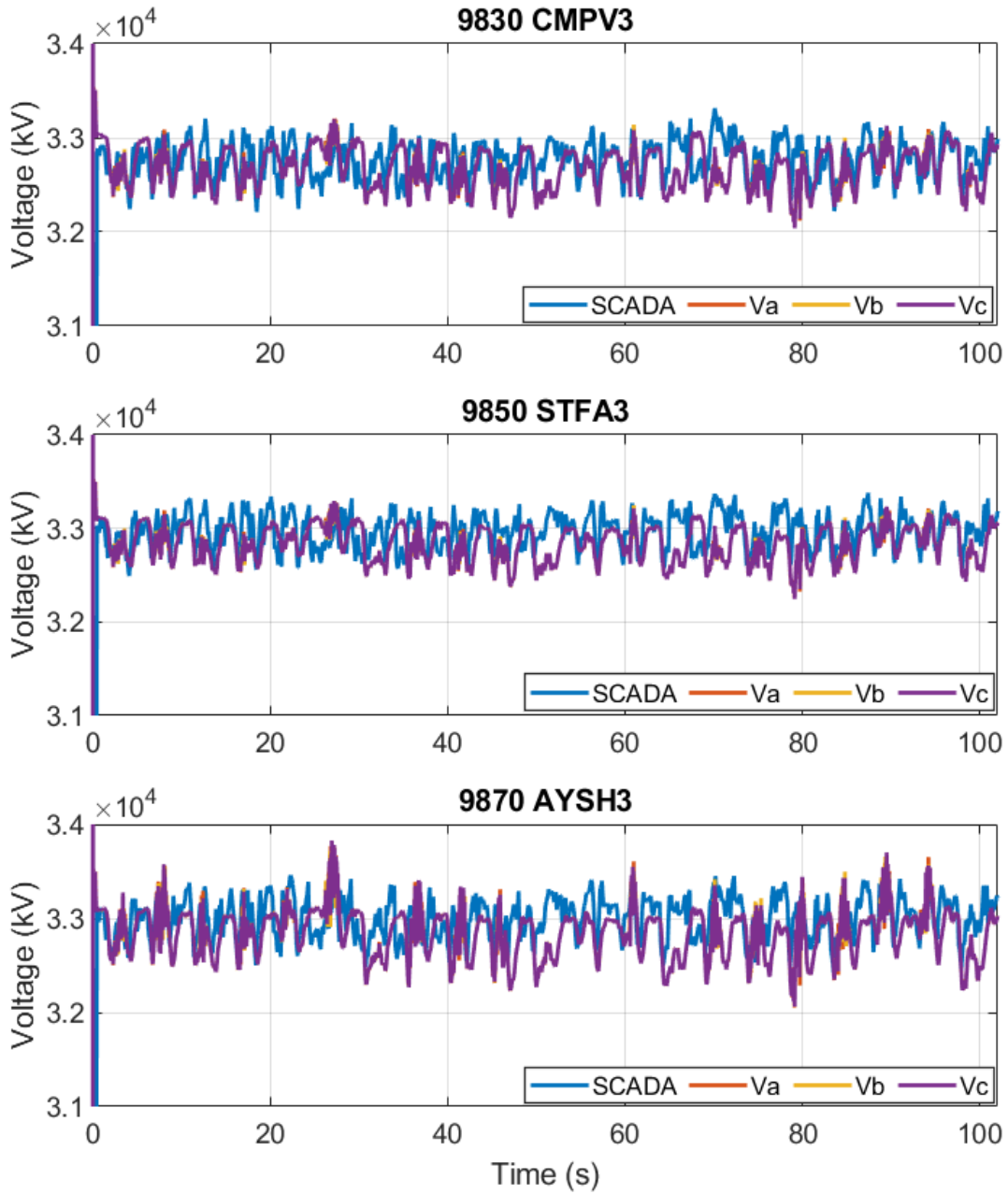
F.1 Results for PV farms

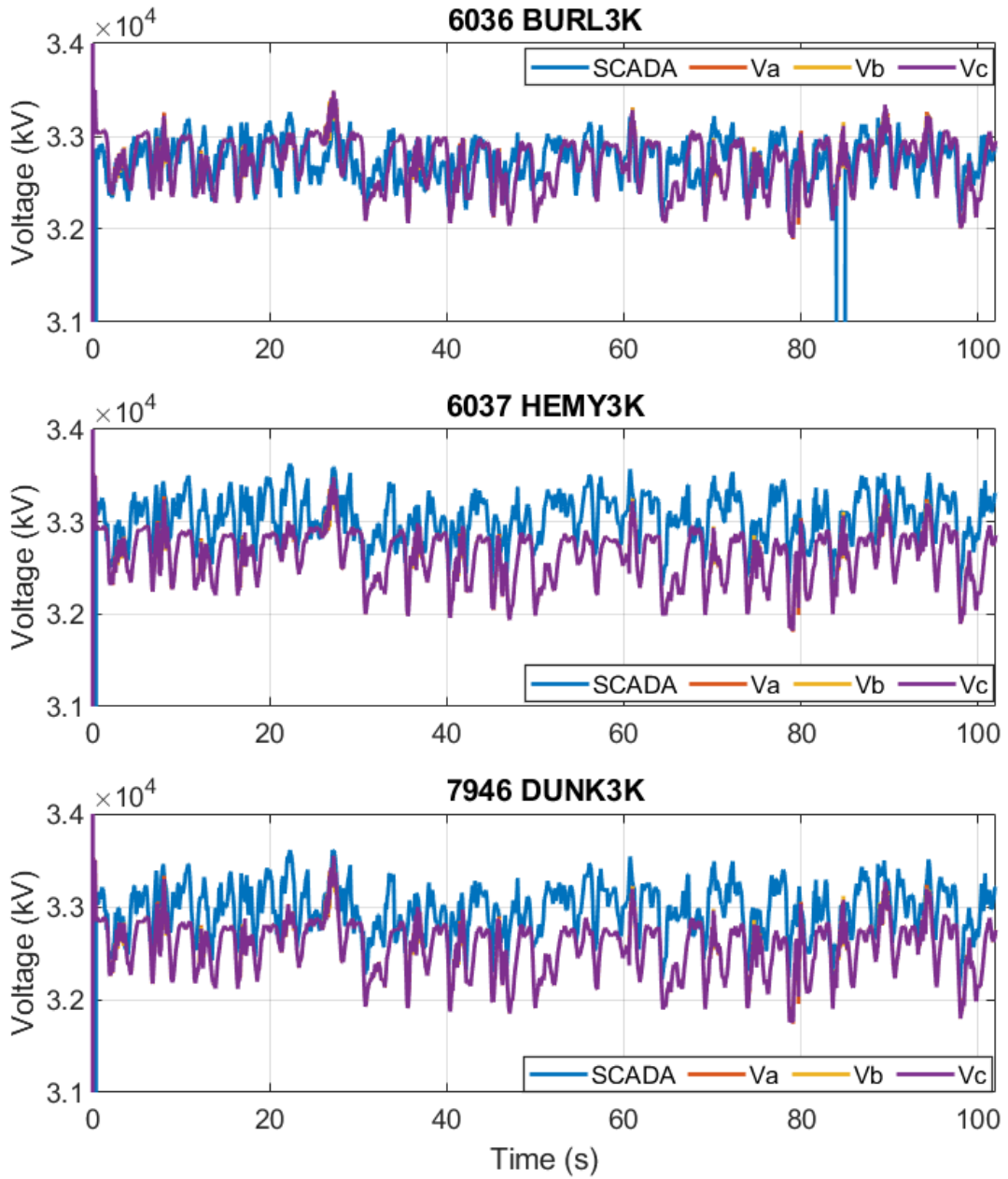


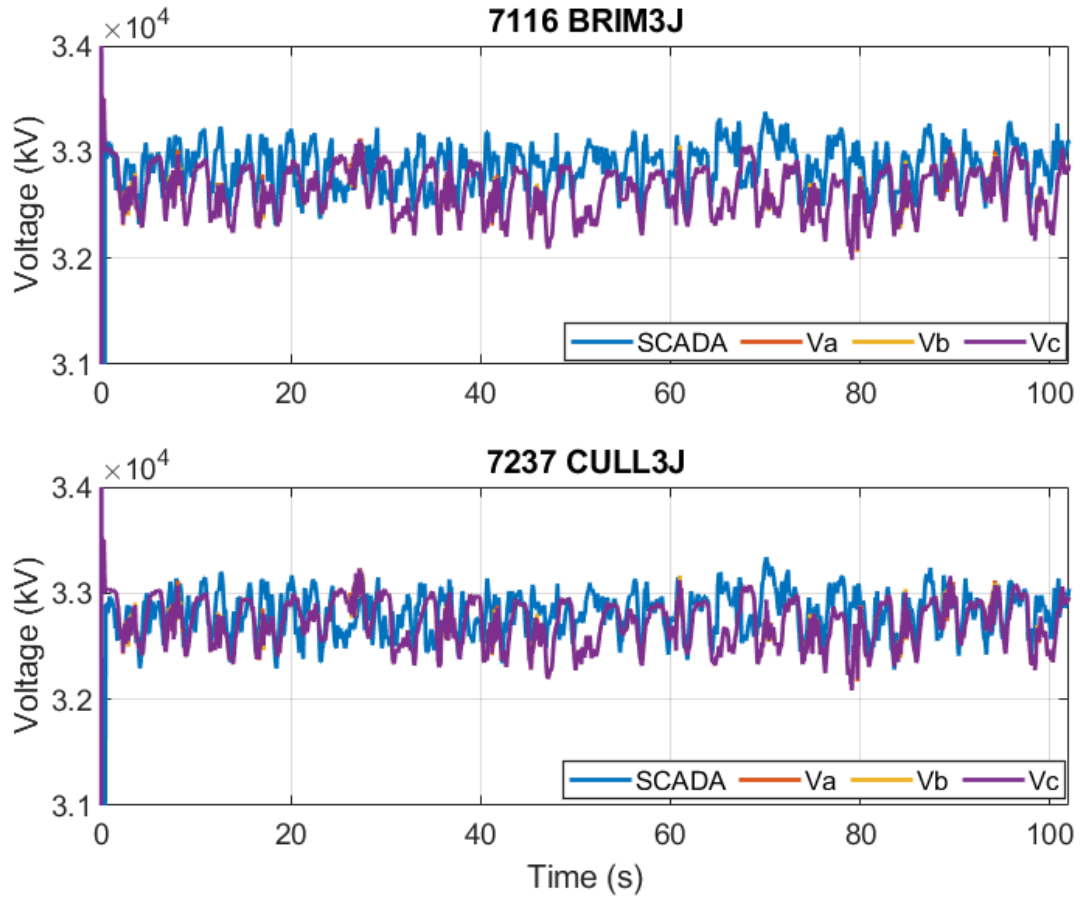
F.2 Results for 33 kV buses – voltage rms

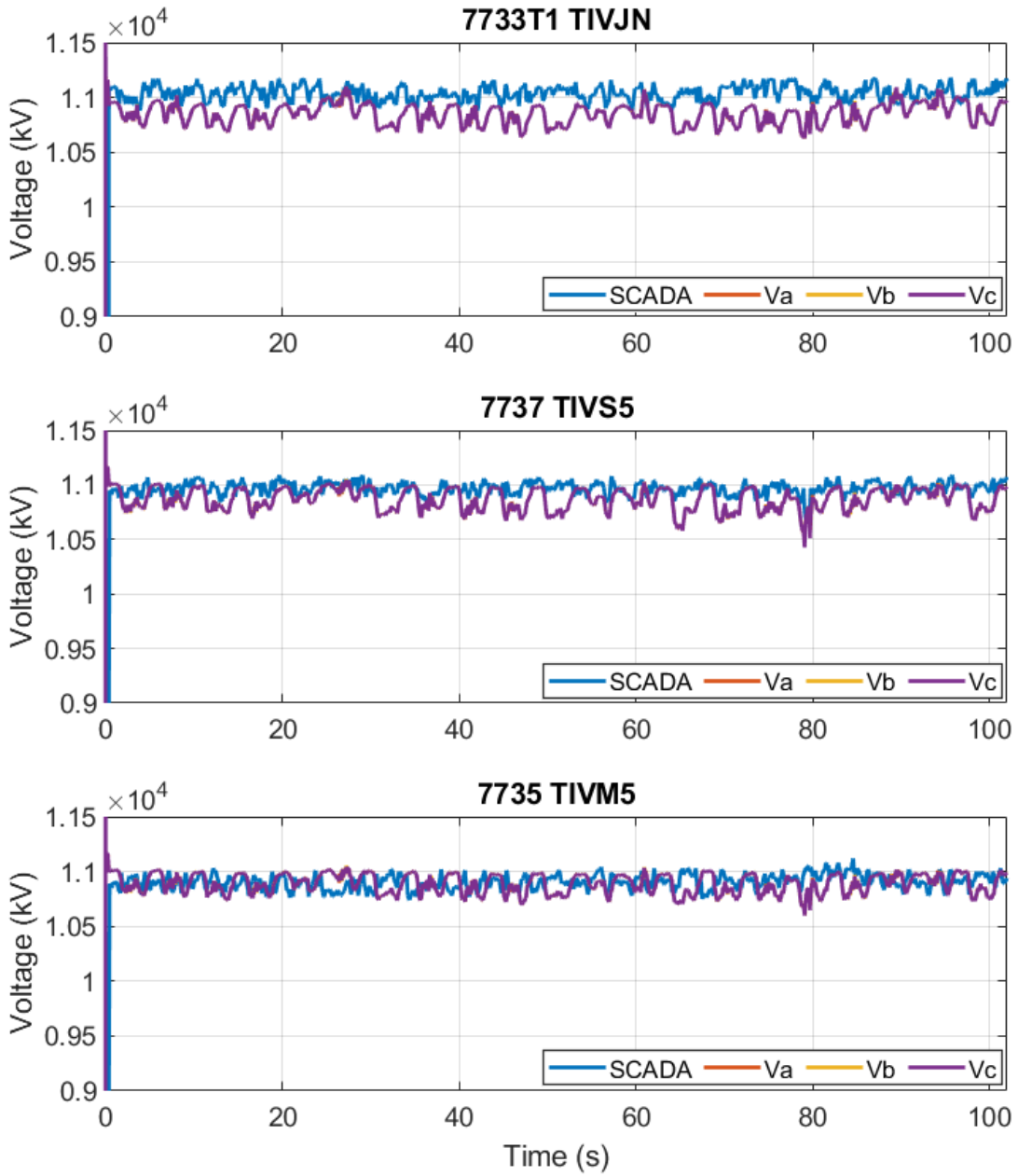


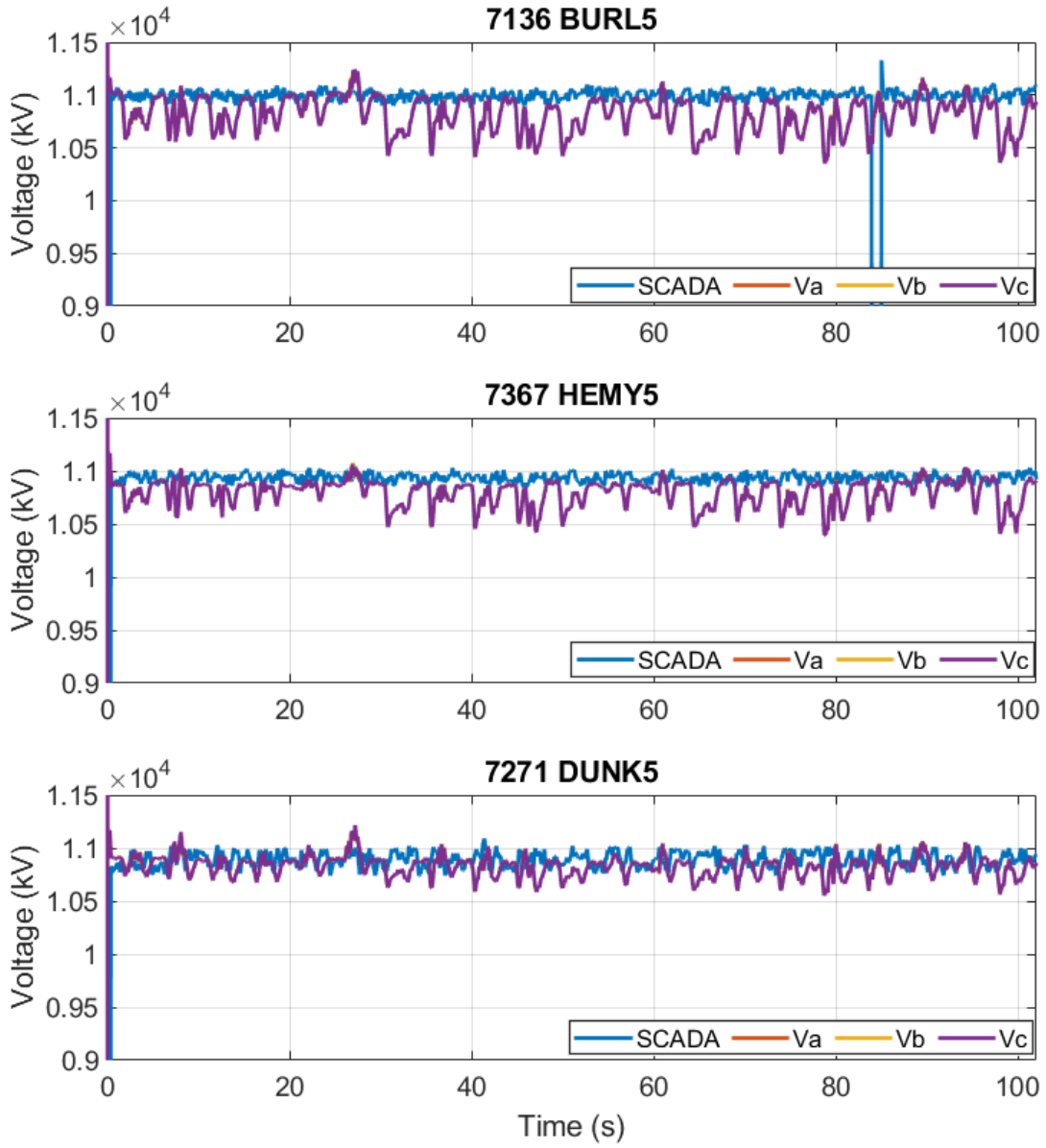
Note: no SCADA 33kV voltage data is available for TIVM3J.

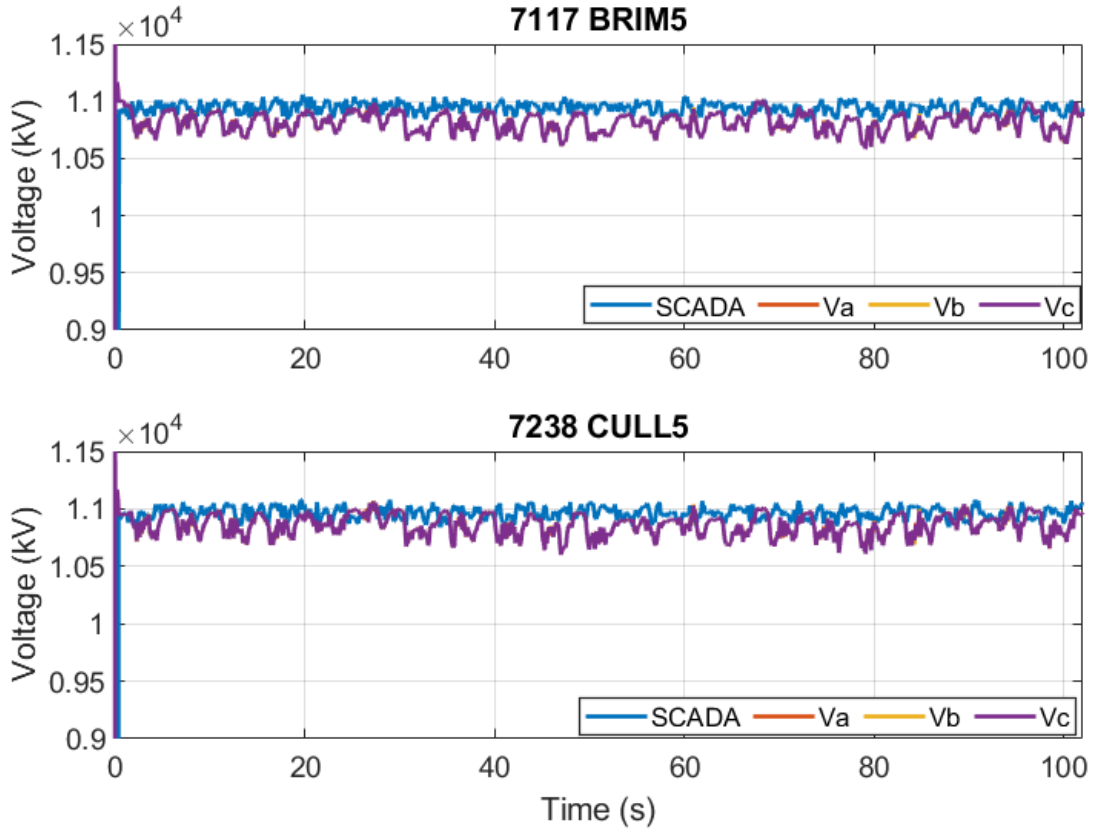




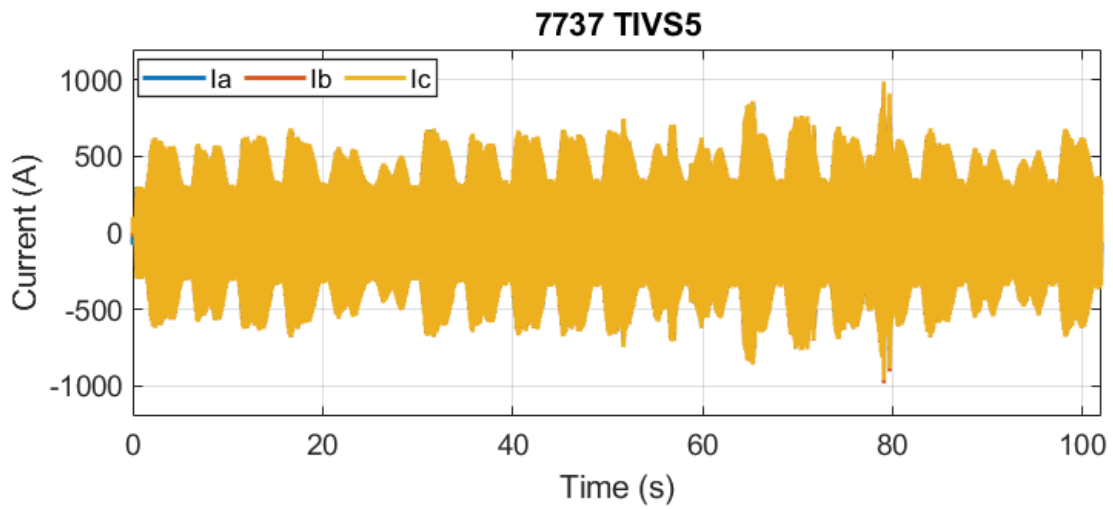
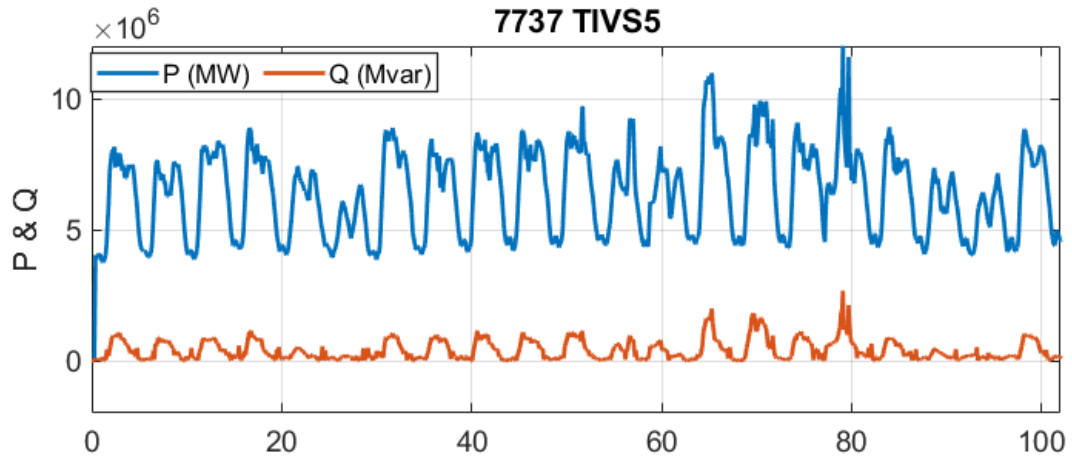


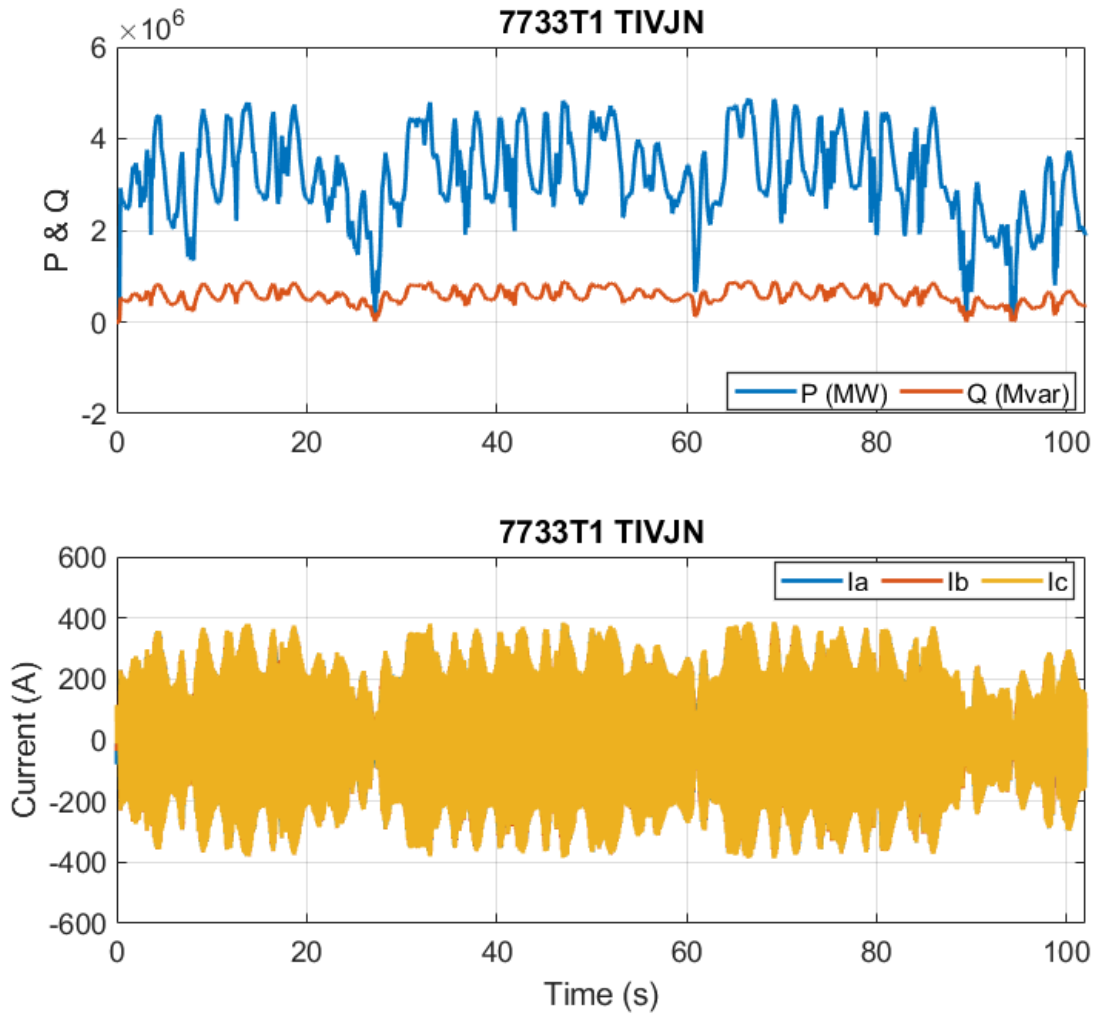


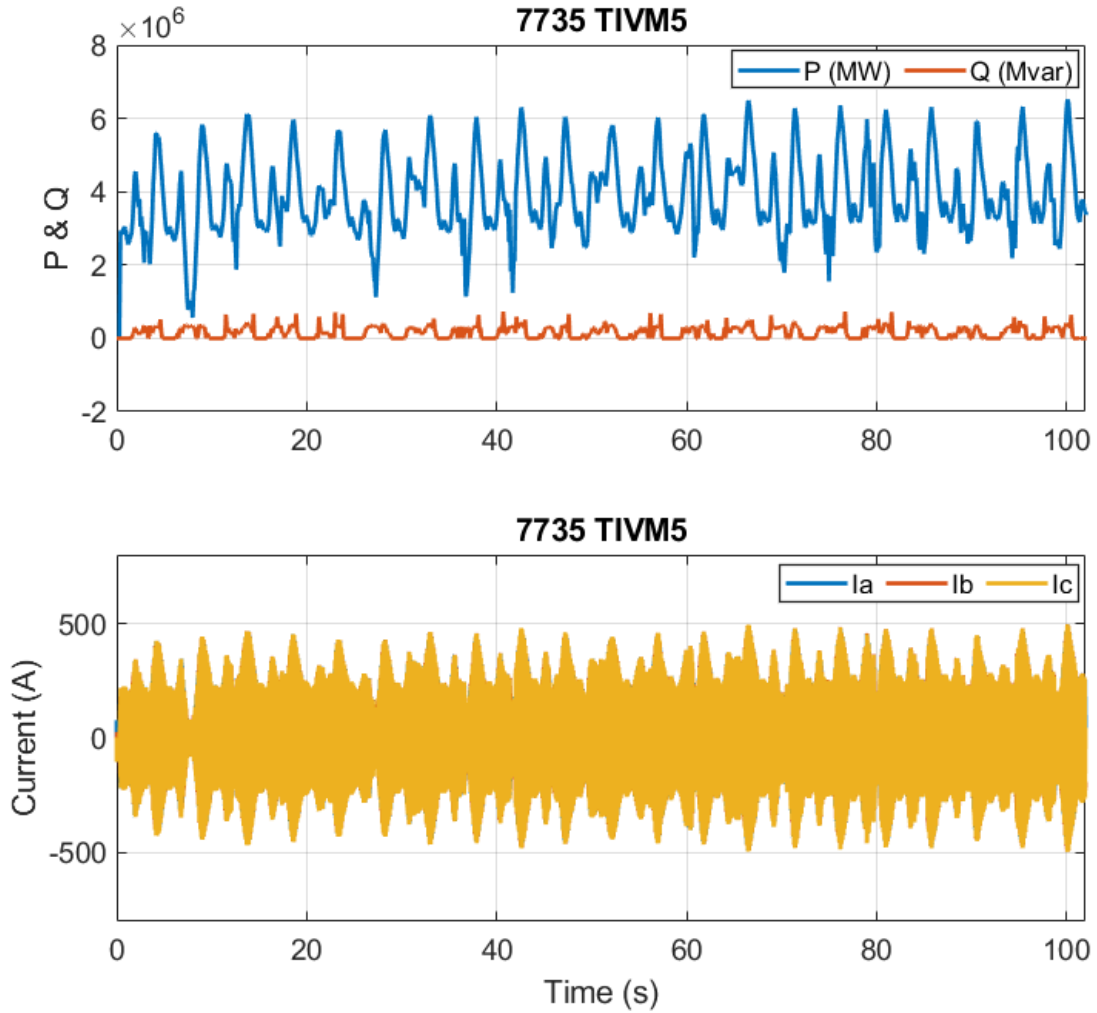


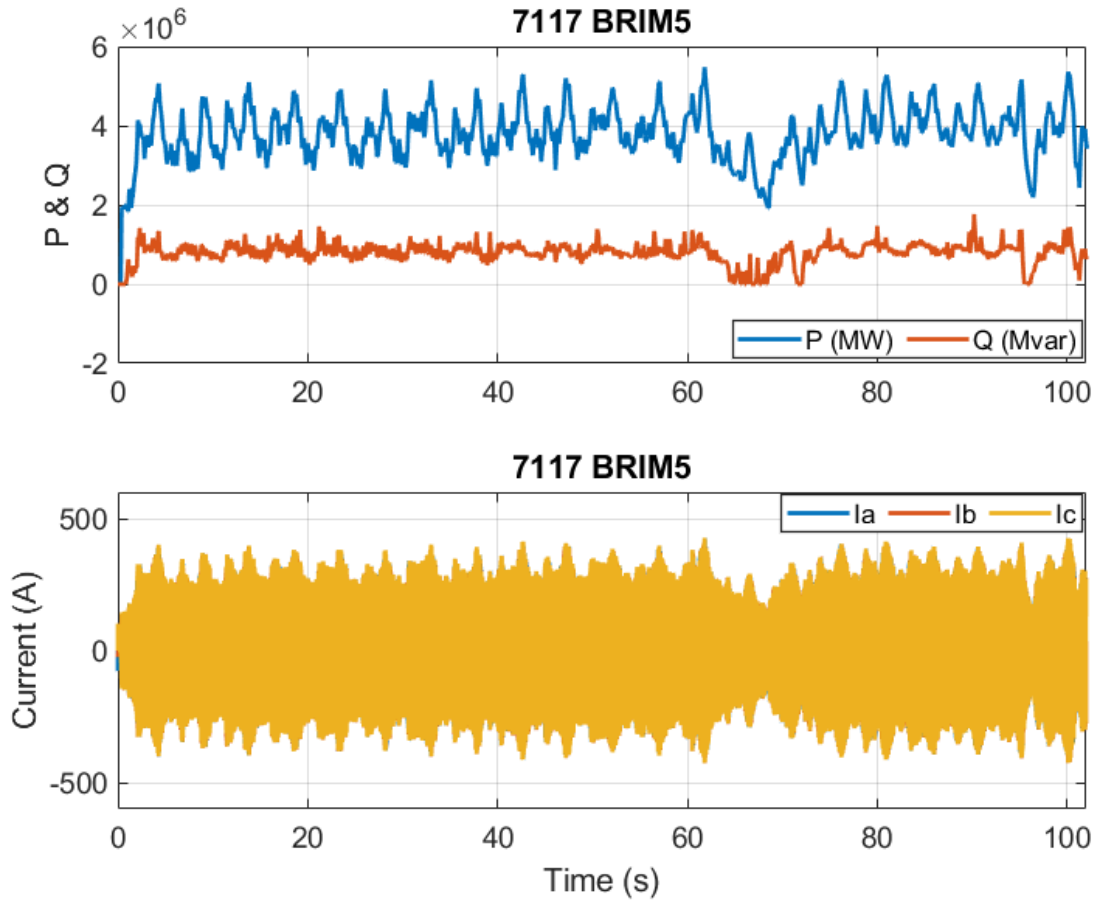


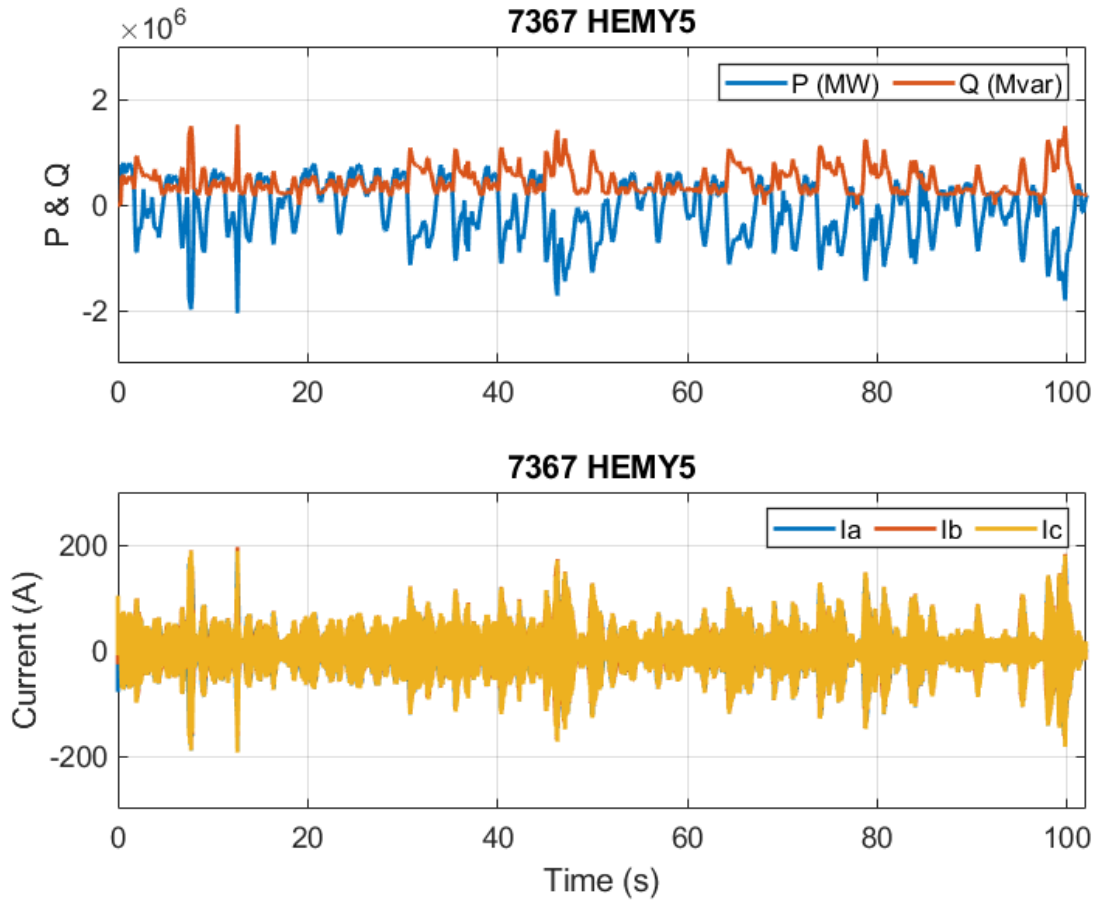
F.3 Results for 11 kV busses – Load active and reactive power

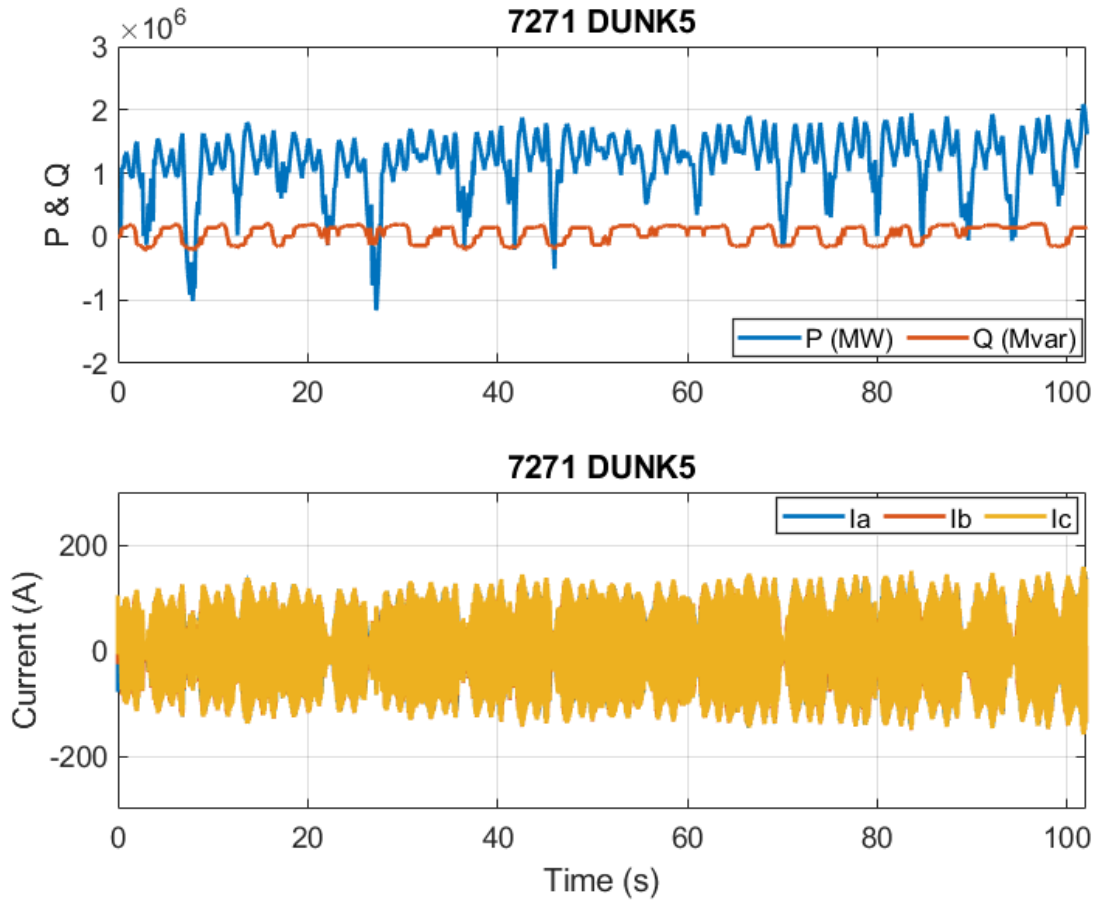


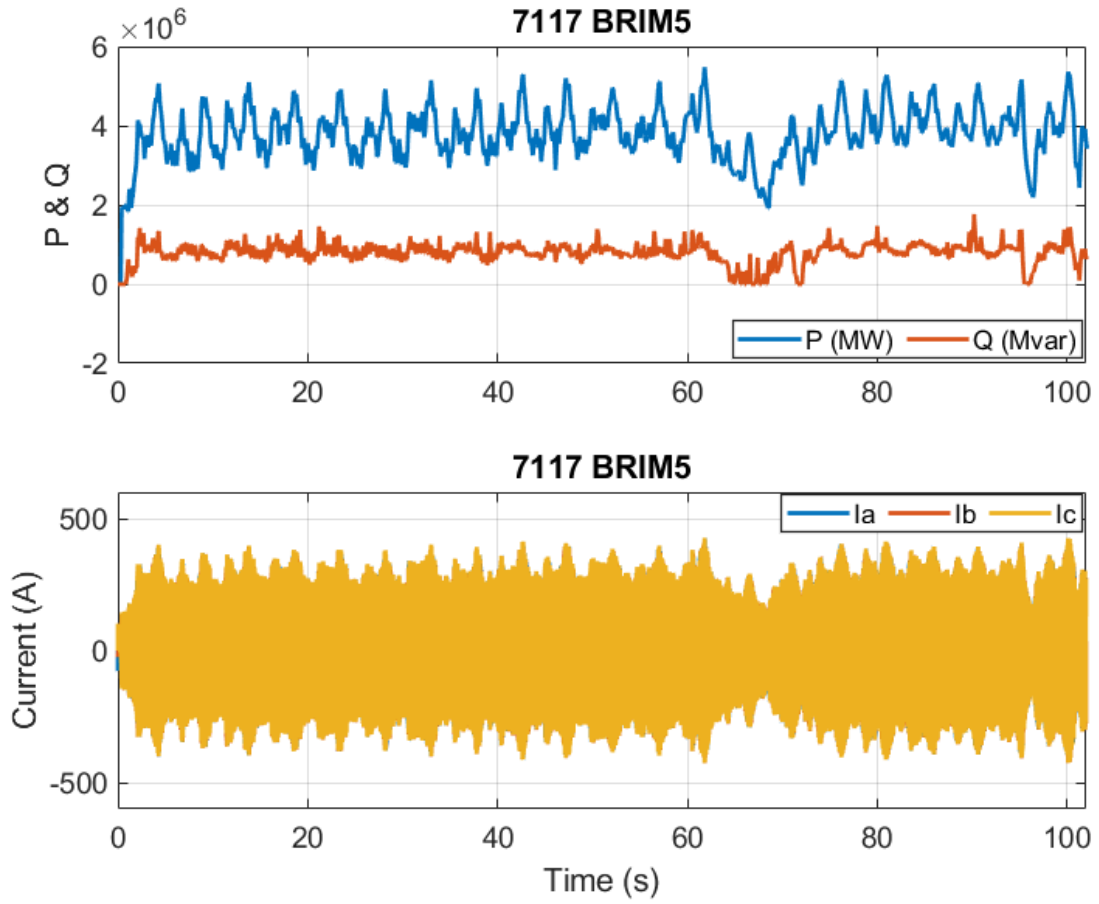


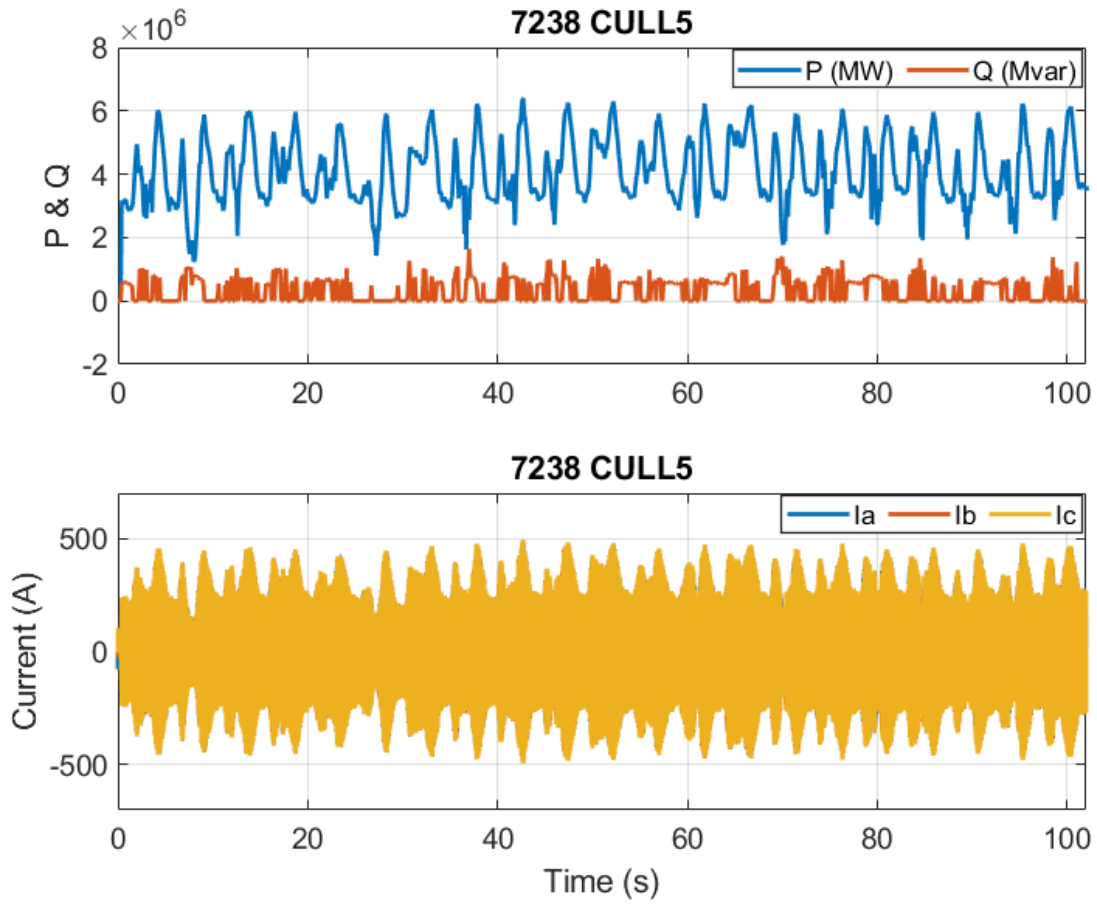












F.4 Results for system boundary

